Impact of Geomorphic Structures on Hyporheic Exchange, Temperature, and Ecological Processes in Streams

Erich T. Hester

A dissertation submitted to the faculty of the University of North Carolina at Chapel Hill in partial fulfillment of the requirements for the degree of Doctor of Philosophy in the Curriculum in Ecology.

Chapel Hill
2008

Approved by:

Martin W. Doyle

Lawrence E. Band

Emily S. Bernhardt

Michael F. Piehler

Seth R. Reice

Abstract

Erich T. Hester: Impact of Geomorphic Structures on Hyporheic Exchange, Temperature, and Ecological Processes in Streams
(Under the direction of Martin W. Doyle)

Water exchange between streams and groundwater (hyporheic exchange) facilitates exchange of heat, nutrients, toxics, and biota. In-stream geomorphic structures (IGSs) such as log dams and steps are common in natural streams and stream restoration projects, and can significantly enhance hyporheic exchange. Hyporheic exchange is known to moderate temperatures in streams, a function important to a variety of stream organisms. Nevertheless, the connection between IGS form, hydrogeologic setting, hyporheic exchange, and hyporheic thermal impacts are poorly known. In this dissertation, I used hydraulic modeling and field experiments to quantify how basic characteristics of IGSs and their hydrogeologic setting impact induced hyporheic water and heat exchange and stream temperature. Model results indicate that structure size, background groundwater discharge, and sediment hydraulic conductivity are the most important factors controlling induced hyporheic exchange. Nonlinear relationships between many such driving factors and hyporheic exchange are important for understanding IGS functioning. Weir-induced hyporheic heat advection noticeably affected shallow sediment temperatures during the field experiments, and also caused slight cooling of the surface stream, an effect that increased with weir height. Nevertheless, such advection was far less important to the stream heat budget than atmospheric heat exchange, indicating streambed hydraulic conductivity was the overriding factor controlling hyporheic influence on surface water temperatures. Lotic organisms are

adapted to the thermal regime typically experienced in their native ranges, and are therefore sensitive to thermal shifts from human activities. However, a basic survey of ecological sensitivity to temperature change in lotic systems is currently lacking. In this dissertation, I generated a quantitative synthesis of ecological sensitivity to temperature from the peer-reviewed scientific literature which I compared to a broad array of human thermal impacts to streams and rivers. Results indicate that on average, lotic organisms are more sensitive to warming than to cooling, and fish are more sensitive than invertebrates. Human thermal impacts entail warming more often than cooling and are of similar magnitude to that required to induce a 50% reduction in organism level functioning, indicating significant potential to impair ecological functioning. My results highlight the need for thermal mitigation in lotic systems at local, regional, and global scales.

Acknowledgements

This dissertation was funded by a United States Environmental Protection Agency Science to Achieve Results (STAR) graduate fellowship (FP-91667601), a William R. Kenan fellowship from the University of North Carolina, and a National Science Foundation grant (CAREER-BCS-0441504). I am grateful to Myles Killar, Meredith Harvill, Frank M. Smith, and Jason Johnson for valuable field assistance, data analysis, and interesting conversation between ibutton downloads. I wish to thank Geoffrey C. Poole for lengthy discussions of stream and river hydraulic and thermal dynamics, professional development, and life in general. Michael N. Gooseff, Tamao Kasahara, Mary I. O'Connor, Jay P. Zarnetske, John Bruno, Jeffrey J. Clark, and John Stofleth provided valuable advice and manuscript review. I am indebted to Karen Henry, Cottie Pasternak, Denise Kenney, Barbara Taylor, Nell Phillips, and Bob Peet, who provided important assistance and advice at many critical administrative junctures. I greatly appreciate the efforts of committee members Larry Band, Emily Bernhardt, Seth Reice, and Mike Piehler for their assistance and guidance during my PhD program. I will be forever grateful to my advisor Martin Doyle for his wisdom, patience, and flexibility over four years. And finally I wish to recognize the patient behind-the-scenes efforts of Linsey Marr, without which my sanity, let alone this dissertation, would be truly impossible.

Table of Contents

List of Tables

List of Figures

List of Abbreviations and Symbols

1D	One-dimensional
2D	Two-dimensional
3D	Three-dimensional
A-D	Advection-dispersion
A	Stream cross sectional area (m^2)
A_c	Chapter 2: Flowpath cross sectional area (m^2) Chapter 3: Area of streambed for conduction calculation (m^2)
A_d	Area of streambed where weir-induced hyporheic flow enters subsurface upstream of weir (m^2)
A_s	Storage zone cross sectional area (m^2)
A_u	Area of streambed where weir-induced hyporheic flow discharges to surface stream downstream of weir (m^2)
C_{bs}	Specific heat of saturated sand (J/kg-ºC)
C_w	Specific heat of water (J/kg-ºC)
d_h	Hyporheic depth (m)
Δh	Hydraulic head difference (m)
i	Hydraulic gradient (m/m)
i_d	Vertical hydraulic gradient downstream of weir (m/m)
i_u	Vertical hydraulic gradient upstream of weir (m/m)
J_a	Hyporheic heat advection (J/s, kJ/day)

J_c	Streambed heat conduction (J/s, kJ/day)
K	Substrate hydraulic conductivity (m/s)
IGS	In-stream geomorphic structure
l_h	Hyporheic pathlength (m)
n	Number of data points
n_e	Effective porosity
PVC	Polyvinyl chloride
Q_d	Downwelling water flux across streambed (m^3/s)
Q_s	Discharge in the surface stream (m^3/s)
R^2	Coefficient of determination
s	Structure size (m, cm)
s_l	Lateral structure width (m, cm)
s_s	Step height (m, cm)
s_w	Weir height (m, cm)
Δt	Travel time along flowpath (s, min, days)
t_r	Hyporheic residence time for water downwelling within the patch scale area (s, min, days)
ΔT_a	Effect of weir-induced hyporheic advection on surface stream temperatures (°C)
ΔT_e	Ecologically relevant temperature changes estimated from thermal performance curve (°C)
$\Delta T_{e\text{-}50}$	Temperature change required to reduce biological process rate below peak value by 50% (°C)

$\Delta T_{e\text{-}10}$	Temperature change required to reduce biological process rate by 10% of its peak value at the steepest part of the performance curve (°C)
T_c	Temperature of subsurface water at conduction depth (°C)
T_d	Temperature of downward hyporheic flow in shallow hyporheic zone upstream of weir (°C)
T_{s1}	Temperature of surface stream water immediately above area of downward hyporheic flow upstream of weir (°C)
T_{s2}	Temperature of surface stream water downstream of weir (°C)
T_{s3}	Temperature of surface stream water upstream of the weir backwater (°C)
T_u	Temperature of upward hyporheic flow discharging to the surface stream downstream of the weir (°C)
USACE	United States Army Corps of Engineers
USGS	United States Geological Survey
v	Average linear groundwater velocity (m/s)
V_h	Hyporheic volume (m^3)
Δx	Flowpath length (m)
Δz	Elevation difference (m)
Δz_c	Vertical distance between conduction depth and sediment surface (m)
λ_{bs}	Thermal diffusivity of saturated sand (m^2/s)
ρ_{bs}	Bulk density of saturated sand (kg/m^3)
ρ_w	Density of water (kg/m^3)

1 Introduction

1.1 Research Rationale

The flow of water in rivers and streams has three basic dimensions. Water flows longitudinally, following gravity to the ocean. Water is exchanged laterally between channel and floodplain, forming the perirheic zone (Mertes 1997). Finally, water is exchanged vertically between channel and groundwater (hyporheic exchange), forming the hyporheic zone (Jones and Mulholland 2000, Brunke and Gonser 1997). Hyporheic exchange facilitates movement of heat, nutrients, toxics, and biota between the surface stream and groundwater. These processes affect the distribution and abundance of organisms in the surface stream and hyporheic zone, nutrient cycling and carbon flux, water quality, and temperature (Jones and Mulholland 2000, Brunke and Gonser 1997).

Temperature is the single most important condition affecting the lives of organisms (Begon et al. 2006). Most lotic organisms are ectotherms (Giller and Malmqvist 1998), which are adapted to the spatial and temporal patterns of thermal regimes typically experienced in their native ranges, and are therefore sensitive to thermal shifts (Lomolino et al. 2006, Begon et al. 2006). Human activities like forestry, agriculture, and urbanization increasingly impact stream temperatures by modifying discharge, riparian shading, channel form, and climate. However, a basic survey of ecological sensitivity to temperature change in lotic systems is currently lacking, and would provide useful context for evaluating the risk posed by anthropogenic temperature change and the need for policy changes.

In-stream geomorphic structures (IGSs) such as debris dams, log dams, boulder weirs, and steps are common in natural streams and can significantly enhance hyporheic exchange (Lautz and Siegel 2006, Kasahara and Wondzell 2003). The density of IGSs on the landscape has been significantly reduced by human activities like modifying flow regimes, removal of large wood, and reduction of riparian and upland forest cover. To help reverse this loss, and provide a variety of ecological and geomorphic benefits, IGSs are commonly installed in stream restoration projects (Bethel and Neal 2003). Geomorphic forms are known to moderate temperatures in streams under certain conditions by exchanging daily and seasonally variable temperature stream water for constant temperature groundwater, a function important to a variety of stream organisms (Poole and Berman 2001). Nevertheless, the connection between in-stream geomorphic form, hydrogeologic setting, hyporheic exchange, and hyporheic thermal impacts remain inadequately characterized.

1.2 Research Questions

The objectives of this research were to characterize the hydraulic and thermal impact of IGSs on streams and their hyporheic zones, and to set those thermal impacts in ecological context. This dissertation therefore addressed three fundamental questions:

1. How do basic characteristics of IGSs and their hydrogeologic setting impact hyporheic exchange in streams?
2. How does IGS presence and size affect heat exchange across the streambed and temperatures in the hyporheic zone and surface stream?

3. How does ecological sensitivity to temperature vary by organism level process and taxonomic grouping, and how do those sensitivities compare to human induced temperature impacts in streams?

1.3 Research Approach

For the first question, which addresses the hydraulic impact of IGSs, I simulated a single IGS in a simplified hypothetical stream by linking numerical models of surface water and groundwater flow. A sensitivity analysis was conducted that varied IGSs size and type, as well as various aspects of the hydrologic and geologic setting of the hypothetical stream reach. A field experiment using an artificial variable height weir in upper Craig Creek near Blacksburg VA was performed to confirm that basic trends in model output were also observed in a more heterogeneous field setting.

For the second question, which addresses the thermal impact of IGSs, I instrumented the Craig Creek field site with a three-dimensional temperature sensor array to measure the impact of weir height on surface and groundwater temperatures. I then used simple heat flux equations to estimate conductive and advective heat fluxes across the streambed in the vicinity of the weir. Third, I used a simple heat mixing model to estimate the impact of weir-induced hyporheic heat advection on surface stream temperatures. Finally, I compared advective heat impacts on surface stream temperatures to actual temperature differences measured as water flowed downstream across the weir.

For the third question, I conducted a quantitative synthesis of ecological sensitivity to temperature in lotic systems. This entailed reviewing the literature for thermal performance curves which relate organism level biological processes like growth, reproduction, and

survival to stream or river water temperature. Sensitivity was calculated for each curve by estimating the temperature shift required to reduce process rates by a given amount. These ecologically relevant temperature changes were then compared among taxonomic groupings and organism level biological processes. Finally, I compared these ecologically relevant temperature changes to the magnitude of a wide range of human impacts on lotic temperatures drawn from the literature.

1.4 Document Organization

Each research question listed above is addressed in a separate chapter in this dissertation (Chapters 2-4). Because these three chapters are each also independent manuscripts for separate peer-reviewed journal publication, Chapters 2-4 contain some repetition of the introductory material in this Introduction.

Chapter 2 covers the hydraulics of hyporheic exchange induced by IGSs. This chapter begins by discussing the importance of hyporheic exchange, the various mechanisms of hyporheic exchange, and the methodological options for quantifying hyporheic exchange. The coupled surface-groundwater modeling approach is described second, followed by a description of the field experiments used confirm the modeling. Results of the modeling sensitivity analysis are provided third, which represent the first comprehensive exposition on how induced hyporheic exchange varies with structure type, structure size, sediment hydraulic conductivity, background groundwater discharge, channel slope, depth to bedrock, and baseflow discharge. Field results are presented fourth, and demonstrate that the modeling approach is able to reproduce basic trends of system response in a more heterogeneous field setting. Fifth, basic hydraulic theory is presented and utilized to explain

some of the nonlinear and non-intuitive trends predicted by the model. Finally, the implications for these hydraulic results for natural streams, stream restoration, and watershed planning are discussed.

Chapter 3 addresses the thermal impact of IGSs (weirs) on surface and groundwater as observed during the field experiments. The impact of structure presence and height on surface and groundwater hydraulics, and surface and subsurface temperature patterns is presented first. This is followed by a discussion of heat fluxes across the streambed in the vicinity of the structure, including hyporheic advective fluxes induced by the structure, as calculated by the heat flux equations using stream and groundwater temperatures measured at the site. Third, the influence of structure-induced hyporheic heat advection on surface stream temperatures, as calculated by the heat mixing model, is compared to actual measured temperature changes as water flows downstream across the structure. Finally, the influence of stream context on structure induced thermal perturbations is discussed, particularly the impact of sediment hydraulic conductivity.

Chapter 4 links ecological sensitivity to temperature with human impacts on temperature in lotic systems. The chapter begins with a literature synthesis on the conceptual importance of thermal performance curves and their similarity across organism types and differences among different organism level processes like growth, development, reproduction, and survival. The methodology for quantitative synthesis of ecologically relevant temperature changes for organism level processes of lotic organisms is presented second. The results of the quantitative synthesis are presented third, including how organism level thermal sensitivity, and asymmetry and nonlinearity of thermal performance curves, vary among taxonomic groupings, and organism level processes. The results of a review of a

wide range of human impacts on stream and river temperatures is presented next, followed by a comparison of these human impacts to the ecologically relevant temperature changes presented earlier. Finally, the implications of human thermal impacts on lotic organisms are discussed, including options for human management of its "thermal footprint."

These three manuscript chapters are followed by a Conclusions chapter that summarizes the key findings of each of the preceding chapters, relates the findings of the chapters to each other, discusses their scientific and management significance, and presents productive directions for future research in this field.

Manuscript details

Chapter 2: Hester, E.T., and M.W. Doyle. 2008. In-stream geomorphic structures as drivers of hyporheic exchange. Water Resources Research, 44, W03417, doi:10.1029/2006WR005810. Note: Sections 2.4.6 and 2.4.7 do not appear in the Water Resources Research article.

Chapter 3: Hester, E.T., M.W. Doyle, and G.C. Poole. 2008. The influence of in-stream geomorphic structures on stream temperature via induced hyporheic exhange. In review.

Chapter 4: Hester, E.T., and M.W. Doyle. 2008. Sensitivity of stream and river organisms to temperature change. In preparation for journal submission.

2 In-Stream Geomorphic Structures as Drivers of Hyporheic Exchange[1]

2.1 Introduction

2.1.1 Hyporheic Exchange and Lotic Ecosystem Management

The hyporheic zone is the area of mixing of surface and groundwater beneath and adjacent to streams (Triska et al. 1989), particularly that region where hydrologic flowpaths leave and return to the stream many times along its length (Harvey and Wagner 2000). Exchange of water between a stream and its hyporheic zone (hyporheic exchange) facilitates important exchanges of heat, chemical solutes, and biota between surface stream and subsurface water (Jones and Mulholland 2000). These processes affect the distribution and abundance of organisms in streams and the hyporheic zone, ecosystem level processes like nutrient cycling and carbon flux, and water quality (Jones and Mulholland 2000, Boulton et al. 1998, Groffman et al. 2005).

In-stream geomorphic structures (IGSs) such as steps, pools, and log dams are common in natural streams and are known to enhance hyporheic exchange (Kasahara and Wondzell 2003). Such structures are also commonly installed in stream restoration projects to recreate habitat for organisms and enhance geomorphic stability (Federal Interagency Stream Restoration Working Group 1998, Bethel and Neal 2003), or even to enhance hyporheic exchange (Doll et al. 2003), a stream function that is increasingly recognized as an important goal of restoration (Boulton 2007). Nevertheless, the impact of structure form and

[1]Chapter 2 is published as an article in the journal Water Resources Research (see Chapter 1 for publication details) and is Copyright © 2008 by the American Geophysical Union (AGU). It is reproduced here with permission of AGU. Sections 2.4.6 and 2.4.7 of this chapter do not appear in the journal article.

hydrogeologic setting on induced exchange both in natural and engineered settings is poorly understood.

A sustainable approach to managing lotic ecosystems will require conservation of remaining natural systems, together with rehabilitation of degraded systems through a combination of direct intervention in heavily degraded cases (e.g., stream daylighting where a stream is remove from a pipe) and larger-scale watershed planning efforts to restore processes that provide long-term maintenance of beneficial channel form (e.g., riparian and watershed reforestation). All such management activities require a better understanding of how channel form and hydrogeologic setting affects hyporheic function.

2.1.2 Mechanisms of Hyporheic Exchange

Hyporheic exchange where hyporheic flowpaths leave and return to a stream multiple times over a reach (Harvey and Wagner 2000) requires hydrologically neutral or gaining conditions. Although IGSs induce a three dimensional pattern of hyporheic flow into the bed and banks, similar to recent studies (e.g., Gooseff et al. 2006), we focus here on vertical exchange into the bed for detailed modeling analysis of controlling factors. Mechanisms that drive primarily lateral exchange such as meander bends are not considered (but see Boano et al. 2006). Further, this discussion focuses strictly on hydrologic exchange mechanisms, ignoring processes such as diffusion that affect only solute flux or heat exchange. In this context, vertical hyporheic exchange can be induced via six basic mechanisms.

1. Darcy flux due to local channel steepening – non-turbulent flux induced by head gradients created by local steepening of the channel slope relative to average reach

channel slope, sometimes called concavity and convexity (Vaux 1968). Examples include steps and riffles.

2. Darcy flux due to backwater – non-turbulent flux induced by head gradients created by water collecting behind obstacles in the channel. Examples include debris dams, large woody debris, boulders, and bars.
3. Darcy flux due to form drag – non-turbulent flux induced by head gradients created by head loss due to form drag as turbulent stream water flows over bed forms that are either permeable like ripples and dunes (Thibodeaux and Boyle 1987) or impermeable like partially buried boulders (Hutchinson and Webster 1998). This effect has been called hydraulic pumping or pumping exchange (Elliott and Brooks 1997) because it is induced by pressure differentials along the streambed, but these terms are not used here as they are ambiguous given that localized streambed steepening (mechanism #1 above) and backwater (mechanism #2 above) can also induce pressure differentials.
4. Darcy flux due to substrate heterogeneity – non-turbulent flux induced by head gradients created by obstructions within the sediments (e.g., areas of lower hydraulic conductivity or shallower bedrock) which induce upwelling upstream and downwelling downstream of the obstruction even in the absence of other exchange mechanisms (Vaux 1968, Salehin et al. 2004).
5. Turbulent flux across the bed – the turbulent energy of flowing water carries momentum and therefore stream water into the subsurface (Shimizu et al. 1990).
6. Turnover exchange – exchange of water as bed forms move, successively trapping and releasing water (Elliott and Brooks 1997).

This study was conducted for baseflow, the most common flow condition. All six hyporheic exchange mechanisms presented above operate in most streams and rivers, but several are relatively insignificant at baseflow. Turnover exchange (mechanism 6) is significant only where bed forms are in motion (i.e., primarily during spates in the absence of large wood or boulders that might otherwise block their advance). Turbulent flux across the streambed (mechanism 5) is insignificant in sands and finer materials and confined to the top 4-6 cm in gravels (Packman and Bencala 2000), although these results potentially overestimate turbulent flux penetration for many gravel or cobble bed streams where sufficient fines are present to fill gaps, or where bed armoring or imbrication has occurred. Further, turbulent flux has been shown to scale with the square of the velocity (Packman and Salehin 2003) which is generally at a minimum during baseflow conditions (Leopold and Maddock 1953). Form drag (mechanism 3) will occur anywhere an obstacle projects into the flow. Debris dams, bars or dunes, partially buried boulders, and large woody debris can all create form drag that is significant under certain conditions. Form drag is maximized for completely submerged conditions and scales with the square of the velocity (Munson et al. 1994) such that it would be least significant at baseflow. Darcy flux induced by local steepening of the streambed (mechanism 1) and backwater behind obstructions (mechanism 2) are therefore generally the primary mechanisms by which IGSs drive water vertically into the hyporheic under baseflow conditions. These mechanisms, along with Darcy flux induced by form drag and substrate heterogeneity (mechanisms 3 and 4), control hyporheic exchange in this setting.

2.1.3 Existing Approaches for Quantifying Hyporheic Exchange

Hyporheic exchange due to mechanisms 1-4 at the reach scale has traditionally been quantified in two ways: transient storage and multi-dimensional approaches. The transient storage approach uses the one-dimensional (1D) advection-dispersion (A-D) equation with off-channel storage areas to quantify solute movement along a stream and exchange with longer residence time storage areas representing both backwater areas in the channel and hyporheic exchange zones. The most commonly used version of this model is also the simplest with one well-mixed storage zone (Bencala and Walters 1983). Other formulations include multiple storage zones (e.g., Gooseff et al. 2004), variable residence time storage zones (e.g., Gooseff et al. 2005), or a diffusive type storage zone (e.g., Packman et al. 2004). Application of the model generally requires release of a conservative tracer in a stream, measurement of concentration history downstream, and fitting the data to the A-D equation using software such as OTIS (Runkel 1998) where storage zone parameters are determined via inverse modeling methods. These parameters include (among others, see Runkel 2002) the cross sectional area of the storage zone (related to hyporheic zone size), the rate of tracer exchange between free flowing stream and storage zone (related to exchange flux rate), and residence times of tracer in the storage zone.

In contrast, the multidimensional approach uses spatially explicit two- (2D) or three-dimensional (3D) analysis of subsurface flow patterns, usually coupling modeling with field or flume data. Field studies (e.g., Wondzell and Swanson 1996, Wroblicky et al. 1998) are usually conducted at the reach or segment scale and are often coupled with site-specific groundwater flow and transport models using well-established software (e.g., MODFLOW, MT3D). Model results are used to calculate hyporheic zone size, exchange flux rate, and/or hyporheic residence time for any desired spatial extent. Flume studies are usually conducted

at the sub-reach scale (e.g., Packman et al. 2004) and, where modeling is conducted, often utilize custom-developed numerical codes (e.g., Salehin et al. 2004). Hyporheic zone size, exchange flux rate, and/or residence time are either measured directly from the flume or output from the model at desired scales. Multidimensional studies have the advantage over transient storage approaches in that hyporheic exchange can be understood as a multidimensional process where individual areas of hyporheic exchange can be isolated and characterized directly for size, flux rate, and residence time. This spatial resolution also allows association of areas of hyporheic exchange with specific geomorphic forms within the reach, allowing correlations to be drawn between form and function (e.g., Kasahara and Wondzell 2003).

2.1.4 Motivation and Approach for Study

The goal of this study was to provide a process-based understanding of how channel form (IGSs) affects hyporheic exchange in streams. This entailed determining the relationships between the magnitude of IGS-induced hyporheic exchange and fundamental characteristics of both the IGSs themselves (size and type) and of their setting (background groundwater discharge rate, sediment hydraulic conductivity, depth to bedrock, in-stream baseflow discharge, and channel slope). The intractability of a primarily laboratory or field approach to creating an array of such relationships required modeling. Multidimensional modeling analysis was chosen over transient storage modeling as the latter is primarily an inverse method where hyporheic response cannot be determined directly for a specified geomorphic form. Unlike previous studies, a sensitivity analysis was conducted to fully quantify the relationships between controlling variables and hyporheic response. We

modeled surface and groundwater response to sensitivity analysis perturbations using a simplified hypothetical stream setting to clearly separate the effects of various driving factors. Widely accepted and well tested models were chosen for this purpose for their reliability and to facilitate the use of this general modeling approach by stream restoration or watershed planning practitioners. This study provides the necessary first step toward understanding how individual structures influence hyporheic exchange, which can later be extended to multiple structures. We briefly describe a field study used to support the modeling approach, but primarily focus on the sensitivity of hyporheic exchange to IGS variability. Basic hydraulic theory is then used to interpret field and model results and demonstrate controlling processes.

2.2 Methods

2.2.1 Modeling

2.2.1.1 Conceptual Model of Hypothetical Stream System

We analyzed coupled surface and groundwater hydraulics in a simplified hypothetical stream reach containing one IGS of varying type. Similar to previous work (e.g., Kasahara and Wondzell 2003), we analyzed baseflow conditions because such conditions are present the majority of the time and lower discharges tend to dominate many stream ecosystem processes (Doyle et al. 2005). Steady-state conditions were therefore assumed. A net gaining condition (i.e. net discharge from groundwater to stream) at the reach scale was assumed based on our previous definition of the hyporheic zone (Harvey and Wagner 2000). We analyzed a small stream (3m wide) because such 1st to 2nd order streams are the most common, are the focus of considerable restoration effort, and IGSs are most prevalent in this

setting. For simplicity, the channel cross section was rectangular with vertical sides and with no floodplain. The channel was straight with a slope of 0.01 m/m for the base case. Sediment and soil were assumed isotropic and homogeneous with respect to the flow of water (similar to Lautz and Siegel 2006, Gooseff et al. 2006). Sediment texture for the base case was sand. Channel discharge was 0.2 m^3/s for baseflow conditions, giving a normal depth (steady uniform depth away from obstructions) of 0.1m. The following types of IGSs were analyzed (Figure 2.1):

1. Steps were vertical drops of the channel bottom with a consistent slope upstream and downstream.
2. Weirs were impermeable channel-spanning obstructions rising vertically out of the bottom of an otherwise consistently sloped bed. The structures were perpendicular to flow, with a horizontal top surface. Weirs represented debris dams, log dams, boulder weirs, and log jams that span the channel and create backwater. Flow was assumed to overtop the weir for this study.
3. Lateral structures were similar to weirs but were of greater height, always exceeding flow depth, and did not completely span the channel. Lateral structures were intended to represent wood or rock structures that do not span the channel and divert water around, but not over, at baseflow.

2.2.1.2 Numerical Modeling Approach

The U. S. Army Corps of Engineers (USACE) 1D river hydraulics model HEC-RAS (United State Army Corps of Engineers 2002b) was used to simulate stream hydraulics for a 3m wide, 30m long reach with a single IGS approximately centered in the reach (Figure

2.2a). Although this 1D representation necessarily makes compromises simulating flow across each of the structure types, we considered this acceptable because 1) the purpose of this study was an exploratory sensitivity analysis evaluating basic trends rather than predicting precise magnitudes of system response, and 2) the focus was on vertical hyporheic exchange in a straight simplified stream with no floodplain. Manning's n was set to 0.03, reasonable for natural sand or gravel bottoms (United State Army Corps of Engineers 2002a). Form drag losses were accounted for in HEC-RAS using the default coefficients for contraction (0.1) and expansion (0.3) except within 1.5m of the lateral structures, where 0.6 and 0.8 were used (United State Army Corps of Engineers 2002a), respectively. HEC-RAS assumes an impermeable bed but can accept user-specified lateral inflows at each cross-section which were used to manually couple cross-streambed flows with MODFLOW.

The U. S. Geological Survey (USGS) 3D groundwater flow model MODFLOW (Harbaugh and McDonald 1996) was used to simulate groundwater hydraulics. The model domain was created such that HEC-RAS cross sections were located directly atop MODFLOW nodes along a central column. There were 21 layers in the base case scenario with vertical discretization of 0.25m, plus one top layer of 0.1m. Horizontal layers were used rather than dipping layers for simplicity and for improved accuracy of particle tracking in MODPATH (Pollock 1994). Horizontal discretization, consistent with the exploratory nature of the study, was fairly coarse with 11 3.0m square cells in each direction. Hydraulic conductivity (K) was assumed uniform and isotropic at 10^{-5} m/s to represent fine sand (Freeze and Cherry 1979) for the base case (Table 2.1). The water surface profile of the stream (calculated by HEC-RAS) was represented as constant head cells in the top MODFLOW layer using the river package. The presence of different size and type IGSs was

expressed in the MODFLOW river package by using a series of different hydraulic head profiles from HEC-RAS and varying the distribution of riverbed thicknesses along the channel. Additional boundary conditions in MODFLOW included constant-head conditions for all model cells at the upstream and downstream ends of the model domain and no-flow conditions for all cells on the sides and bottom (Gooseff et al. 2006). Constant heads at the ends of the model were set above (0.1m for base case; Table 2.1) the normal depth of flow in the stream at the respective HEC-RAS cross sections, creating higher heads in groundwater than in the stream and hence gaining conditions. The no-flow boundary condition on the bottom of the model represents bedrock at depth (5m deep for base case; Table 2.1). The USGS program ZONEBUDGET (Harbaugh 1990) was used to extract hyporheic exchange fluxes from MODFLOW output files for cells at the streambed interface.

In order to fully simulate the exchange of water across the streambed, the surface and groundwater models were coupled at the surface-groundwater interface. This was accomplished by an iterative process where heads and flows along the streambed are passed back and forth between HEC-RAS and MODFLOW until values converge. An initial set of iterated model runs was conducted to gauge the extent of this feedback on results. Results indicated that the impact of hydraulic feedback is imperceptible on in-stream flows and hyporheic exchange metrics for the base case K (10^{-5} m/s). The effect of hydraulic feedback was significantly greater for K of 10^{-2} m/s, but still relatively minor. Iteration was therefore performed only for sensitivity analysis model runs where K was increased to 10^{-2} m/s.

The USGS program MODPATH (Pollock 1994) was used to simulate particle tracking in groundwater and calculate residence times of hyporheic flowpaths induced by the modeled IGSs. Particles were released at the surface water-groundwater interface along the

centerline of the stream channel. Effective porosity was set to 0.3, a reasonable value for sand (Freeze and Cherry 1979). Particle tracks determined by MODPATH were visualized using the USGS program MODPLOT (Pollock 1994).

We quantified hyporheic exchange induced by a given IGS as that which downwells within the "patch scale area" just upstream (within 1 channel width) of the structure. This water then flows downstream beneath the structure and upwells downstream of the structure, forming the "patch scale hyporheic flow cell," which is approximately 2 channel widths long. This is in contrast to the "full hyporheic flow cell" which incorporates all the hyporheic flow induced by the IGS (Figure 2.2a). While the model domain was chosen to be much larger than the patch scale hyporheic flow cell, the patch scale was chosen for reporting results because the most intense hyporheic flow occurs in this area, because hyporheic exchange metrics for this area are less sensitive to boundary artifacts of the model than those for the larger full hyporheic flow cell, and because various geomorphic features longitudinally constrain hyporheic flow cells in real streams. In other words, while the full hyporheic flow cell will vary enormously with stream context, patch scale dynamics are the most important subset that is always present, regardless of geomorphic context (see also Section 2.4.1). This choice is arbitrary but reasonable as IGSs are often spaced on the order of 2-5 channel widths in natural streams (Montgomery et al. 1995), and presumably at similar distances in restored reaches.

A variety of fundamental metrics of hyporheic exchange were generated from model output for the patch scale area (Table 2.2). Downwelling flux rate and hyporheic volume were defined for all water downwelling within the patch scale area. Residence time, hyporheic depth, and hyporheic pathlength were defined for the particle that downwelled at

the center of the patch scale area, representing a median value for the patch scale. While in reality there are many flowpaths emanating from the patch scale area that have a distribution of lengths and residence times, for this study it was useful to constrain the results to a single characteristic flowpath in order to focus on the trends of system response to driving factors.

2.2.1.3 Sensitivity Analysis

The primary objective of this study was to determine the independent effect of a wide range of potential controls on the vertical hyporheic exchange induced by a single IGS. This was accomplished by a sensitivity analysis where each of the parameters of interest was varied separately. Factors varied included structure type (weir, step, lateral structure) and size (s), represented by weir height (s_w), step height (s_s), and lateral structure width (s_l) (Table 2.1, Figure 2.1). Stream discharge, background groundwater discharge, sediment hydraulic conductivity (K), channel slope, and depth to bedrock (Table 2.1) were also varied, but due to the extensive number of model runs and volume of output, this was undertaken only for weir type structures. When each factor was varied, all remaining factors were held constant at base case values. Note that when stream discharge rate was varied, the constant head boundary conditions for groundwater were adjusted to maintain a constant level of background groundwater discharge to the stream. This is appropriate for examining the effects of varying baseflow discharge but not for evaluating response to hydrographs.

2.2.2 Field Experiment

A simple field experiment was conducted to discern if trends and patterns observed in the model results were also observed in the field despite more heterogeneous conditions. We

focused on groundwater (and hence MODFLOW) behavior due to higher uncertainty relative to surface hydraulics. We constructed a single, fully-spanning, variable height weir in the upper portions of Craig Creek in the Jefferson National Forest near Blacksburg VA. This stream reach (width 1-2m, baseflow discharge 0.5-5.0 L/s, gravel and cobble surface substrate with increasing proportions of sand with depth) was somewhat smaller than the hypothetical stream used in the model to allow easier weir construction. As weir height was varied, vertical head gradient (proportional to downwelling flux rate) was measured within the downwelling zone just upstream of the weir using a 1.25" polyvinyl chloride (PVC) piezometer with a single screen 20-25 cm below the streambed. Simultaneously, the residence time of hyporheic flow beneath the structure was estimated by injecting a concentrated salt slug into separate piezometer just upstream of the weir (0.5" PVC with a single screen 10-15 cm below the streambed) and determining the inflection time (time to reach half the peak electrical conductivity) of the resultant salt breakthrough curve in a piezometer just downstream of the weir (1.25" PVC with a single screen 10-25 cm below the streambed) using an electrical conductivity probe. All three piezometer screens were located (horizontally and vertically) within the area equivalent to the patch scale hyporheic flow cell from the modeling (Figure 2.2a), allowing the most rigorous comparison with patch scale modeling results. Field data were evaluated as a function of weir height, and resulting trends compared to model output. The parameters measured in the field were chosen because of their primary importance among the results of the modeling and also for ease and accuracy of measurement in the field.

2.3 Results

2.3.1 Field Experiment

Field data confirmed that principal trends observed in the modeling results (for weirs) were also observed in a more heterogeneous field setting. Specifically, vertical head gradient (proportional to downwelling flux rate, Q_d, via Darcy's Law) in the patch scale area increased linearly with weir height for both model and field results (Figure 2.3a). Similarly, hyporheic residence time for water downwelling within the patch scale area (t_r) decreased roughly exponentially with weir height across most weir heights (Figure 2.3b). Field and model t_r results diverged at the smallest weir heights, likely because the salt injection port had to be set deep enough to prevent salt solution escaping to the stream which prevented measurement of the shortest flowpaths created during the lowest weir heights.

2.3.2 Modeling Sensitivity Analysis

Modeling indicated that an IGS in a gaining alluvial stream will induce downwelling into the subsurface upstream of the structure if it is of sufficient size. Much of this downwelling water moves downstream beneath the structure within the alluvium and then re-emerges (Figure 2.2a). This IGS-induced flux manifests as a characteristic pattern of downwelling and upwelling along the channel bed (Figure 2.2b). Model results indicate this pattern varies in magnitude with IGS size and type, as well as with hydrologic and geologic setting, but overall shape remains similar.

2.3.2.1 Effect of Structure Size and Type

For all structure types and patch scale hyporheic exchange metrics, there were minimum structure sizes required to overcome the background gaining conditions. In the

plots of hyporheic exchange metrics versus structure size (Figure 2.4), this effect manifests as a section at the left (small structure) end of each curve that does not rise above zero exchange. All results discussed below refer to exchange induced by structures larger than this minimum size.

As weir and step height increased (s_w and s_s), downwelling flux rate (Q_d, Table 2.2) increased linearly, but the flux rate for steps was always about half as high as for weirs (Figure 2.4a). For lateral structures, structure width (s_l) had little effect on Q_d until s_l exceeded approximately 50% of total channel width (Figure 2.4a). For all IGS types, hyporheic residence time (t_r, Table 2.2) varied nonlinearly with structure size, initially increasing steeply and then decreasing asymptotically (Figure 2.4b). The trends for steps and weirs were similar, with peak t_r at approximately the same structure size, but t_r for weirs was approximately double that for steps.

The trends of the three hyporheic size zone metrics, depth (d_h), pathlength (l_h), and volume (V_h) (see Table 2.2 for calculation methods), were similar and mostly nonlinear (Figure 2.4c-e). For both weirs and steps, all three metrics increased steeply at small s, and then became independent of s at larger s. Hyporheic zone size metrics for weirs exceeded those of steps for all s, with d_h and l_h for weirs about twice that for steps. The d_h asymptotes were considerably shallower than depth to bedrock because these pathlines originated within the patch scale area (i.e., close to the structure), and therefore did not penetrate as deeply as particles originating further from the structure (Figure 2.2a). For lateral structures, hyporheic zone size metrics also increased with s, but either increased approximately linearly with s_l (d_h and l_h, Figure 2.4c-d), or increased roughly exponentially with s_l (V_h, Figure 2.4e).

Interestingly, the ratios of l_h to d_h for each of the IGS types approached approximately 3 at larger structure sizes.

2.3.2.2 Effect of Hydrologic and Geologic Setting

The effect of hydrologic and geologic variables on patch scale hyporheic exchange is presented in two ways. First, the plots of exchange metrics (Q_d, t_r, and d_h) versus s_w are expanded to each include three curves: the original base case curve along with two additional values of the hydrologic or geologic variable being evaluated. This type of plot is shown to quantify response over the full range of structure sizes. Second, additional plots are created of Q_d, t_r, and d_h versus the hydrologic or geologic setting variable itself. These are included to directly quantify the impact of the hydrologic or geologic variable. d_h is the only metric of hyporheic zone size included because our focus here is the shapes rather than the magnitudes of trends, and trends for l_h and V_h share the same basic shape as those for d_h.

The shape of the relationships between s_w and Q_d, t_r, and d_h changed little with baseflow discharge (Figure 2.5, left). As baseflow discharge increased (with background groundwater discharge held constant) at a representative s_w of 0.2m, Q_d increased approximately 51%, t_r decreased approximately 15%, and d_h increased approximately 10% (Figure 2.5, right). All three relationships between hyporheic exchange and baseflow discharge were nonlinear, becoming independent of discharge at higher discharges.

Hyporheic exchange metrics responded significantly to background groundwater discharge rate (i.e. degree of gaining). The shape of the relationships between s_w and the various hyporheic exchange metrics were all similar (Figure 2.6, left), and Q_d, t_r, and d_h all decreased to zero as background groundwater discharge increased (Figure 2.6, right).

Some metrics of hyporheic exchange responded substantially to changes in hydraulic conductivity (K) while others did not (Figure 2.7). Both Q_d and t_r responded dramatically over many orders of magnitude as K increased from 10^{-8} m/s to 10^{-2} m/s at a representative s_w of 0.1m (Figure 2.7, right). Specifically, Q_d increased linearly with K (Figure 2.7 shows trend as linear on a log-log plot, but trend would also be linear on a linear-linear plot) and t_r decreased logarithmically with K (Figure 2.7 shows trend as negatively linear on a log-log plot, which would look approximately negatively exponential on a linear-linear plot). On the other hand, d_h changed little with increasing K, decreasing approximately 9%, with all of the decrease occurring at a K of 10^{-2} m/s (Figure 2.7, right). In all cases the shape of the relationships between exchange metrics and s_w varied little if at all with K (Figure 2.7, left).

Hyporheic exchange metrics responded significantly to channel slope (Figure 2.8). The shape of the relationships between s_w and Q_d, t_r, and d_h changed relatively little with slope, except for t_r which peaked at increasing s_w with increasing slope (Figure 2.8, left). The relationships between Q_d, t_r, and d_h and slope are mostly nonlinear, increasing at low slopes and decreasing at higher slopes (Figure 2.8, right). Peak exchange generally occurred at slopes of 0.005 - 0.01 m/m. The one exception was t_r for s_w = 1.0m, which increased slightly with slope.

Finally, hyporheic exchange responded significantly to depth to bedrock (Figure 2.9). The shape of the relationships between s_w and Q_d, t_r, and d_h varied somewhat with depth to bedrock but were generally consistent (Figure 2.9, left). The largest change was for t_r which peaked at increasing s_w as depth to bedrock increased. For most weir heights, Q_d, t_r, and d_h increased with increasing depth to bedrock, although all three trends were also reversed at small s_w (< ~0.1-0.2 m). Two different curves are therefore shown for Q_d, t_r, and d_h versus

depth to bedrock (Figure 2.9, right). All such relationships were nonlinear, exhibiting a rise (moderate to large s_w) or drop (small s_w) at shallower bedrock depths and a leveling off at greater bedrock depths.

2.4 Discussion

2.4.1 Model Confidence and Spatial Scale

Issues of scale and model confidence are discussed together because the issues are related and many lines of evidence available to address one issue also address the other. There are four lines of evidence supporting the validity of the model results as presented in this study. First, model software (MODFLOW and HECRAS) is well-developed and has been extensively tested and refined. Second, the models were used for comparative purposes (i.e. determining trends of system response in a sensitivity analysis) in a simplified hypothetical setting rather than for predictive purposes at a heterogeneous real site. Third, the field experiment indicated the model was accurately quantifying trends of hyporheic response to varying weir height. These field results do not explicitly confirm model performance with other structure types, and additional field or flume studies would be useful. However, the field experiment for weirs is at least somewhat relevant to steps and lateral structures because these other structure types, like weirs, drive hyporheic flow by creating hydraulic head perturbations in the stream that propagate into the subsurface. Fourth, trends from the modeling and field experiment appear reasonable when simple hydraulic theory is used to interpret the hydraulic processes behind them.

These lines of evidence also inform the application of these model results to other scales. First, the field experiment and modeling results show similar trends of system

response to weir height, despite differences in the size of the streams. This supports the idea that modeled trends are not specific to a particular size stream. Second, modeled trends of system response are congruent with application of hydraulic theory where no scale was specified (see Sections 2.4.3 and 2.4.4). This further supports the idea that modeled trends are not specific to a particular size stream, but also indicates that modeled trends are not specific to a particular scale of observation (e.g., patch scale vs. full hyporheic flow cell). We acknowledge that the very shortest flowpaths induced by the structure were outside the scope of the field experiment, and that the modeling did not address turbulent flux and scour that might affect these short flowpaths under certain circumstances. However, the overall Darcy flux hyporheic response characterized in these results appears relevant to a range of scales.

These scale issues then bear on the rationale and justification for choosing the "patch scale area" and the corresponding "patch scale hyporheic flow cell" for presenting the results. Note the patch scale was merely the scale for reporting the results, whereas the scale of the model domain was considerably larger (see Section 2.2 for details). To begin, the patch scale was not chosen as an expedient compromise, but rather was intentionally implemented as both a necessary and highly useful way to broaden the applicability of the results. Specifically, we originally evaluated results for the full hyporheic flow cell induced by the IGS, but this proved untenable, because as structure size increased, the flow cell would eventually encompass the entire MODFLOW model domain in the longitudinal direction, which artificially constrained hyporheic metrics at greater structure sizes. To remedy this problem, the length of the model domain for weir scenarios was increased several times up to approximately 200m, but the larger weirs still induced a hyporheic flow cell that pressed up

against at least one end of the model domain. While this effect might be somewhat less for other structure types or steeper channel slopes, for much of the sensitivity analysis presented in this study, the full hyporheic flow cell was an ill-defined concept in the context of this modeling study. Furthermore, such long model domains devoid of constraints from other hyporheic flow cells induced by other geomorphic forms are meaningless when applied to real streams. We further discovered that patch scale hyporheic exchange metrics did not change significantly as the length of the model domain changed, and were therefore independent of the arbitrary model boundary conditions. This fact, combined with the typical presence of other structures up and downstream in real streams, rendered patch scale results more generally applicable than results for the full hyporheic flow cell. In other words, while the full hyporheic flow cell will vary enormously with stream context, patch scale dynamics are the most important portion that is always present, regardless of geomorphic context.

We acknowledge that the patch scale hyporheic flow cell takes up a variable percentage of the full hyporheic flow cell as the full hyporheic flow cell varies in size as controlling factors are varied in the sensitivity analysis. This effect is probably most significant for hyporheic zone size metrics, but even then, this issue affects the details, not the overall shape, of the relationships between driving factors and hyporheic response. For example, hyporheic depth levels off with increasing structure height for both patch scale and full hyporheic flow cells, just at different values. An alternative approach to a fixed size patch scale area would be to vary the patch scale as some percentage of the full hyporheic flow cell. However, as discussed above, the full hyporheic flow cell is not defined for larger

structures in our modeling context, so this approach would place significant limits on the structure sizes included.

2.4.2 Magnitude of Structure-Induced Hyporheic Exchange

The degree of hyporheic exchange induced by an IGS can be better understood when set within its stream context. For example, the magnitude of downwelling flux (Q_d, Table 2.2) induced by an IGS can be viewed as a portion of baseflow stream discharge. This percentage varies with hydraulic conductivity (K) and degree of gaining, but will often be much less than 100% for natural sediments. We calculated this percentage from our modeling results (presented previously in Figure 2.4a) by dividing the downwelling flux rate by in-stream discharge rate. Q_d values from the base case ($K = 10^{-5}$ m/s, appropriate where the finest sediment size fraction is medium sand) were all less than about 0.015% of surface discharge (Figure 2.10a). For $K = 10^{-2}$ m/s (appropriate where the finest sediment size fraction is gravel), induced Q_d can approach 25-50% of the stream discharge. The latter values, while substantial, reflect the largest size of the most effective type of IGS (weirs), and most structures would therefore induce significantly less flux, even in coarse substrate. This is consistent with most hyporheic studies on streams and rivers with either hydrologically gaining or approximately net neutral conditions which report a small fraction of surface flow moving through the hyporheic due to relatively fine sediments (e.g., Lautz and Siegel 2006, Kasahara and Wondzell 2003, Storey et al. 2003). Only a few studies report K values high enough that relatively large fractions of surface flow may move through the hyporheic zone (e.g., Poole et al. 2004).

Hyporheic residence times (t_r, Table 2.2) (Figure 2.4b) for the base case scenario (sandy sediment, see Table 2.1) were mostly in the range of days to weeks and much greater than typical surface water residence times, generally in the range of seconds to hours. Like Q_d, t_r is highly dependent on K. These results are similar to those found by others for sandy bed streams (e.g., Lautz and Siegel 2006, Cardenas et al. 2004), and greater than those for streams of generally coarser sediments (e.g., Kasahara and Wondzell 2003).

Hyporheic pathlengths (l_h, Table 2.2) and depths (d_h, Table 2.2) (Figure 2.4c-d) were in the range of a few meters, with l_h generally in the range of three times d_h. Corresponding hyporheic volumes (V_h, Table 2.2) ranged over a few to a few tens of cubic meters. To allow an order of magnitude comparison with other studies, these hyporheic zone size metrics can be expressed in transient storage terms, where storage zone cross sectional area is divided by stream cross sectional area (A_s/A). We calculated A_s as V_h/l_h, which estimates the average cross sectional area (normal to flow) of V_h. We calculated A as the channel width times the normal depth used in the HEC-RAS simulations. The resulting patch-scale A_s/A estimates for our model simulations range with structure size up to 5-25, depending on structure type (Figure 2.10b). A_s values used in Figure 2.10 are for the patch scale area, and those for the full hyporheic flow cell would be larger. However, given t_r is in the range of days to weeks for our hypothetical stream (Figure 2.4b) and in the range of hours to days duration of most transient storage experiments, transient storage experiments run on our hypothetical stream would probably detect a patch scale or smaller hyporheic contribution to transient storage. Nevertheless, transient storage analyses on real streams would generally also detect a surface water storage component (Ensign and Doyle 2005). We did not attempt to estimate a surface storage component for our hypothetical stream, but it would presumably be significant for the

weir and lateral storage cases, and insignificant for the step case. Our A_s estimates therefore would be greater than or equal to the reported values if we accounted for surface storage. Overall then, given that our method of calculating A_s may both tend to overestimate A_s by including longer residence time hyporheic pathlengths than are typical of tracer studies and tend to underestimate A_s by not including surface storage, we would expect literature values from field studies to agree with our modeling results, at least at an order of magnitude level. This is indeed the case, as literature values tend to range from 0 to nearly 10 (Harvey and Wagner 2000) and our results range from 0 up to a maximum anywhere between 5 and 25, depending on structure type (Figure 2.10b).

2.4.3 Effect of Structure Size and Type

Structure size was a critical factor in determining the relationship between IGS morphology and hyporheic exchange. Relationships between IGS size (s; weir height s_w, step height s_s, lateral structure width s_l) and the hyporheic exchange metrics (Figure 2.4) were of similar shape for weirs and steps, but different for lateral structures. Q_d increased approximately linearly with s_w and s_s, but increased nonlinearly (approximately exponentially) with s_l (Figure 2.4a). This is consistent with our field experiment for weirs (Figure 2.3), and also with Kasahara and Wondzell (2003) who reported that larger steps induce greater flux than smaller steps. Similarly, Storey et al (2003) found an increase in downwelling flux with head drop across a riffle. This increase in head drop is analogous to an increase in s in our modeling study, because increasing s increases in-stream head drop and associated hyporheic Darcy flux processes due to channel steepening, backwater and/or form drag mechanisms (mechanisms 1, 2, and 3 in Section 2.1.2). In fact, this connection

between structure size, head drop, and induced hyporheic flux can be understood by applying Darcy's Law to the hyporheic flow originating within the patch scale area. Because s is varied in this study under conditions of constant K, Darcy's Law can be simplified,

$$Q_d = K \frac{\Delta h}{l_h} A_c \propto \frac{\Delta h}{l_h} A_c \tag{2.1}$$

where A_c is the cross sectional area of the subsurface (hyporheic) flowpath and Δh is the in-stream head drop across the structure. Because the relationships between Δh and s (Figure 2.11a) have the same shapes as the relationships between Q_d and s (Figure 2.4a), it is clear that Δh in equation (2.1) is more important than A_c or l_h in determining Q_d and that an IGS controls Q_d primarily by controlling Δh.

In contrast to Q_d, t_r varied nonlinearly with s for all three IGS types, with large initial increases and then asymptotic decreases (Figure 2.4b). This result is less intuitive than the linear increase of Q_d with s. However, while only the falling portion of this curve was reproduced at our field site (Figure 2.3), the processes giving rise to the entire relationship can be understood for weirs and steps by applying equation (2.1) to the flowpath originating at the center of the patch scale area. To start, average linear groundwater velocity (v) along the flowpath can be derived from equation (2.1) by dividing Q_d by A_c and the effective porosity (n_e).

$$v = K \frac{\Delta h}{l_h n_e} \tag{2.2}$$

Further, velocity is defined as

$$v \equiv \frac{\Delta x}{\Delta t} = \frac{l_h}{t_r} \tag{2.3}$$

where Δt is the travel time along a flowpath, i.e. the residence time, t_r. Equations (2.2) and (2.3) can be combined and solved for t_r, and recognizing that n_e and K are constant for this analysis,

$$t_r \propto \frac{l_h}{\Delta h / l_h} = \frac{l_h^{\,2}}{\Delta h} \tag{2.4}$$

Examining the numerator and denominator of equation (2.4) in turn, we focus on how each varies with s, and how their behavior differs between small and large values of s. For the numerator, our model results indicate that l_h increases with s for small values of s but levels off to a constant value at large values of s (Figure 2.4d). Because such an asymptotic curve retains its basic shape when all the ordinate values are squared, the relationship of l_h^2 with s will also have rising and constant sections that correspond to the same ranges of s. For the denominator of equation (2.4), Δh increases linearly with s for weirs and steps (Figure 2.11a), and thus Δh^{-1} relates inversely to s (Figure 2.11b). Comparing these trends for the numerator (Figure 2.4d) and the denominator (Figure 2.11b) which combine per equation (2.4) to produce the t_r versus s relationship for weirs and steps (Figure 2.4b), l_h appears to dominate the relationship at small s and Δh appears to dominate the relationship at large s (Figure 2.12). This seems to clarify the processes behind the relationship observed in the modeling, indicating that under gaining conditions, weirs and steps control t_r at small s primarily by controlling l_h and control t_r at large s primarily by controlling Δh. Even at small s, however, l_h is ultimately controlled by Δh (Figure 2.4d), tying the observed pattern back to the hyporheic Darcy flux processes (mechanisms 1, 2, and 3 in Section 2.1.2). Further investigation would be useful to confirm this hypothesis in real streams, particularly for the rising portion of the curve where dynamics at small s are influenced by scour patterns downstream from the weir and turbulent flux in coarser sediment.

All hyporheic zone size metrics (d_h, l_h, and V_h) relate nonlinearly to s_w and s_s, increasing rapidly at small s, and then becoming independent of s at greater s (Figure 2.4c-e). The processes behind this pattern can be understood by examining how the effect of geologic and geomorphic constraints increases with structure size. First, under gaining conditions, no hyporheic exchange will be induced in the absence of a structure, such that d_h, l_h, and $V_h \rightarrow 0$ as $s \rightarrow 0$. Second, as s increases, d_h, l_h, and V_h will eventually be constrained both vertically and longitudinally by nearby geologic or geomorphic features. Specifically, as s increases, the vertical extent of the hyporheic zone induced by the structure will eventually be constrained by geologic units such as bedrock or clay layers. At the same time, the longitudinal extent of the hyporheic zone will eventually be constrained by other IGS-induced hyporheic zones up and downstream, other geomorphic features, or bedrock outcrops. The net effect is a relationship between V_h (and therefore d_h and l_h) and s that increases from zero and then asymptotes. By contrast, hyporheic zone size metrics (d_h, l_h, and V_h) do not appear to level off with s_l, (Figure 2.4c-e), but this is expected because lateral structures in this study are infinitely tall (never overtopping), so Δh increases rapidly at large s_l to an undefined condition at s_l =1.0. Literature data for comparison are relatively rare. Gooseff et al (2006) showed that mean hyporheic depth (analogous to d_h) both increased and decreased with reach-averaged step height in various modeling studies informed by field data (their Figure 7a), although they did not explain the contradiction. Lautz and Siegel (2006) showed that for small dam structures (analogous to weirs), hyporheic volume increased with head drop (their Table 2). This increasing trend is similar to ours, but because they used a "hydrochemical" (> 10% of water from stream) delineation of the hyporheic zone and other parameters varied between structures, the results may not be directly comparable. Because

little existing work is directly comparable to our hyporheic zone size results, additional field or flume studies in this area, particularly those that more realistically address turbulent flux and scour in shallow sediments downstream of the structure, would be beneficial.

Taken together, the impact of IGS size on the various hyporheic exchange metrics, at least for weirs and steps under gaining conditions where turbulent hyporheic flux is minimal, appears to be determined by its effect on both Δh induced in the stream, and on the size of the induced hyporheic flow cell (d_h, l_h, and V_h) relative to the available subsurface flow domain that is subject to various geologic, geomorphic, and hydraulic constraints. In particular, for Q_d, changes in Δh are always the dominant controlling factor that translates changes in structure size to changes in hyporheic Darcy flux processes due to structure-induced channel steepening, backwater and/or form drag (mechanisms 1, 2, and 3 in Section 2.1.2). On the other hand, for hyporheic zone size, Δh is the dominant factor for small values of s but geomorphic constraints are dominant for large values of s, yielding an overall nonlinear trend. Finally, for t_r, Δh is dominant for large values of s, but only because hyporheic zone size has been constrained in this range, which allows Δh to operate along a relatively fixed length flowpath.

The type of IGS was also a critical factor in inducing hyporheic exchange. Channel-spanning structures (weirs, steps) were generally more effective than partially-spanning lateral structures. Lateral structures had relatively little influence on hyporheic exchange until they spanned a substantial portion of the stream width (~ 50%). In addition, hyporheic exchange metrics for weirs exceeded those for steps at all structures sizes (Figure 2.4). These results are somewhat non-intuitive, as greater Q_d for weirs than steps of the same height should be accompanied by greater v and lesser t_r, everything else being equal. Instead,

greater t_r is observed for weirs, due in part to greater l_h, but also due to greater divergence of the flowpaths originating in the patch scale area for weirs relative to steps, leading to greater reduction in velocities along the weir flow paths, and therefore greater values for t_r. The larger l_h for weirs is itself due also to this divergence of flow that does not occur in the step case, which overwhelms the extra pathlength increment for steps that results from the shallower water column and hence deeper sediment upstream of the structure. Some existing studies are relevant to portions of these results. For example, Lautz and Siegel (2006) found that debris dams (weirs) were more effective at driving downwelling flux than meander bends in a real stream. Further, Kasahara and Wondzell (2003) found that steps generally induced more hyporheic exchange flow (analogous to Q_d) of shorter residence time than geomorphic features such as secondary channels and sinuosity (their Figures 5, 7, and 9). Although these results do not directly address weirs vs. steps, they seem to indicate that IGSs may induce more downwelling flux than planform features, but such a conclusion is probably premature given the full range of feature configurations and sizes were not evaluated.

2.4.4 Effect of Hydrologic and Geologic Setting

Studies of hyporheic exchange have been conducted across a range of hydrologic and geologic settings. It is likely that this variety of settings has shaped our understanding of the hyporheic zone, but its influence remains somewhat uncertain. Although we discuss each factor separately in this section, together they bear on the broader impact of setting. For example, varying stream and groundwater discharge under baseflow conditions allows us to examine the effect of not only different discharge regimes, but also the impact of seasons, climate, and climate change. Varying substrate hydraulic conductivity, together with stream

and groundwater discharge, allows us to examine the effect of land use changes like urbanization. Factors like channel slope, depth to bedrock, and substrate hydraulic conductivity relate to topographic setting. Finally, the combination of all these factors allows us to evaluate the effect of position within the stream network hierarchy. While our results are specific to weir type structures, the effect of these parameters should be relevant at some level to all IGS-induced hyporheic perturbations.

Varying in-stream baseflow discharge in this study had a relatively minor effect on hyporheic exchange (Figure 2.5). As discussed earlier, variation in Δh controls the process of hyporheic Darcy flux due to structure-induced channel steepening, backwater and/or form drag (mechanisms 1, 2, and 3 in Section 2.1.2), reflected in this case in the similarity in the shape of the relationships between these two parameters and baseflow discharge (Figure 2.13a). This minor effect implies that hyporheic exchange might not vary that much while groundwater heads and hence baseflow discharge vary throughout their annual cycles. This variation of baseflow discharge should be distinguished from discharge variation in spates, where stream stage can be temporarily elevated without commensurate increases in groundwater levels. Although discussion of the flood pulse cycle is beyond the scope of this study, others have found a more significant hyporheic effect in that situation (e.g., Saenger et al. 2005).

Background groundwater discharge had a substantial effect on all hyporheic exchange metrics that was consistent across weir heights (Figure 2.6). As groundwater discharge increased, downwelling flux rate (Q_d), hyporheic residence time (t_r), and hyporheic depth (d_h) all decreased markedly. This result is reasonable because higher groundwater discharge entails a greater rate of background upwelling within the reach which would tend to oppose

structure-induced hyporheic flux. This is consistent with Storey et al. (2003) who found that increased groundwater discharge led to decreased downwelling flux, and with Lautz and Siegel (2006) who found that increased areal recharge to groundwater (i.e. increased precipitation, which would increase background groundwater discharge rate) decreased hyporheic volume. Similarly, Cardenas and Wilson (2006) found that increasing ambient groundwater discharge decreased both exchange flux and residence time of bedform-induced subsurface flow. Taken together, these results imply that hyporheic exchange would be less prevalent in areas with strong gaining conditions (e.g., wetter climates, areas of topographic convergence) and more prevalent elsewhere.

Increases in hydraulic conductivity (K) significantly affected exchange, inducing increases in Q_d, decreases in t_r, but having little impact on d_h (Figure 2.7). The impact of K on Q_d is consistent with Darcy's Law (equation (2.1)) which indicates that Q_d is proportional to K where Δh, l_h, and A_c are constant, yielding a linear relationship. The inverse relationship between K and t_r is also expected because as Q_d increases, average linear groundwater velocity (v) increases, and t_r decreases, all else being equal. Because the sediment was homogeneous, what little variation occurred in d_h occurred at higher values of K due to stream-groundwater feedback (See section 2.2.1.2), and K had no affect on any hyporheic zone size metric for K of 10^{-5} m/s or less. These results (Figure 2.7) generally agree with those of Storey et al (2003) for downwelling flux and hyporheic depth across much of the range of K, but were more complicated for residence time, possibly because they varied other parameters between runs in addition to K (e.g., groundwater discharge). Contrary to our findings, Lautz and Siegel (2006) reported that hyporheic volume increased with K, but they defined the hyporheic zone "hydrochemically" which is dependent on transport parameters

(some of which can vary with K), and their site was heterogeneous with respect to K. Overall, our results imply that hyporheic zones in areas with coarser substrate (e.g., steep mountainous regions, glacial outwash) may have greater downwelling flux rates whereas areas with finer substrates (e.g., lower gradient plains or coastal regions) may have greater hyporheic residence times, all else being equal. Hyporheic zone size will depend on the delineation method, and the degree of substrate heterogeneity.

In general, all hyporheic exchange metrics exhibit a maximum at a channel slope of 0.005-0.01 m/m (Figure 2.8). This is true across the full range of weir heights evaluated, with the sole exception of t_r at large weir heights. As discussed earlier, variation in Δh controls the hyporheic Darcy flux processes induced by the structure (Q_d), reflected in this case in the similarity in the shape of the relationships between these two parameters and channel slope (Figure 2.13b). Minor deviations in shape between these two curves likely result from variations in the other parameters besides Δh on the right hand side of equation (2.1), but the overall correspondence confirms Δh is the primary driver. It then becomes important to understand why Δh peaks at an intermediate slope of 0.01: Δh decreases as slope decreases from 0.01 because the decreased slope decreases the Froude number further below 1 and therefore normal flow depth increases in the stream (discharge is held constant). As this occurs, the weir, which remains at constant height, becomes more drowned, decreasing Δh. On the other hand, as slope increases above 0.01, while normal depth does continue to decrease, this effect is overwhelmed by the increasing channel slope and corresponding downvalley groundwater head gradient, which progressively reduces the effective head drop by reducing the perturbation that a constant height weir can have on the subsurface flowfield. Although not evaluated in this study, it is expected that the slope at

which hyporheic exchange peaks for a given structure type and height may vary with certain conditions such as baseflow discharge and background groundwater discharge. The results for slopes less than 0.01 m/m have not, to our knowledge, been previously reported. However, the results for slopes greater than 0.01 are consistent with those of Storey et al (2003), who found that increasing channel slope surrounding a riffle from 0.01 to 0.08 m/m decreased the residence time through the riffle and decreased hyporheic depth. In addition, Gooseff et al (2006) reported that the length of the hyporheic flow cell induced by steps and riffles decreased as channel slope increased from 0.04 to 0.10 m/m in simulations of both synthetic and field profiles of streams (their Figure 4a). These results would be consistent with our results if hyporheic size decreased at the same time. On the other hand, Storey et al (2003) found little effect on downwelling flux at the head of a riffle as slope increased from 0.01 to 0.08 m/m. Overall, these results indicate that, all else being equal, hyporheic exchange is probably less prevalent in steep streams (e.g., slopes of 0.08-0.10 m/m) than in shallower ones, but more research is necessary to confirm this finding, corroborate our results at slopes less than 0.01 m/m, and determine how universally applicable they are.

Varying depth to bedrock had arguably the most complex effect on weir-induced hyporheic exchange (Figure 2.9), although all metrics increased with depth to bedrock for most structure sizes. The increase in hyporheic exchange with depth to bedrock makes sense because as depth to bedrock increases, hyporheic flow is progressively less vertically constrained, as discussed earlier. This implies that hyporheic exchange should increase in prevalence when moving from locations of shallow bedrock to areas of deeper bedrock, all else being equal (e.g., moving from steep mountainous locations to lowland areas). To our knowledge the impact of this parameter has not been isolated in previous work, and makes

our results difficult to generalize. For example, depth to bedrock was varied with stream order in Gooseff et al (2006), but not independently.

In discussing the effect of each of the setting descriptors in turn, we note that many geographic variations observed in these parameters are at least somewhat related to watershed position within the stream network hierarchy. For instance, in some cases, steep headwater areas tend to have steeper channel slopes, greater groundwater discharge, and coarser substrate relative to areas further downstream. In such cases, headwater areas should, according to our results, generally exhibit smaller hyporheic zones of shorter residence time relative to areas further downstream. In the end, however, each of these controlling factors can vary in complex ways throughout the stream network hierarchy, and broad generalizations concerning the effect of position within that hierarchy are probably premature.

2.4.5 Primary Factors Controlling Hyporheic Exchange

We did not explicitly quantify the relative impacts of each driving factor on overall hyporheic exchange. However, based on our sensitivity analysis we can conclude qualitatively that IGS size, background groundwater discharge rate, and hydraulic conductivity are most important when considering all hyporheic exchange metrics together. Somewhat less but still important are IGS type and depth to bedrock. Channel slope appears to be of low to moderate importance, and baseflow discharge was found to be relatively unimportant. These results generally agree with those of other studies. Both Kasahara and Wondzell (2003) and Lautz and Siegel (2006) indicate that structure type is important in controlling exchange. Storey et al (2003) conclude that hyporheic exchange through a riffle

is controlled primarily by head drop across the riffle (related to riffle size), sediment hydraulic conductivity, and background groundwater discharge rate (in that order), and secondarily by channel slope. Saenger et al (2005) report that *K* is more important than stream discharge for controlling hyporheic exchange flux. Finally, Woessner (2000), Cardenas et al (2004), and Salehin et al (2004) show heterogeneity to be significant, a factor that we did not address.

2.4.6 Implications for Natural Streams

Steps, impermeable weirs, and impermeable lateral structures as discussed in this study are simplifications. IGSs found in natural (i.e. minimally impacted by humans) streams are often more complex, and natural weirs (e.g., debris dams, log dams, boulder weirs) and lateral structures are of varying permeability (Manners et al. 2007). Furthermore, many of these structures induce scour of the streambed, particularly downstream of the structure. Nevertheless, this analysis provides a starting point for analyzing a wider range of IGSs. Most natural streams have IGSs, and they are constantly being formed, transformed, and destroyed. However, despite this constant change, in many natural streams, structure creation and destruction balance each other out over the long term, creating a dynamic equilibrium where IGSs are generally present. Formation and evolution mechanisms fall into two broad categories based on whether or not wood is involved in formation.

Wood-formed IGSs tend to go through a lifecycle involving a log or branch falling across a stream, or a root or previously buried log being exposed, followed by collection of leaves and other debris reducing the permeability of the IGS and forming a log dam (weir), followed by sediment accumulation behind the weir eventually transforming the weir to a

step (Manners and Doyle 2008). Lateral structures have a similar formation process although they probably become steps less frequently. Structures can be destroyed at various stages in the lifecycle, generally during spates. Specific causes include hydraulic erosion, decay of wood members, and burial by sediment. Wood-formed IGSs commonly form in forested regions, but they can also occur in prairie or desert regions where woody riparian vegetation exists. Weirs and steps can also form in the absence of wood where larger rocks back up water or capture sediment. Rock-formed IGSs are generally formed in spates when rocks are mobilized from upstream or banks by higher flows. Alluvial processes can also form IGSs from finer sediment materials (e.g., bars and riffles), and while some implications discussed here apply to bars and riffles, such structures are beyond the scope of this study. Superimposed on this formation-destruction lifecycle is the clogging cycle where fine sediments accumulate (abiotic clogging or colmation) and algae and microbes grow (biotic clogging) in the interstices of surface sediments between spates, and fine sediments are mobilized and living accretions broken up during bedload transport during spates (Saenger et al. 2005).

Hyporheic zones and their exchange metrics will evolve in parallel with these cycles. As fallen logs or exposed roots collect leaves, their induced backwater will increase, the size of the induced hyporheic flow cell and the induced Q_d will increase, while t_r will decrease (Figure 2.4). As these log dams subsequently collect sediment and evolve toward steps, their exchange metrics will likely decrease. Superimposed on this will be the effects of the clogging cycle where surface sediment K decreases between spates, reducing Q_d, increasing t_r, and possibly reducing hyporheic zone size because clogging creates spatial heterogeneity. Clogging will be greater for weirs than steps because weirs reduce in-stream velocities

upstream whereas steps do not. This would lead to increased deposition between spates and less flushing during spates for weirs. This effect may reduce the differences between weirs and steps in terms of the induced hyporheic exchange shown in Figure 2.4. However, because some weirs will become steps, trapped fines collected during the weir stage may reduce exchange during the step stage, perhaps countering this effect.

2.4.7 Implications for Stream Restoration and Watershed Planning

Ecological conditions in human-impacted streams can be improved on two scales. The first directly manipulates a stream to create a more natural form that it is hoped will improve ecological conditions. Consistent with common usage, we will describe this process as stream restoration, even though watershed planning can also improve stream conditions. The second approach, watershed planning, involves modifying larger scale land use patterns to recreate landscape processes which automatically maintain healthy streams. Stream restoration has immediate effects and can be appropriate where extreme degradation has occurred (e.g., removing a stream from a pipe, known as stream daylighting). However, its effects are local and often short lived, particularly if watershed level issues are not addressed. By contrast, watershed planning can take longer to improve in-stream conditions, but is more sustainable. Both approaches are currently necessary, and are now discussed in the context of restoring hyporheic exchange through restoring IGSs.

2.4.7.1 Stream Restoration

The stream restoration community is becoming aware of the importance of hyporheic rehabilitation (Boulton 2007), and that restoration of geomorphic form can enhance

hyporheic exchange (Doll et al. 2003) and associated ecosystem functions such as temperature moderation and nutrient processing (Jones and Mulholland 2000, Boulton et al. 1998). However, the potential efficacy of such restoration activities for hyporheic restoration is poorly understood. The analyses presented here provide the foundation necessary to understand the potential for IGSs in stream restoration projects to enhance hyporheic exchange, in terms of both site design and site selection. These concepts could be applied to a specific project in a variety of ways, including qualitative use of results presented in this study, application of standardized design guidance developed from our results, or construction of a site-specific hydraulic model. The following example design process could utilize any of these techniques. Developing design guidance from our results is a potentially useful next step, but beyond the scope of this paper.

The example of enhancing hyporheic exchange to lower peak summer stream temperatures is used to illustrate the design process and show how restoration of geomorphic form might restore hyporheic function. Although the connection between specific hyporheic exchange metrics and summer stream cooling is still the subject of much research (but see Chapter 3 of this dissertation), we assume for this exercise that increasing downwelling flux and hyporheic depth benefits stream cooling. While also significant, hyporheic residence time is ignored in this example to simplify the discussion and help focus on the general utility of this study in the design process. Based on these assumptions, our results suggest that weirs (e.g., log dams or rock weirs) are more effective than steps or lateral structures to maximize cooling. Maximizing weir height then maximizes downwelling flux and hyporheic depth (Figure 2.4) for an individual weir. Because the relationship between downwelling flux rate and weir height is linear, there is no optimum height for this hyporheic exchange

metric relative to weir cost, assuming weir cost increases with weir height. However, because hyporheic depth levels off with increasing height, an intermediate height at this break in slope could optimize hyporheic depth relative to structure height. In addition, because structure spacing also generally increases with height (for a given slope), there is probably an intermediate combination of structure height and spacing that optimizes cooling on a reach basis. Of course, other factors relevant to stream cooling need to be considered, for example that weirs may reduce in-stream velocity more than steps, leading to greater solar heating than for steps, which could negate the thermal benefit of greater downwelling flux induced by weirs (see Chapter 3).

While adding in-stream structures is relatively easy, hydrologic and geologic setting also needs to be considered, and is generally more difficult to manipulate than structure size or type. Substrate texture is perhaps the most amenable to direct control, and channel designs often specify placement of specific substrate materials. For the purposes of the example design for summer stream cooling, coarser substrate would probably be beneficial. Nevertheless, ongoing watershed level processes can cause siltation, burial, or loss of sediments whose size is incompatible with watershed conditions. Channel slope is somewhat more difficult to manipulate, although in many projects there is some flexibility in channel sinuosity, which affects channel slope. According to our results and assumptions, a slope of about 0.01 m/m or less would probably enhance summer cooling, although the effect of slope on downwelling flux and hyporheic depth may not be significant enough to justify adjusting design slope. Depth to bedrock and background groundwater discharge are even more difficult to manipulate, but some control might be possible at a particular site through selection of particular channel configurations. Avoiding areas with greater background

groundwater discharge and avoiding areas with shallow bedrock, assuming bedrock depths are known, might be beneficial to summer cooling.

Although we have discussed each controlling factor separately, all structure characteristics (e.g., size, type, and number of structures) and hydrologic and geologic setting characteristics (e.g., channel slope and depth to bedrock) collectively determine the impact that IGSs in a particular stream restoration project have on peak summer stream temperatures or any other design goal. These multiple factors needed to be optimized together rather than in isolation. Factors that are easier to manipulate become design specifications, while those that are more difficult to manipulate become site selection criteria. A detailed example of multiple parameter optimization is beyond scope of this study. Finally, the temporary nature of constructed IGSs and associated hyporheic enhancement must be acknowledged in the design process. As with naturally formed structures, functions will eventually be lost by demise of the structure itself, and may be subject to periodic clogging between spates.

2.4.7.2 Watershed Planning

The transient and local effects of direct stream intervention need to be complemented on the watershed scale by appropriate planning. In addition to determining priority areas for direct stream manipulations within a watershed (as discussed above), planning should focus on restoring or maintaining riparian-level and watershed-level land use to induce a self-sustaining process of IGS formation and their associated functions. For example, restoring riparian forests is important for restoring natural formation of wood-induced IGSs in lotic environments (Berg et al. 2003, Abbe et al. 2003, Manners and Doyle 2008), and particularly

in restoring a mixture of wood sizes needed to create woody debris jams that alter stream hydraulics in a way that increases hyporheic exchange (Manners et al. 2007).

The restoration goal from the previous section can then be applied, where we assumed summer cooling would increase with induced downwelling flux rate and hyporheic depth. If we assume that naturally formed wood-induced IGS height is roughly proportional to the largest size trees in the riparian forest, structure-induced cooling would increase with riparian forest age. However, given that hyporheic depth levels off above a certain height structure, there might be an optimum forest age if occasional forest thinning is also a desired management goal. The hydrologic and geologic setting results might then be useful for determining where in a watershed riparian restoration might most effective. For instance, areas with particularly fine sediments or steep slopes might be avoided. Similarly, agricultural or rapidly urbanizing areas might be less suitable due to higher delivery of fine sediments to waterways, whereas fully built out environments might be more suitable.

2.5 Summary and Conclusions

Hyporheic exchange is increasingly recognized as important in streams and rivers for the ecologically relevant functions it provides. The in-stream geomorphic structures (IGSs) analyzed in this study (weirs, steps, lateral structures) drive significant hyporheic exchange in streams under baseflow conditions mainly by inducing Darcy flux through both local steepening of the streambed and creating backwater behind obstructions. A multidimensional modeling approach was necessary to rigorously evaluate hyporheic response to a suite of controlling factors associated with IGSs. Sensitivity analysis results yielded many insights relevant to understanding IGSs under baseflow conditions in the

context of natural streams, and informing stream restoration and watershed planning activities. Structure size, background groundwater discharge rate, and hydraulic conductivity appear to be the most important factors controlling hyporheic exchange, followed by structure type, depth to bedrock, and channel slope. Downwelling flux rate and hyporheic zone size generally increase with structure size, while hyporheic residence time peaks at a small or intermediate size. Nonlinear elements of these trends appear to be related to how the size of the induced hyporheic flow cell increases with structure size until it is constrained by geologic, geomorphic, or hydrologic constraints. Hydrogeologic setting appears to be important, with reduced background groundwater discharge, increased depth to bedrock, and low to intermediate slopes tending to maximize hyporheic exchange, while the impact of substrate hydraulic conductivity varies depending on the exchange metric of interest. Structure types vary in their ability to induce hyporheic flow with channel spanning structures (weirs, steps) generally more effective than partially spanning structures (lateral structures), and weirs more effective than steps.

A field experiment determined that our modeling approach anticipates key trends of hyporheic response to driving factors observed in a more heterogeneous field setting, at least for one structure type. Trends observed in both field and model results appear reasonable when interpreted with simple hydraulic theory, which indicates that structures modulate hyporheic exchange mainly through their effect on head drop in the stream. While further testing of these results with field or flume studies is recommended, and additional modeling or generation of design guidance would be necessary for their application at a particular site, many lines of evidence support their basic form. This knowledge should provide key insights not only for stream restoration design, but also for broader scale planning efforts to

restore watershed conditions and processes that promote creation of in-stream geomorphic structures and associated hyporheic exchange. For example, the relationships among many controlling factors and hyporheic exchange metrics such as hyporheic residence time and hyporheic zone size are nonlinear, exhibiting breaks in slope that suggest strategies for maximizing these aspects of hyporheic exchange relative to structure installation costs during stream restoration.

Table 2.1. Parameters varied in sensitivity analysis.

Category	Parameter	Description	Base Case	Min	Max	Notes
Structure	Structure type	Step, weir, and lateral structure (Figure 2.1)	N/A	N/A	N/A	
	Structure size	Step height, s_s (Figure 2.1)	N/A	0.0 m	1.0 m (10x normal flow depth)	
		Weir height, s_w (Figure 2.1)	N/A	0.0 m	1.0 m (10x normal flow depth)	
		Lateral structure width, s_l (Figure 2.1)	N/A	0.0 m	2.7 m (90% of channel width blocked)	
Hydrology	Baseflow discharge	Baseflow discharge rate in surface stream	0.2 m^3/s	0.2 m^3/s (0.1 m normal depth)	5.0 m^3/s (0.78 m normal depth)	Used weir structure type only; Groundwater discharge held constant by raising boundary condition heads as flow depth increased with stream discharge
	Background groundwater discharge	Values at right are background groundwater discharge rates per streambed area within the patch scale area in absence of any IGS[1].	$1.8x10^{-7}$ m/s (head differential = 0.1 m)	$-4.1x10^{-9}$ m/s (head differential = 0.0 m)	$1.8x10^{-6}$ m/s (head differential = 1.0 m)	Used weir structure type only
Geology	Sediment hydraulic conductivity (K)	Homogeneous and isotropic: single *K* value for entire model domain	10^{-5} m/s (silty sand)	10^{-8} m/s (fine silt or clayey silt)	10^{-2} m/s (gravel)	Used weir structure type only
	Channel slope	Background channel slope for reach	0.01 m/m	0.001 m/m	0.1 m/m	Used weir structure type only
	Depth to bedrock	Depth from bottom of top model layer (represents bottom of in-stream structure) to no flow boundary condition at bottom of model domain	5 m	1 m	25 m	Used weir structure type only; No flow boundary condition at uniform depth throughout model

[1]This flux was varied by adjusting the constant-head boundary conditions in MODFLOW; the difference between this constant-head value and the elevation of the normal depth in the stream (head differential) is also shown at right.

Table 2.2 Hyporheic exchange metrics used to report results of modeling study.

Parameter		Dimensions	Description
Downwelling flux rate, Q_d		L^3/T	Downward flux rate of water across streambed within patch scale area; extracted from MODFLOW results by ZONEBUDGET
Hyporheic residence time, t_r		T	Travel time of MODPATH particle that originates at center* of patch scale area between when it enters and exits the groundwater model domain.
Hyporheic zone size	Hyporheic depth, d_h	L	Maximum depth the particle in MODPATH released at center* of patch scale area reaches below streambed at downstream side of the IGS; estimated from MODPLOT visualizations of hyporheic pathlines.
	Hyporheic pathlength, l_h	L	Length of subsurface flowpath of MODPATH particle released at center* of patch scale area; estimated from MODPLOT visualizations of hyporheic pathlines.
	Hyporheic volume, V_h	L^3	Product of downwelling flux rate Q_d [L^3/T] and hyporheic residence time t_r [T]; representative of the patch hyporheic scale flow cell.

*Use of particle originating at center of patch scale area approximates median value for water downwelling along centerline of channel within patch scale area.

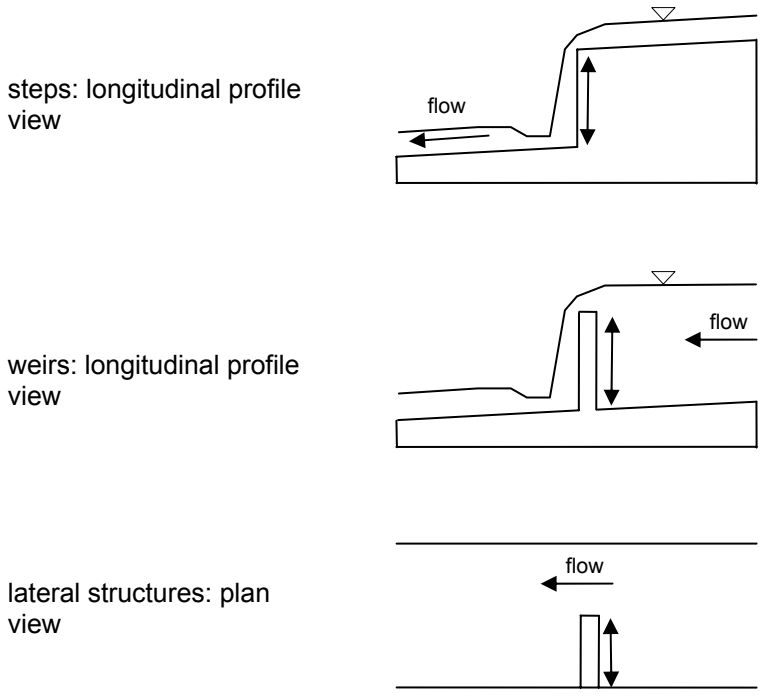

Figure 2.1 Cartoon views of in-stream structures analyzed. Double ended arrows indicate size dimension varied in sensitivity analysis.

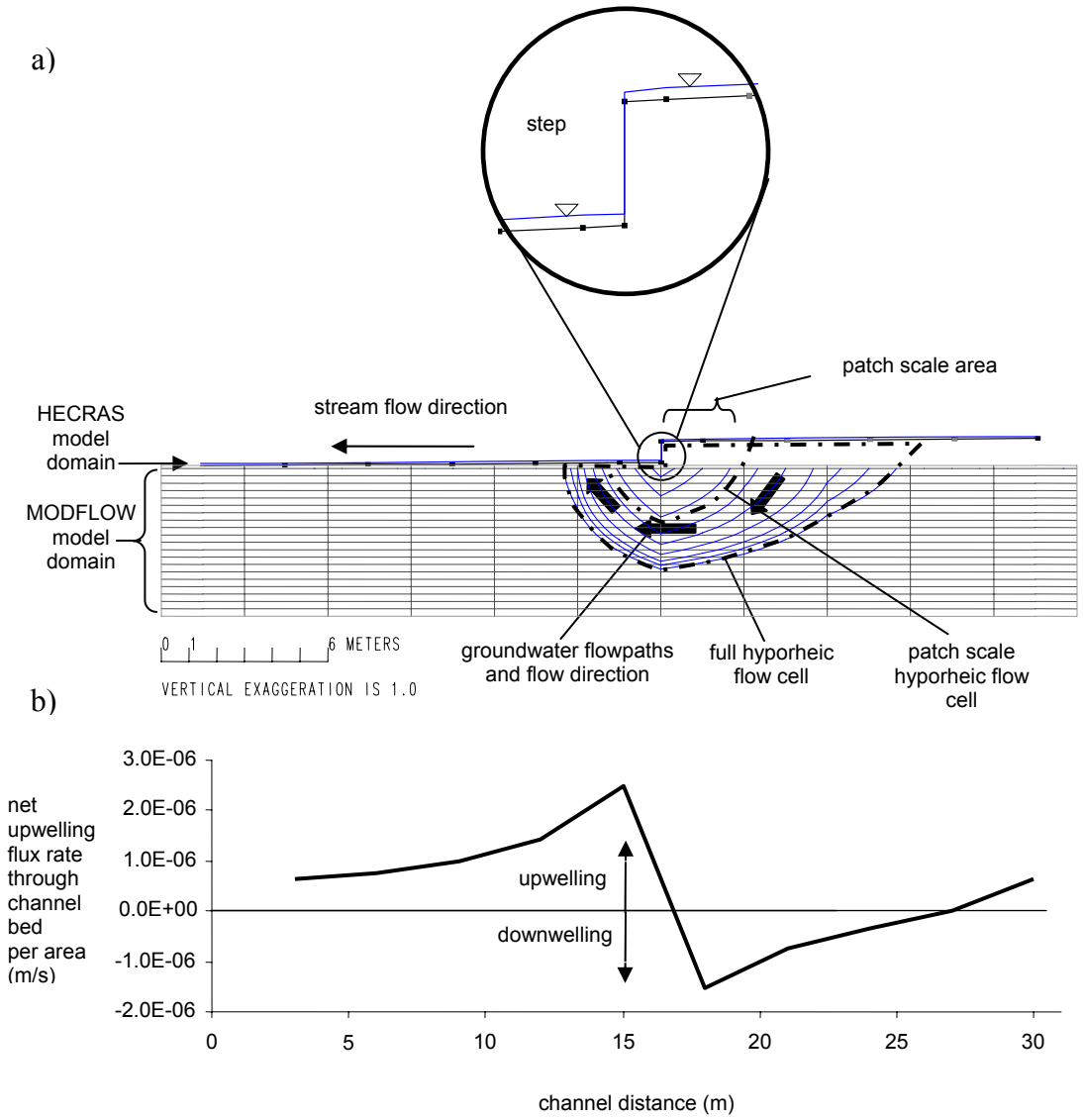

Figure 2.2 (a) Example longitudinal profile view of model of hypothetical stream showing water surface profile (from HEC-RAS) and groundwater flowpaths (from MODPATH) for a step (step height, s_s =1.0m) scenario. (b) Example longitudinal pattern of flux across the streambed (lines up with longitudinal profile in panel a).

a)

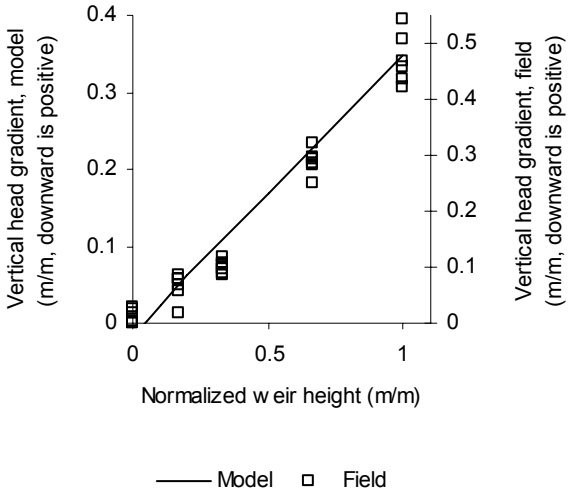

b)

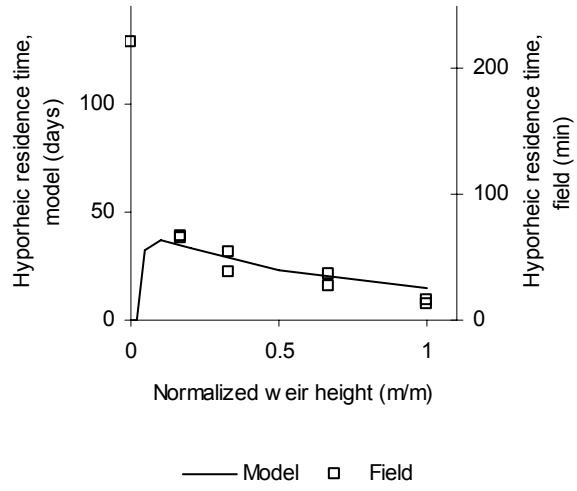

Figure 2.3 Vertical head gradient (a) and residence time (b) showing modeling (solid line) and field experiment (open squares) results. Note that y-axes are different for field and model results, and weir heights (x-axes) are normalized by maximum weir height to allow superposed presentation. This is consistent with comparing the shape (rather than magnitude) of field and model trends.

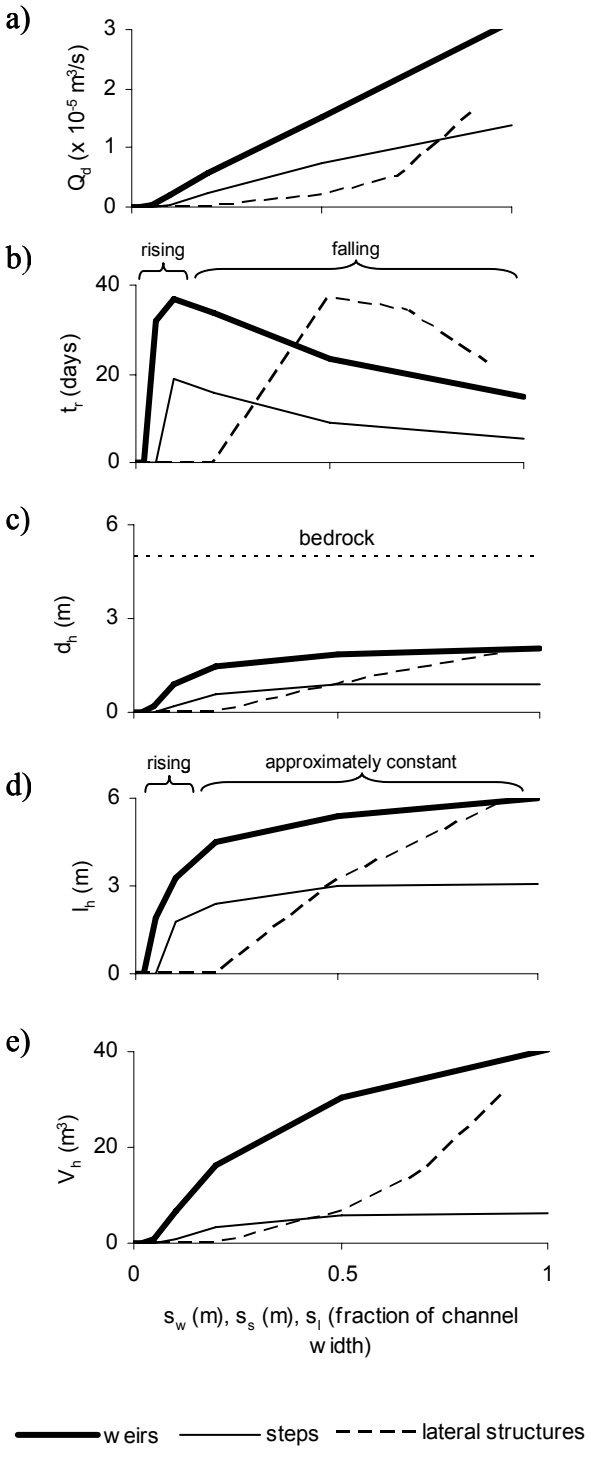

Figure 2.4 (a) Downwelling flux rate (Q_d), (b) hyporheic residence time (t_r), (c) hyporheic depth (d_h), (d) hyporheic pathlength (l_h), and (e) hyporheic volume (V_h) versus IGS size for weir, lateral structure, and step cases. All non-specified parameters are set at base case values (Table 2.1). Brackets apply only to weirs and steps. Breaks in slope occur at data points generated by individual model runs.

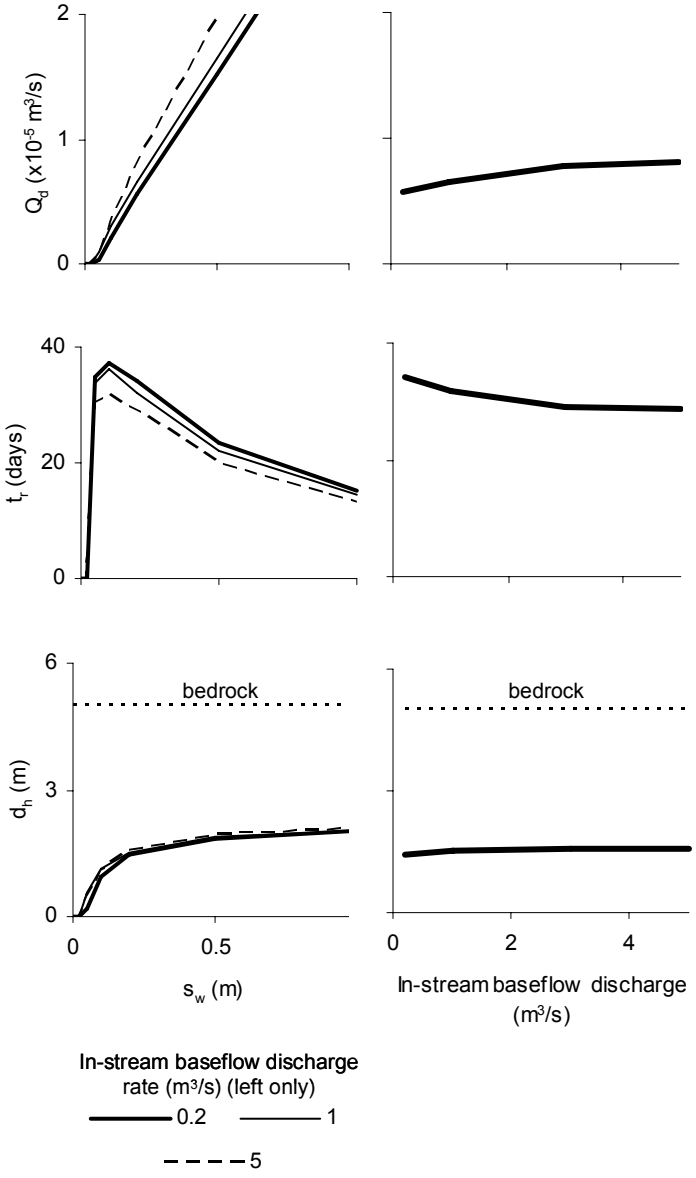

Figure 2.5 Downwelling flux rate (Q_d), hyporheic residence time (t_r), and hyporheic depth (d_h) versus weir height (s_w) for three different in-stream baseflow discharge rates (left) and versus in-stream baseflow discharge rate for s_w = 0.2m (right). Breaks in slope occur at data points generated by individual model runs.

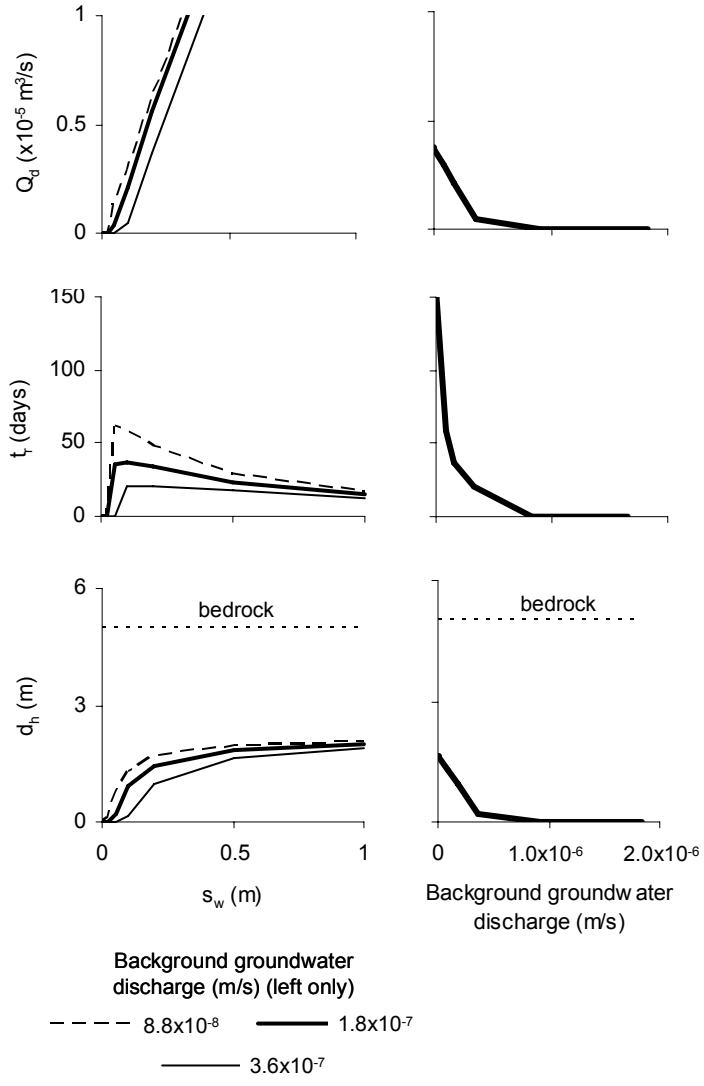

Figure 2.6 Downwelling flux rate (Q_d), hyporheic residence time (t_r), and hyporheic depth (d_h) versus weir height (s_w) for three different background groundwater discharges (left) and versus background groundwater discharge for s_w = 0.1m (right). Background groundwater discharge rate is presented on a per streambed area basis within the patch scale area, giving units of m/s. Breaks in slope occur at data points generated by individual model runs.

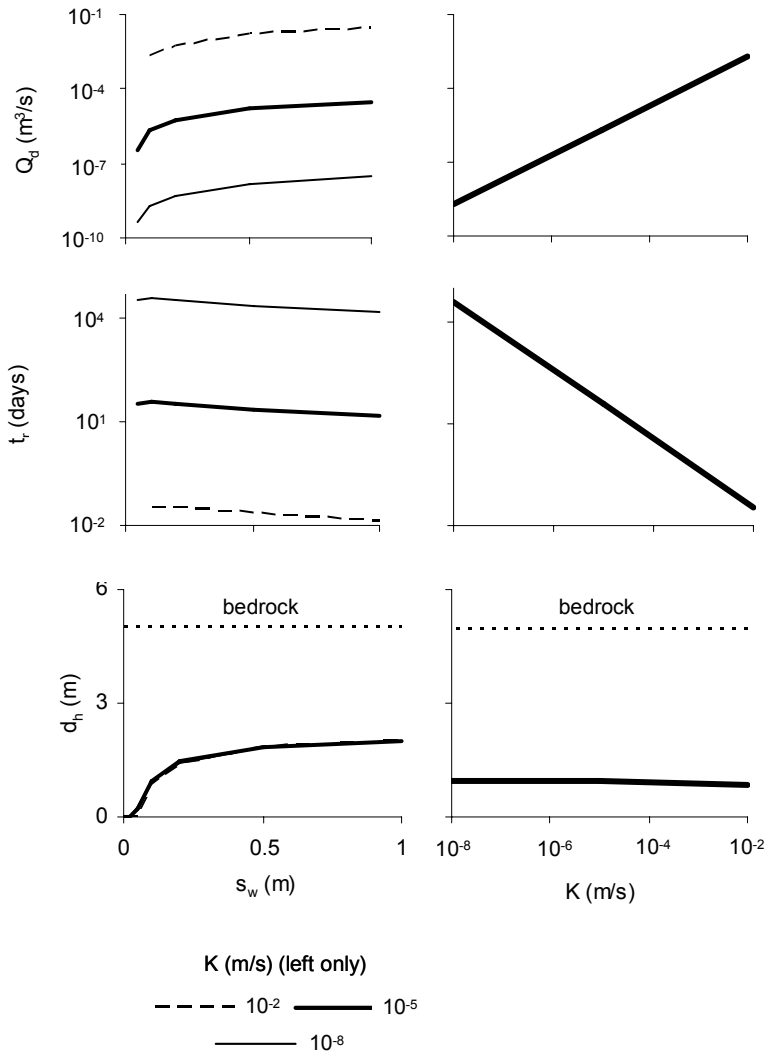

Figure 2.7 Downwelling flux rate (Q_d), hyporheic residence time (t_r), and hyporheic depth (d_h) versus weir height (s_w) for three different hydraulic conductivities (K's, left) and versus K for s_w = 0.1m (right). Several axes use logarithmic scales as K naturally varies over many orders of magnitude. Breaks in slope occur at data points generated by individual model runs.

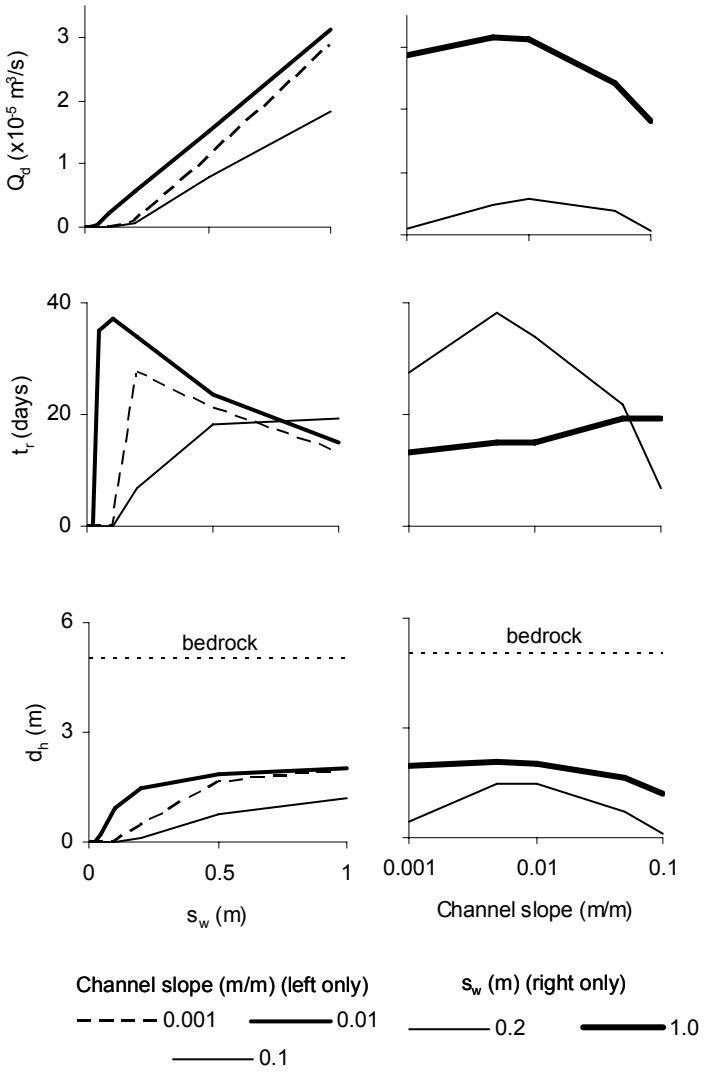

Figure 2.8 Downwelling flux rate (Q_d), hyporheic residence time (t_r), and hyporheic depth (d_h) versus weir height (s_w) for three channel slopes (left) and versus channel slope for two different weir heights (right). Channel slope axis (right) is logarithmic due to natural variability over several orders of magnitude. Breaks in slope occur at data points generated by individual model runs.

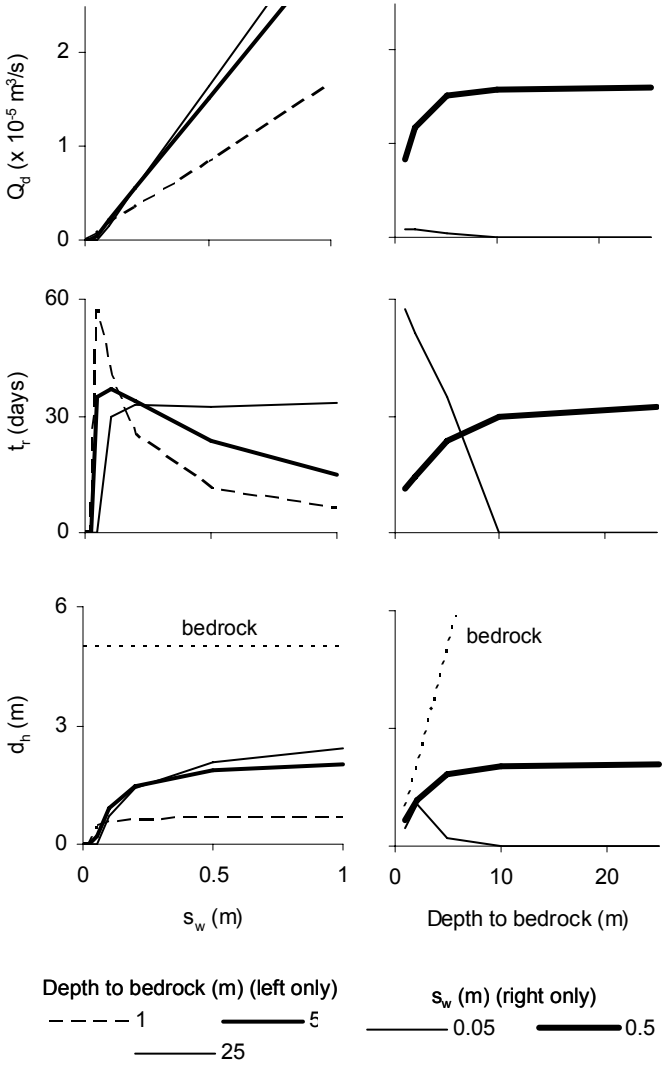

Figure 2.9 Downwelling flux rate (Q_d), hyporheic residence time (t_r), and hyporheic depth (d_h) versus weir height (s_w) for three depths to bedrock (left) and versus depth to bedrock for two different weir heights (right). Breaks in slope occur at data points generated by individual model runs.

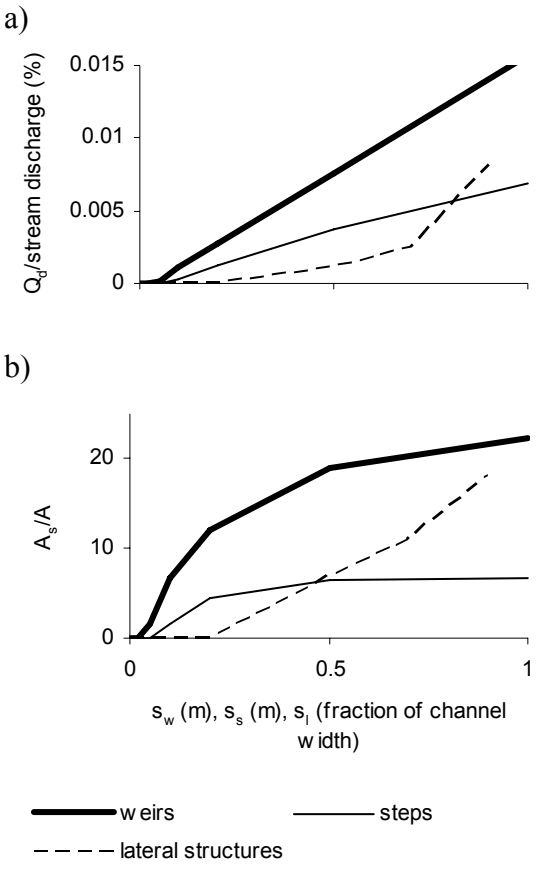

Figure 2.10 (a) Downwelling flux rate (Q_d) as percentage of in-stream discharge and (b) storage zone cross sectional area divided by stream cross sectional area (A_s/A) versus IGS size for weir, lateral structure, and step cases. Breaks in slope occur at data points generated by individual model runs.

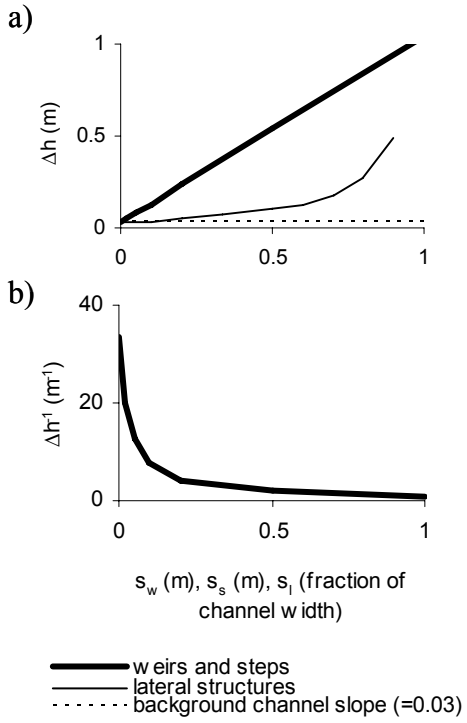

Figure 2.11 (a) Head drop across IGS (Δh) versus weir height (s_w), step height (s_s), and lateral structure width (s_l); and (b) Δh^{-1} versus height (s_w), step height (s_s). Breaks in slope occur at data points generated by individual model runs.

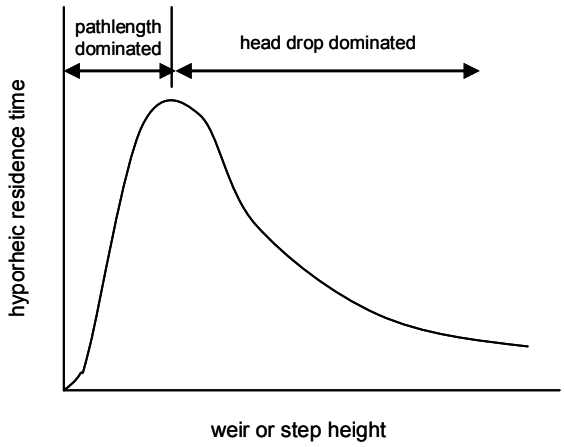

Figure 2.12 Conceptual relationship between hyporheic residence time and IGS structure size (weir and step height). Breaks in slope occur at data points generated by individual model runs.

a)

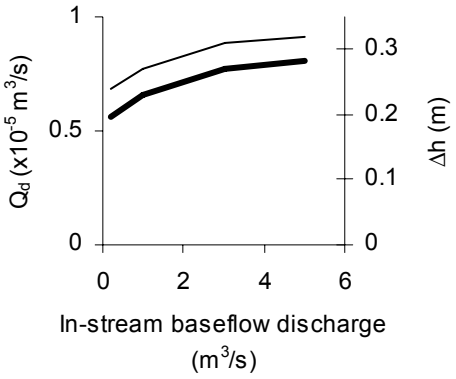

b)

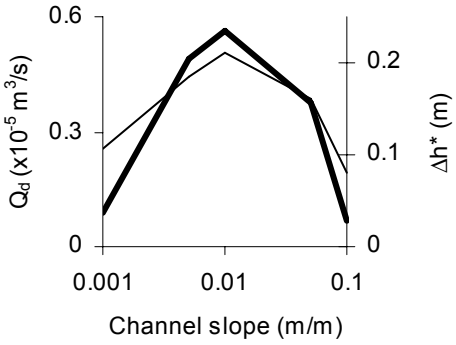

Figure 2.13 (a) Downwelling flux rate (Q_d) and (b) head drop across IGS (Δh) versus baseflow discharge and channel slope. Left y-axes show scale for Q_d and right y-axes show scale for Δh. Q_d values taken from MODFLOW results; Δh values taken from HEC-RAS results. Slope and baseflow discharge values for weir height = 0.2m. *Δh has been adjusted by subtracting that portion of Δh that is due to the channel slope itself, which does not contribute to hyporheic flow due to parallel downvalley groundwater gradients. This resulting "effective Δh" is the Δh across the structure abov e and beyond what would be there in absence of the structure. Breaks in slope occur at data points generated by individual model runs.

3 The influence of in-stream geomorphic structures on stream temperature via induced hyporheic exchange

3.1 Introduction

Temperature is the single most important condition affecting rates of both organism and ecosystem level functions (Begon et al. 2006, Brown et al. 2004). Understanding the thermal dynamics of streams is therefore important to understanding ecological stream function. In addition, organisms are adapted to the thermal regimes typically experienced in their native ranges (Hill et al. 2004, Lomolino et al. 2006), and are therefore sensitive to thermal shifts (Walther et al. 2002). Human impacts on stream temperature may therefore stress organisms and impact ecosystem function. Consequently, understanding the potential thermal impacts of geomorphic features that are common in natural streams and stream restoration projects will be useful for understanding heat dynamics in streams and assessing the ecological impact of stream restoration projects in the context of anthropogenic thermal change.

The hyporheic zone is the area of mixing of surface and groundwater beneath and adjacent to stream channels (Jones and Mulholland 2000). Exchange of water between stream channels and hyporheic zones (hyporheic exchange) facilitates ecologically and biogeochemically important exchanges of heat (Loheide and Gorelick 2006, Brunke and Gonser 1997). In-stream geomorphic structures such as steps, log dams, riffles, and gravel bars are common in natural streams and stream restoration projects, and are known to enhance hyporheic exchange (Kasahara and Wondzell 2003) by creating a hydraulic drop in

the channel, which induces curvilinear hyporheic flows paths with downward hyporheic flow upstream of the structure and upward hyporheic flow downstream of the structure (Gooseff et al. 2006, Thibodeaux and Boyle 1987, Vaux 1962). More specifically, this type of hyporheic response has been established for weir-type structures (e.g., debris dams, log dams, boulder weirs) by modeling (Chapter 2) and analogy to underflow patterns for dams (Freeze and Cherry 1979).

Previous studies have characterized the distribution of temperatures in streambed sediments (Crisp 1990, Ringler and Hall 1975), and related temperature patterns to sediment porewater movement (Silliman and Booth 1993, Hansen 1975) and heat flux (Moore et al. 2005b, Hondzo and Stefan 1994). Such patterns have also been used to distinguish areas of upward and downward hyporheic flow (Stonestrom and Constantz 2003, Lapham 1989). The connection between geomorphic form and hyporheic exchange of water and heat in streams and rivers has been well documented (Fernald et al. 2006, Poole et al. In Press, Arrigoni et al. In Press). For example, distinct water exchange patterns and associated hyporheic temperature patterns have been documented for specific types of in-stream structures like riffles (Evans and Petts 1997, White et al. 1987), dunes (Cardenas and Wilson 2007), and steps (Moore et al. 2005b). Nevertheless, we are unaware of prior studies that have experimentally manipulated in-stream structures to determine resulting effects on hyporheic temperature, heat exchange across the streambed (streambed heat flux), and surface stream temperature.

Net heat flux across the streambed induced by hyporheic water exchange (hyporheic heat advection) can moderate benthic and surface stream temperatures over diel and annual cycles (Loheide and Gorelick 2006, Lapham 1989). Relative to diel or annual temperature

cycles in the surface stream, temperature cycles in upwelling hyporheic water may have a different daily average temperature (i.e., may be cooler or warmer), a reduced diel temperature range (i.e., may be buffered) or a delayed phase (i.e., may be lagged) (Arrigoni et al. In Press). Because of the ecological importance of temperature, understanding the relationships between geomorphology and temperature will then be useful for understanding the thermal dynamics of streams and the impacts of stream restoration projects in the context of human impacts on stream temperatures. The goals of our study were therefore to determine the impact of weir-type in-stream geomorphic structure presence and size on 1) hyporheic temperature patterns, 2) structure-induced hyporheic heat advection, and 3) surface stream temperature.

3.2 Methods

3.2.1 Field Experiments

We performed field experiments during the summers of 2006 and 2007 in a 1st order headwater reach of Craig Creek in the Jefferson National Forest near Blacksburg, Virginia. The stream surface is 1-2 m wide with baseflow discharge of 0.5-5.0 L s^{-1} with hydrologically neutral to gaining (catchment groundwater typically discharges to stream channel) conditions. The reach is a fairly straight 10 m long riffle located between pools at the adjacent upstream and downstream meander bends. It has a gravel and cobble surface substrate, with increasing proportions of sand at depth.

We constructed a single, channel-spanning, variable height weir perpendicular to the channel (Figure 3.2). The weir was not keyed into the substrate and thus did not inhibit induced hyporheic flow paths beneath the structure (Chapter 2). Subsurface water levels

were measured with automatic stage recorders (Onset U20-001-01 hobos) and manual well sounder readings (using Solinst Model 101M) in a series of 6 piezometers distributed longitudinally along the centerline of the channel up- and downstream of the weir (shaded piezometers in Figure 3.2) and screened at approximately 0.23 m below the streambed surface. Water levels in the surface stream were measured along the right side of the channel with automatic stage recorders (Onset U20-001-01 hobo and Intech WT-HR 1000) installed in perforated pipes at rows 3 and 4, and with manual stage gauges located at rows 1, 2, 4, and 6 (Figure 3.2). Surface stream stages were also measured along the centerline of the channel using manual well sounder readings with the Solinst 101M on the outside of the hydraulic piezometers in rows 1 to 6 (shaded gray in Figure 3.2). Salt slug tracer injections were conducted to measure residence time of hyporheic water in the subsurface (Chapter 2) (piezometers with diagonal stripes in Figure 3.2) and surface stream discharge (Moore 2005).

Temperatures were measured with a three-dimensional array of thermochron ibutton temperature sensor-loggers (Dallas Semiconductor models DS1921-Z and DS1921-H) placed in two columns of piezometers in the streambed (white piezometers in Figure 3.2) and mounted in the surface stream both in the pool formed behind the weir, and further up- and downstream (Figure 3.2). Temperature data were calibrated using correction factors specific to each individual sensor. Correction factors were determined by noting the difference in temperature readings between each ibutton and highly accurate ASTM mercury thermometers when placed in each of several constant temperature water baths that spanned the range of temperatures observed in the field experiments. Calibration improved the accuracy of the ibutton data from +/- 1.0°C as reported by the manufacturer (http://www.ibutton.com) to approximately +/- 0.1°C (fig. 3 of Johnson et al. 2005).

3.2.2 Calculations

We used hydraulic and temperature data to estimate a variety of hydraulic and thermal quantities. Values and sources for input parameters used in the calculations are listed in Table 3.1.

3.2.2.1 Vertical Hydraulic Gradient

We calculated the vertical hydraulic gradient between the surface stream and subsurface water (i, defined as negative when downward into the streambed) [m/m] for a variety of locations as

$$i \equiv \frac{\Delta h}{\Delta z} \tag{3.1}$$

where Δh is the hydraulic head difference between the piezometer and the surface stream adjacent to the piezometer [m] and Δz is the difference in elevation between the piezometer screen and the streambed surface adjacent to the piezometer [m] (Table 3.1).

3.2.2.2 Advective Heat Flux

We estimated downward flow of water across the streambed from the surface stream into the hyporheic zone upstream of the weir [m^3/s] (downward hyporheic flow rate, Q_d) using Darcy's Law

$$Q_d = K i_d A_d \tag{3.2}$$

where K is the hydraulic conductivity of the sediments [m/s], i_d is the hydraulic gradient upstream of the weir [m/m], and A_d is the area of downward hyporheic flow across the streambed [m^2] (Table 3.1). Equation (3.2) utilized hourly hydraulic data from the first piezometer upstream of the weir (row 4 in Figure 3.2). These hydraulic data were applied to the area A_d, which extends from the weir upstream to midway between piezometer rows 4 and 5 and across the full width of the channel. We chose the area closest to the weir because hydraulic gradients were strongest there (see Section 3.3, Figure 3.3) indicating that most of the downward hyporheic flow induced by the weir occurred near the weir, regardless of weir height. Although not shown in Figure 3.3, head gradients would be even higher at the upstream face of the weir than at piezometer row 4 due to a gradient discontinuity at the weir (Chapter 2), such that piezomter row 4 is reasonably representative of area A_d.

We estimated net heat flux across the streambed due to weir-induced flow of water through the hyporheic flow cell (hyporheic heat advection, J_a) [J/s] n an hourly basis by (Moore et al. 2005b)

$$J_a = \rho_w C_w Q_d \left(T_u - T_{s1}\right) = \rho_w C_w K i_d A_d \left(T_u - T_{s1}\right) \tag{3.3}$$

where ρ_w is the density of water [kg/m^3], C_w is the specific heat of water [J/kg-ºC], T_u is the temperature of upward hyporheic flow discharging to the surface stream downstream of the weir [ºC], and T_{s1} is the temperature of surface stream water immediately above the area of downward hyporheic flow upstream of the weir [ºC] (Table 3.1, Figure 3.2). Equation (3.3) assumes that water induced into the hyporheic zone upstream of the weir in the area specified

by A_d flows downstream beneath the weir and then returns to the surface stream by upward hyporheic flow downstream of the weir in an area specified by A_u [m^2], forming a weir-induced hyporheic flow cell (Chapter 2). This assumption is an approximation, but is reasonable given the net hydrologic balance of our study reach was neutral to slightly gaining, and the exploratory nature of our analysis (Moore et al. 2005b). We were unable to measure A_u directly, but because the same hyporheic flow (Q_d) passes through both A_d and A_u, and because we assume sediment hydraulic conductivity (K) remains constant (Table 3.1), we estimate A_u as

$$A_u = A_d \frac{-i_d}{i_u} \tag{3.4}$$

where i_u is the hydraulic gradient at the end of the hyporheic flow cell (i.e., downstream of the weir) [m/m]. We estimated T_u (Table 3.1) by averaging temperatures from the two ibutton piezometer locations closest to the weir (row 3, Figure 3.2) because the greatest flow occurs in this area (see Section 3.3, Figure 3.3).

3.2.2.3 Conductive Heat Flux

We estimated the heat flux between the surface stream and subsurface water due to vertical conduction (streambed conduction, J_c) on an hourly basis [J/s] by (Moore et al. 2005b)

$$J_c = \rho_{bs} C_{bs} A_c \lambda_{bs} \frac{T_c - T_{s1,2}}{\Delta z_c} \tag{3.5}$$

where ρ_{bs} is the bulk density of saturated sand [kg/m^3], C_{bs} is the specific heat of saturated sand [J/kg-ºC], A_c is the area of the streambed of interest [m^2], λ_{bs} is the thermal diffusivity of saturated sand [m^2/s], T_c is the temperature of subsurface water at depth [ºC], $T_{s1,2}$ represents the temperature of surface stream water above the sediment [ºC], and Δz_c is the depth of the subsurface temperature measurement T_c [m] (Table 3.1, Figure 3.5a). Equation (3.5) utilized hourly temperature data to calculate streambed conduction. In order to compare estimated streambed conduction with estimated weir-induced hyporheic advection, A_c was set equal to the sum of A_d and A_u, averaged across all weir heights and both years (Table 3.1). We divided A_c into four sections (corresponding to piezometers in rows 3 and 4, left and right), calculated conduction for each section, and summed the four sections, providing the net flux rate for the area A_c.

3.2.2.4 Response of Surface Stream Temperatures

We estimated the effect of weir-induced hyporheic advection calculated by Equation (3.3) on surface stream temperatures (ΔT_a) [ºC] by (Story et al. 2003):

$$\Delta T_a = \frac{Q_d}{Q_s}\left(T_u - T_{s3}\right) = \frac{Ki_d A_d}{Q_s}\left(T_u - T_{s3}\right) \tag{3.6}$$

where Q_s is the discharge in the surface stream [m^3/s] and T_{s3} is the temperature of surface stream water upstream of the weir backwater area [ºC] (Table 3.1, Figure 3.2). Equation (3.6) estimates the influence of weir-induced hyporheic heat advection in isolation, independent of streambed heat conduction or atmospheric heat fluxes. Equation (3.6) applies to a length of

stream that includes just the hyporheic flow cell induced by the weir (i.e., encompassing A_d and A_u as defined previously), and hence no other water fluxes crossing the streambed. While J_a does not explicitly appear in Equation (3.6), its effect manifests through Q_d and T_u, which are the same for both Equation (3.3) and Equation (3.6).

3.3 Results

3.3.1 Hydraulics

In the presence of the weir, vertical hydraulic gradient (i) along the channel centerline was generally downward upstream of the weir, and upward downstream of the weir (Figure 3.3). This pattern was much weaker or non-existent in the absence of the weir. Among the representative vertical head gradient profiles in Figure 3.3, hydraulic gradient just upstream of the weir (i_d, piezometer row 4) tended to increase in magnitude with weir height to -0.50 m/m for the 22.8 cm high weir in 2006, and -0.15 m/m for 15.2 cm weir in 2007. Conversely, hydraulic gradient just downstream of the weir (i_u, piezometer row 3) reached 0.04 m/m for the 22.8 cm high weir in 2006 and the 15.2 cm weir in 2007. By comparison, in the absence of a weir, downward and upward hydraulic gradients never exceeded -0.03 m/m and 0.02 m/m, respectively, for both years combined. Because the magnitude of i_d exceeds that of i_u, A_u is larger than A_d (Equation 3.4). A_u/A_d varied considerably based on variations in weir height, surface stream discharge, and other factors, but was always 3.0 or greater. Consistent with the vertical hydraulic gradient data, diel temperature oscillations penetrated deeper into subsurface upstream of the weir than downstream of the weir whenever a weir was present, and this pattern abated in the absence of the weir (Figure 3.4).

3.3.2 Subsurface Water Temperatures

Shallow subsurface water warmed up during the afternoon with or without a weir present (Figure 3.5a, Figure 3.7). However, when a weir was present, heating extended further into subsurface upstream of the weir, creating a drop in temperature in the shallow hyporheic zone upstream (T_d, Figure 3.2) to downstream (T_u, Figure 3.2) across the weir, both during the day (up to approximately 1.5ºC, Figure 3.5a) and averaged over the diel cycle (up to approximately 0.5ºC, Figure 3.5c, Figure 3.7). Furthermore, T_u was generally cooled (lower daily average temperature, Figure 3.5c), buffered (smaller daily temperature range, Figure 3.5d), and lagged (delayed phase of temperature peaks and/or troughs, Figure 3.6) relative to T_{s1} and T_d.

3.3.3 Streambed Heat Flux

Net heat conduction across the streambed (streambed heat conduction, J_c) and net weir-induced hyporheic heat advection across the streambed (hyporheic heat advection, J_a) exhibited diel cycles in which net heat flux is from the surface stream to the subsurface (i.e., cooling effect on surface water) over much of the day and net heat flux is from the subsurface to the surface stream (i.e., warming effect on surface water) for a short period in early morning (Figure 3.8a), mirroring temperature differences between the surface stream and the subsurface (Figure 3.8b). Average daily total weir-induced hyporheic heat advection was always negative (i.e., cooling effect on surface water), and increased in magnitude with weir height (Figure 3.9a), from approximately -300 kJ/day for a 3.8 cm weir to -1600 kJ/day for a 22.8 cm weir (~450% increase) in 2006, and from approximately -300 kJ/day for a 7.6 cm weir to -1200 kJ/day for a 15.2 cm weir (~300% increase) in 2007. Using linear regression, the coefficients of determination (R^2) for daily total weir-induced hyporheic heat

advection versus weir height were 0.59 and 0.68 for the 2006 and 2007 data, respectively, and 0.59 for both years combined. The slopes of all regression lines were significantly different than zero ($p < 0.01$). The magnitude of average daily total streambed heat conduction was always greater than weir-induced hyporheic heat advection (note y-axis scales in Figure 3.9) and was similarly a consistent cooling influence on the surface stream, ranging from -3800 kJday to -7500 kJ/day in 2006, and -2700 kJ/day to -4400 kJ/day in 2007. There was not a consistent conduction response to weir height (Figure 3.9b). Using linear regression, R^2 values for daily total streambed heat conduction versus weir height were 0.46 and 0.26 for 2006 and 2007, respectively, and 0.20 for both years combined. The slopes of the regression lines were different than zero at varying levels of significance ($p<0.01$ and $p<0.1$ for the 2006 and 2007 data, respectively, and $p<0.01$ for both years combined).

3.3.4 Surface Stream Temperatures

The estimated effect of weir-induced hyporheic heat advection on surface stream temperatures (ΔT_a, Figure 3.10) followed the same diel pattern as hyporheic heat advection (Figure 3.8) with cooling over much of the day and warming in early morning (up to ~0.01ºC in magnitude). The observed temperature changes that occurred as stream water flowed across the weir were estimated as the difference between stream temperatures downstream of the weir and stream temperatures upstream of the weir's backwater (T_{s2} and T_{s3} in Figure 3.2), and were generally much greater than the estimated effect of weir-induced hyporheic heat advection, and did not appear to follow the same diel cycle except in late afternoon (up to ~0.4ºC in magnitude, Figure 3.10). The daily average effect of weir-induced hyporheic heat advection was cooling from the perspective of the surface stream, and increased in magnitude with weir height from -0.001ºC at 7.6 cm to -0.003ºC at 15.2 cm for 2007 (Figure

3.11a). In comparison, the daily average observed temperature change across the weir (T_{s2}-T_{s3}, Figure 3.2) ranged from -0.01ºC to 0.03ºC, but exhibited no discernible trend with weir height (Figure 3.11b, R^2=0.04). In addition, when a weir was present, thermal heterogeneity was observed in surface water upstream of the weir both during the day (up to ~1.0ºC, Figure 3.5a) and averaged over the diel cycle (up to ~0.5ºC, Figure 3.5c).

3.4 Discussion

3.4.1 Hydraulics

Hydraulic data collected at the site confirmed that backwater created by the weir produced a curved hyporheic flow cell (Figure 3.2) that is expected based on the literature (Freeze and Cherry 1979, see also Chapter 2 of this dissertation). The roughly vertical component of hyporheic flow at either end of the hyporheic flow cell was confirmed by longitudinal patterns of vertical head gradient along the channel centerline (Figure 3.3) which indicated downward hyporheic flow upstream of the weir and upward hyporheic flow downstream of the weir. Further, vertical subsurface water temperature profiles up- and downstream of the weir (Figure 3.4) showed deeper and shallower subsurface penetration of diel temperature oscillations, respectively, indicating areas of downward and upward hyporheic flow (Lapham 1989). The horizontal component of weir-induced hyporheic flow in the downstream direction beneath the weir was confirmed by tracer tests (Chapter 2) in which slugs of concentrated salt solution injected into subsurface water upstream of the weir were consistently detected in subsurface water downstream of the weir (see Figure 3.2 for injection and monitoring piezometer locations). Hydraulic data (Chapter 2) also indicate that downward hydraulic gradient upstream of the weir (i_d, row 4 in Figure 3.2) and therefore

downward hyporheic flow rate (Q_d, Equation (3.2)) increases consistently with weir height, which is important for interpreting weir-induced hyporheic heat advection results (below). Upwelling area (A_u) consistently greater than downwelling area (A_d) indicates divergence of hyporheic flowpaths from upstream to downstream, as expected for weir type structures (Chapter 2).

3.4.2 Temperatures and Streambed Heat Flux

Surface and subsurface water temperature patterns at our experimental site exhibited a number of important characteristics even in the absence of a weir. First, surface stream water was warmer on average than groundwater beneath, and hyporheic water showed a gradation of temperatures between the two end points (Figure 3.4, Figure 3.5c). Second, diel temperature oscillations were observed in both surface stream and subsurface water, with subsurface oscillations being buffered and lagged relative to the surface stream and with increasing depth (Figure 3.4, Figure 3.5d, Figure 3.6, Figure 3.7). This suite of summer stream temperature patterns has been widely reported (Stonestrom and Constantz 2003, Lapham 1989, Arrigoni et al. In Press) and is due to oscillation in atmospheric heating of the surface stream on annual and diel cycles, which propagates into subsurface water beneath by conduction and sometimes advection of heat across the streambed (Silliman and Booth 1993, Lapham 1989).

3.4.2.1 Effect of Weir Presence and Height

The addition of the weir to the experimental site increased average temperature in the shallow hyporheic zone upstream of the weir, creating a drop in average temperature in the

shallow hyporheic upstream to downstream across the weir (Figure 3.5c, Figure 3.7). The presence of the weir probably affected temperatures in the ecologically important (Hynes 1970) benthic zone in a similar fashion, although we did not measure temperatures in the shallowest sediments (< 10 cm depth). This hyporheic temperature modification was caused by advection of heat from the warmer (on average) surface stream through the weir-induced hyporheic flow cell. On average, hyporheic water cooled as it flowed through the hyporheic flow cell and thus imparted a cooling effect on the surface stream when the hyporheic water discharged downstream of the weir (Figure 3.9a).

The general pattern of weir-induced hyporheic temperature modifications observed at our site is consistent with a large body of literature. Surface water temperatures have been shown to propagate further into subsurface water in areas of downward hyporheic flow or groundwater recharge from surface water than in areas of upward hyporheic flow or groundwater discharge to surface water (Stonestrom and Constantz 2003, Anderson 2005, Lapham 1989). Furthermore, the observed drop in shallow hyporheic temperature downstream across the weir is consistent with other summertime studies that show similar temperature drops across steps (Moore et al. 2005b) and riffles (Hendricks and White 1991, Evans and Petts 1997, White et al. 1987). In contrast, such temperature drops are only sometimes observed at gravel bars (Fernald et al. 2006, Arrigoni et al. In Press), possibly indicating less interaction of shallow hyporheic flow paths with deeper reservoirs of cooler water or sediments (Fernald et al. 2006).

Observed temperature changes in stream water as it flowed across the weir did not indicate net cooling and were greater in magnitude than would be expected if either streambed heat conduction (J_c) or our estimate of weir-induced hyporheic heat advection (J_a)

were dominating the surface stream heat budget (Figure 3.8, Figure 3.9, Figure 3.10, Figure 3.11). Atmospheric heat flux processes (net radiation, sensible heat transfer, evaporation/condensation) across the stream surface were therefore probably responsible for the majority of observed downstream surface water temperature changes across the weir. Although we did not measure atmospheric heat flux processes, they are probably important because there appears to be significant surface heating in the pool behind the weir (Figure 3.5a). This is consistent with studies that have shown atmospheric heat flux processes to dominate the heat budgets of many streams (Webb and Zhang 2004, Brown 1969, Sinokrot and Stefan 1993), sometimes even where heat advection across the streambed is important (Evans et al. 1998, Moore et al. 2005b), and particularly where riparian shading had been removed (Johnson 2004).

While weir-induced hyporheic heat advection appeared to have a negligible impact on bulk surface water temperatures, its impact on surface water thermal heterogeneity might be important. For instance, such advection might have thermal impacts on bottom boundary layer temperatures that are greater than in the bulk flow above. In particular, cooler water upwelling downstream of the weir during the day may create a boundary layer with of a temperature significantly cooler than the bulk flow in the stream above it. Cool upwelling water may also fill depressions in the stream bottom to create pockets of cooler water. As our data do not address this question, this is an area for future research.

Weir height was positively correlated with J_a (Figure 3.9a), and therefore, with cooling effect on surface water (Figure 3.11a). Weir height explained >50% of the variation in J_a. The weir's impact on J_a was due mainly to increased weir-induced hyporheic water exchange (Q_d, Equation (3.3), see also Figure 2.3). While the magnitude of J_a is directly

dependent on the hydraulic conductivity of the sediments (K), the trend of increasing J_a with increasing weir height should be independent of K. Because the stream is hydrologically neutral to gaining, the weir-induced hyporheic flow cell may divert catchment groundwater that would otherwise discharge to the stream at that location. Our experiment does not address this issue, but it seems likely that such diverted catchment groundwater would discharge to the stream elsewhere in the reach, with minimal overall impact to this component of the stream heat budget.

J_c was also generally a cooling influence on the surface stream, was generally larger than J_a (although still within an order of magnitude), and did not exhibit a consistent response to weir height (Figure 3.9b). The lack of trend with weir height is consistent with an increase in weir height leading to an increase in mixing between the weir-induced hyporheic flow cell and cooler deeper groundwater. In contrast, if the hyporheic flow cell remained largely separate from deeper groundwater, a decrease in J_c with increasing weir height would be expected as the cooler groundwater was pushed further down into the streambed, and vertical thermal gradients consequently declined. Variation in J_c with weir height is therefore most likely due to variation in surface stream temperature due to weather variability. Our results are for a summer experiment; the relative magnitudes of J_a and J_c, as well as the trend of J_a with weir height, may vary with season.

3.4.2.2 Effect of Stream Context

Hyporheic heat advection across the streambed induced by an individual weir (J_a) caused local anomalies of subsurface water temperatures (Figure 3.5, Figure 3.7), a response that is expected to be widespread among different streams. However, in contrast with many studies that have linked hyporheic water exchange with surface stream temperature effects

(Loheide and Gorelick 2006, Moore et al. 2005b, Bilby 1984), our estimates indicate weir-induced hyporheic heat advection had negligible impact on surface stream temperature (ΔT_a, Figure 3.10, Figure 3.11).

Variation among different streams of ΔT_a induced by a given weir height (and hence the relative magnitudes of J_a and J_c) can be understood by evaluating the relative importance of the various hydrologic and geomorphic contextual parameters represented by each of the input variables in Equation (3.6). We discuss these parameters in descending order of importance. The most important parameter in controlling ΔT_a is sediment hydraulic conductivity (K, a function of sediment texture), which varies directly with ΔT_a, and can vary among streams by nearly 10 orders of magnitude, ranging from bedrock to very coarse alluvium (Freeze and Cherry 1979, Calver 2001). For J_a to dominate relative to J_c, and for ΔT_a to be ecologically relevant, it appears K would need to be at least an order of magnitude greater than estimated for our experimental site (i.e., $>\sim 10^{-3}$ m s^{-1}, corresponds to fine gravel). The effect of large variations in K among streams and rivers probably explains why hyporheic exchange and its attendant impacts as reported in some coarse-bedded rivers in western North America (Poole et al. 2006, Stanford and Gaufin 1974) are much larger than we observed, and indicates that our results might be more typical for most eastern streams and even many western streams where hyporheic zones are composed of sand or finer-grained sediment.

In most settings, the second most important parameter is surface stream discharge (Q_s), which varies inversely with ΔT_a, and can vary over at least 4 orders of magnitude between streams (Leopold and Maddock 1953), but can also vary widely among seasons and weather conditions in a given stream. Temperature differences between the surface stream

and the weir-induced hyporheic flow cell (T_u - T_{s3}) and hydraulic gradients induced by a given weir (i_d) both vary directly with ΔT_a and should vary less than an order of magnitude between streams, but also vary over time and with structure height in a given stream. Temperature differences may also vary between different structure types and shady versus sunny reaches. The area of downward hyporheic flow across the streambed (A_d) also varies directly with ΔT_a over a couple orders of magnitudes between streams. Much of this variation is due to channel width, although some may also be due to structure height.

Although streambed heat conduction (J_c) does not vary directly with K (Equation (3.5)), an increase in K would increase Q_d, which might decrease the temperature difference between the surface stream and subsurface water upstream of the weir (T_c - T_{s1}) and increase the temperature difference downstream of the weir (T_c - T_{s2}). Because J_c is a summation of conduction upstream and downstream of the weir, the effect of K on thermal gradients in these two areas may partially cancel out, with little net impact on J_c. This is an area for future research. Independent of variation in K, T_c - $T_{s1,2}$ and the area of the streambed of interest (A_c, in terms of channel width) are the only parameters in Equation (3.5) that vary considerably between streams, and such variations influence J_a in much the same way they influence J_c. For this reason, sediment texture, through its wide natural variability and control of K, is the primary control on the relative magnitudes of J_a and J_c (Cardenas and Wilson 2007). Therefore, while J_a and J_c happen to be of a similar order-of-magnitude in our study (Figure 3.8a), their relative magnitude could vary markedly between sites.

Our experiments only address a single isolated geomorphic structure. However, such structures always exist within a reach context. It is therefore interesting to consider whether any reach scale thermal impacts accrue to a series of weirs. Our data do not directly address

this question, but some insight comes from Figure 3.10a, which indicates that water flowing across the structure, averaged across a typical day, has little impact on surface water temperatures. This indicates there would probably be little cumulative average thermal impact of weir-induced hyporheic advection on the reach scale. Nevertheless, periods of warming and cooling that typically occur around noon and late afternoon, respectively (Figure 3.10a), may have a temporary cumulative impact on reach temperatures. The occurance and significance of such a cumulative impact depends on the spacing of the structures and the nature of atmospheric heat fluxes. The greater the atmospheric heat exchange, or the more widely spaced the structures, the more likely surface stream water flowing over a given structure will return to thermal equilibrium with the atmosphere before it encounters the next structure downstream. If the stream returns to equilibrium between structures, cumulative impacts will not occur. These concepts apply not only to the net thermal impact of the structure (as discussed above), but also to any particular heat flux process going on at the structure, such as the hyporheic heat advection induced by the structure.

3.4.2.3 Parameter Uncertainty

The degree of uncertainty associated with each of the input parameters in Equations (3.1-3.6) varies widely among the parameters, and this has important implications for the conclusions presented in this paper. Sediment hydraulic conductivity (K) is highly heterogeneous in streambeds (Cardenas and Zlotnik 2003) and the falling head tests used in this study measure K only in relatively small areas in the vicinity of the test piezometer. Further, K can vary over many orders of magnitude (Freeze and Cherry 1979, Calver 2001),

and is therefore by far the most uncertain parameter in our calculations, and the only one that can affect our conclusions which rest on the magnitude of weir-induced hyporheic heat advection (J_a, Figure 3.8a, Figure 3.10). If our estimate of K were off by an order of magnitude, our estimate of weir-induced hyporheic heat advection induced by the weir would be off by the same factor (Equation (3.3)). Regardless of the direction of the error, the magnitude of the error would invalidate the conclusion that streambed heat conduction (J_c) and J_a are of similar magnitude (Figure 3.8a). Further, the conclusion that weir-induced hyporheic advective impact on surface stream temperature (ΔT_a) is negligible (Figure 3.10) would be invalidated if K was underestimated by an order of magnitude. ΔT_a would increase by a factor of 10 to peak at approximately 0.1ºC rather than 0.01ºC (Figure 3.10), which has potential to be important both in terms of the surface stream heat budget and ecologically. In fact, the period of greatest observed cooling as water flows across the weir (late afternoon daily, Figure 3.10a) coincides with the period of greatest hyporheic advective impact of the weir (late afternoon daily, Figure 3.10b). It is therefore possible that averaged across a daily cycle, the hyporheic cooling induced by the structure is balancing out the heat due to insolation and other atmospheric heat flux processes, and that the hyporheic impact of the weir is greater than we estimate. Without atmospheric measurements we cannot resolve this question, which remains ripe for future research.

In contrast to K, all other sources of uncertainty in Equations (3.1-3.6) (e.g., that associated with methods for estimating upwelling area (A_u) from downwelling area (A_d), choice of piezometer locations used to represent hydraulic gradient or temperature, and methods for measuring surface stream discharge) are far smaller than that for K (i.e., less than an order of magnitude) and consequently would not affect those conclusions which rest

on the order of magnitude of weir-induced hyporheic heat advection. Finally, none of the input parameter uncertainty has the potential to affect our conclusions that are based on temperature or hydraulic head patterns (Figure 3.3, Figure 3.4, Figure 3.5, Figure 3.6, Figure 3.7, Figure 3.8b, Figure 3.11b) or trends of response to weir height (Figure 3.9, Figure 3.11a).

3.4.2.4 Ecological Significance

The impacts of in-stream geomorphic structures on stream temperature presented in this chapter help us understand one way in which these common structures may affect ecological stream function in summer. For instance, thermal heterogeneity induced in the shallow hyporheic zone (and therefore benthic zone) by hyporheic advection induced by our experimental weir (up to ~1.5ºC, Figure 3.5, Figure 3.7), may be large enough to have direct ecological consequences. Similarly, thermal heterogeneity induced in the surface stream by increased atmospheric heat fluxes with the backwater behind the weir (up to ~1.0ºC, Figure 3.5), may also be important (although this would be less important for structures such as steps which do not create backwater). On the other hand, the thermal impact of hyporheic heat advection induced by our single experimental structure on bulk summer surface stream temperatures (<0.01ºC, Figure 3.10), as estimated in this study, would be negligible. Nevertheless, the effect of weir-induced hyporheic advection on the temperature of certain parts of the surface stream water column such as bottom boundary layers and depressions in the streambed (e.g., pools), may be more important, even in sandy sediments like those at our site. These conclusions may vary among streams and seasons, particularly the hyporheic effect on surface stream temperatures which could vary widely with sediment hydraulic

conductivity. As discussed previously, the significance of cumulative reach-scale hyporheic impact of multiple structures may be greater than for a single structure.

Organisms are adapted to the thermal regimes typically experienced in their native ranges (Hill et al. 2004, Lomolino et al. 2006), and are therefore sensitive to human-induced thermal shifts (Walther et al. 2002). Humans can impact stream temperature in many important ways, most of which increase average stream temperatures, particularly in summer (see Chapter 4). Thermal effects of structure-induced hyporheic exchange may therefore prove beneficial in helping mitigate human-induced thermal stress in streams. Enhanced thermal heterogeneity induced by structures in both the hyporheic zone and the water column may provide cool summer thermal refugia for organisms in living in streams that have warmed due to human activities. For example, cooler boundary layers and pool bottoms may provide thermal protection for periphyton, benthic macroinvertebrates, and possibly even small fish. Cooler patches of the hyporheic zone may provide refugia for benthic or hyporheic microbes and meiofauna, as well as fish eggs. Furthermore, in settings where structure-induced hyporheic exchange has significant impact on bulk surface stream temperatures (e.g., coarse streambeds), moderation of daily or annual peak temperatures may help buffer stream temperatures against human activities. Finally, the impact of structures on both groundwater and surface water temperatures should also affect the rates of biogeochemical processes occurring in those areas, as many such processes are strongly temperature dependent (Westrich and Berner 1988, Nimick et al. 2003).

Table 3.1 Values and sources for input parameters used in hydraulic and thermal calculations.

Parameter	Symbol	Units	Value	Source
Area of streambed where weir-induced hyporheic flow enters subsurface upstream of weir	A_d	m^2	0.99 (2006) 1.07 (2007)*	measured
Area of streambed where weir-induced hyporheic flow discharges to surface stream downstream of weir	A_u	m^2	6.5	estimated using Equation (3.4), averaged across both years
Area of streambed used for streambed conduction heat flux calculations	A_c	m^2	7.5	sum of A_d and A_u averaged across both years
Specific heat of sand and water, bulk	C_{bs}	J/(kg-ºC)	1372	(Jobson 1977)
Specific heat of water	C_w	J/(kg-ºC)	4187	(Lindeburg 2001)
Hydraulic head difference between surface stream and subsurface water	Δh	m	varies hourly, multiple locations	measured
Estimated vertical hydraulic conductivity of sediments in area used for Equation (3.3)	K	m/s	1.39×10^{-5} (2006) 4.54×10^{-5} (2007)	geometric mean of horizontal hydraulic conductivities measured by falling head tests in streambed piezometers; divided by 2 for vertical:horizontal anisotropy (reasonable for shallow sediments in active channel)
Downward hyporheic flow rate	Q_d	m^3/s	varies hourly	estimated using Equation (3.2)
Surface stream discharge	Q_s	m^3/s	varies hourly	measured
Temperature of subsurface water at conduction depth	T_c	ºC	varies hourly, multiple locations	measured, used deepest ibuttons available at each location
Temperature of surface stream water immediately above the area of downward hyporheic flow upstream of the weir (marked by square and "T_{s1}" in Figure 3.5a)	T_{s1}	ºC	varies hourly	measured
Temperature of surface stream water downstream of the weir (marked by square and "T_{s2}" in Figure 3.5a)	T_{s2}	ºC	varies hourly	measured
Temperature of surface stream water upstream of the weir backwater (marked by square and "T_{s3}" in Figure 3.5a)	T_{s3}	ºC	varies hourly	measured

Parameter	Symbol	Units	Value	Source
Temperature of upward hyporheic flow downstream of weir (marked by square and "T_u" in Figure 3.5a)	T_u	ºC	varies hourly, multiple locations	measured
Depth of piezometer screen used for estimating vertical hydraulic gradient	Δz	m	0.23 (2006) 0.235 (2007)	measured
Vertical distance between conduction depth and sediment surface	Δz_c	m	multiple locations and years; 0.435m - 0.575m	measured
Thermal diffusivity of sand and water, bulk	λ_{bs}	m^2/s	$7.7x10^{-7}$	(Jobson 1977)
Density of water	ρ_w	kg/m^3	1000	(Lindeburg 2001)
Bulk density of sand and water, average density, mixed grain size	ρ_{bs}	kg/m^3	2075	(Lindeburg 2001)

* channel was slightly wider and sediments slightly more hydraulically conductive in 2007 than in 2006 due to effects of intervening winter storms

Figure 3.1 View of field site, looking downstream, showing piezometers, and with location of weir shown by board across stream at center of photograph.

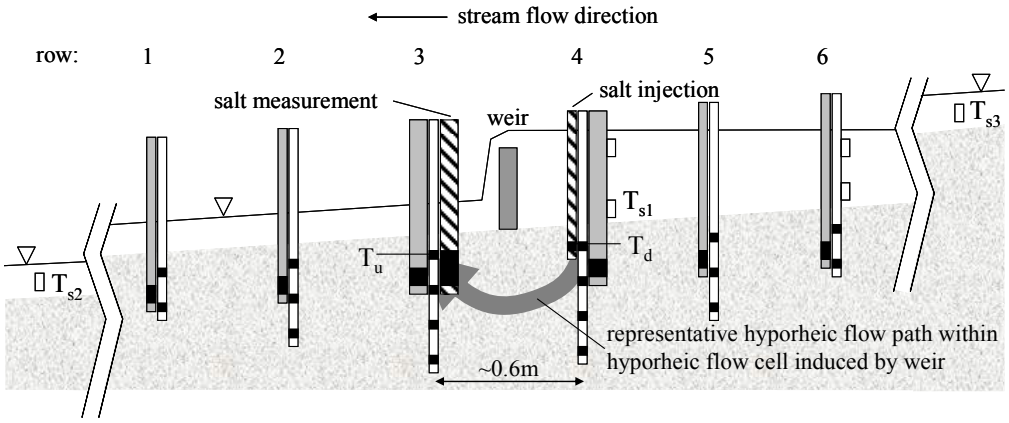

Figure 3.2 Schematic showing longitudinal arrangement of piezometers. Piezometers shaded gray were used for measuring hydraulic head along centerline of channel. Piezometers shown in white were used for measuring temperature in two longitudinal columns, one each approximately 0.23 m to the left and right of the central column of hydraulic piezometers (only one column of temperature piezometers shown). Areas shaded black indicate piezometer screen locations. Temperature sensors (ibuttons) were located at each well screen shown, with baffles inserted between sensors to isolate the water in each piezometer in vertical intervals. Piezometers shaded with diagonal stripes were used for injection of salt solution into the hyporheic zone upstream of the weir and measurement of the salt breakthrough curve using a conductivity logger downstream of the weir. Temperature sensor locations in the surface stream are indicated by open rectangles. Water surface is indicated by inverted triangles.

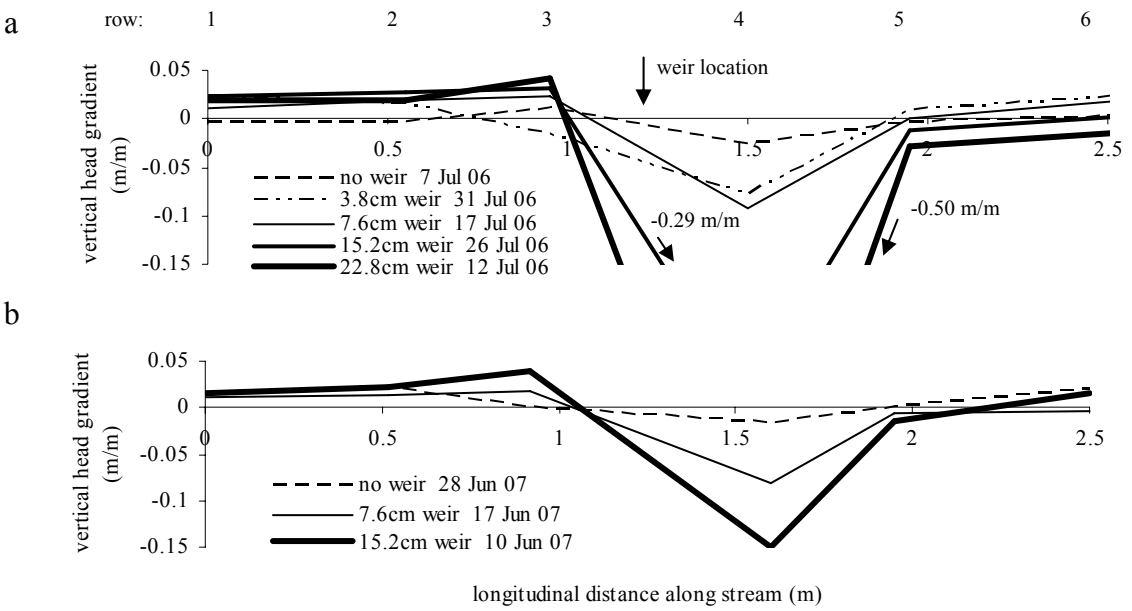

Figure 3.3 Representative longitudinal profiles of channel center vertical hydraulic gradients between surface stream and subsurface water for 2006 (a) and 2007 (b). Row numbers indicate piezometers rows as in Figure 3.2.

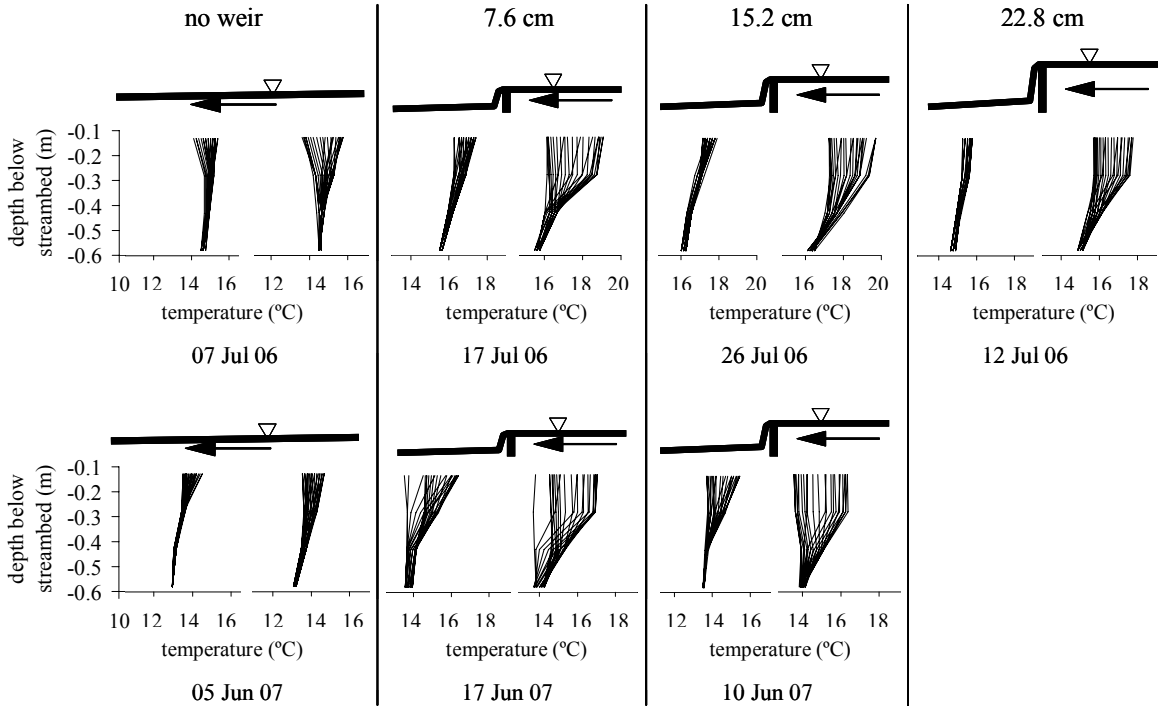

Figure 3.4 Profiles of subsurface water temperature versus depth below streambed for the 24-hour periods beginning at 10:00 h on the dates shown. Each profile contains separate lines for each of 24 separate hourly intervals spanning the day specified. Left and right profiles for each weir height and year combination are for downstream (row 3 in Figure 3.2) and upstream (row 4 in Figure 3.2) of the weir, respectively. Corresponding weir heights are shown across the top. Results from 2006 and 2007 are shown in the first and second row of the figure, respectively. Longitudinal water surface schematics immediately above each plot are for visual orientation and are not to scale (inverted triangles indicate water surface, arrows indicate direction of flow). Plots shown are for left-hand column of temperature piezometers (see Figure 3.2); results for right-hand column are similar but not shown.

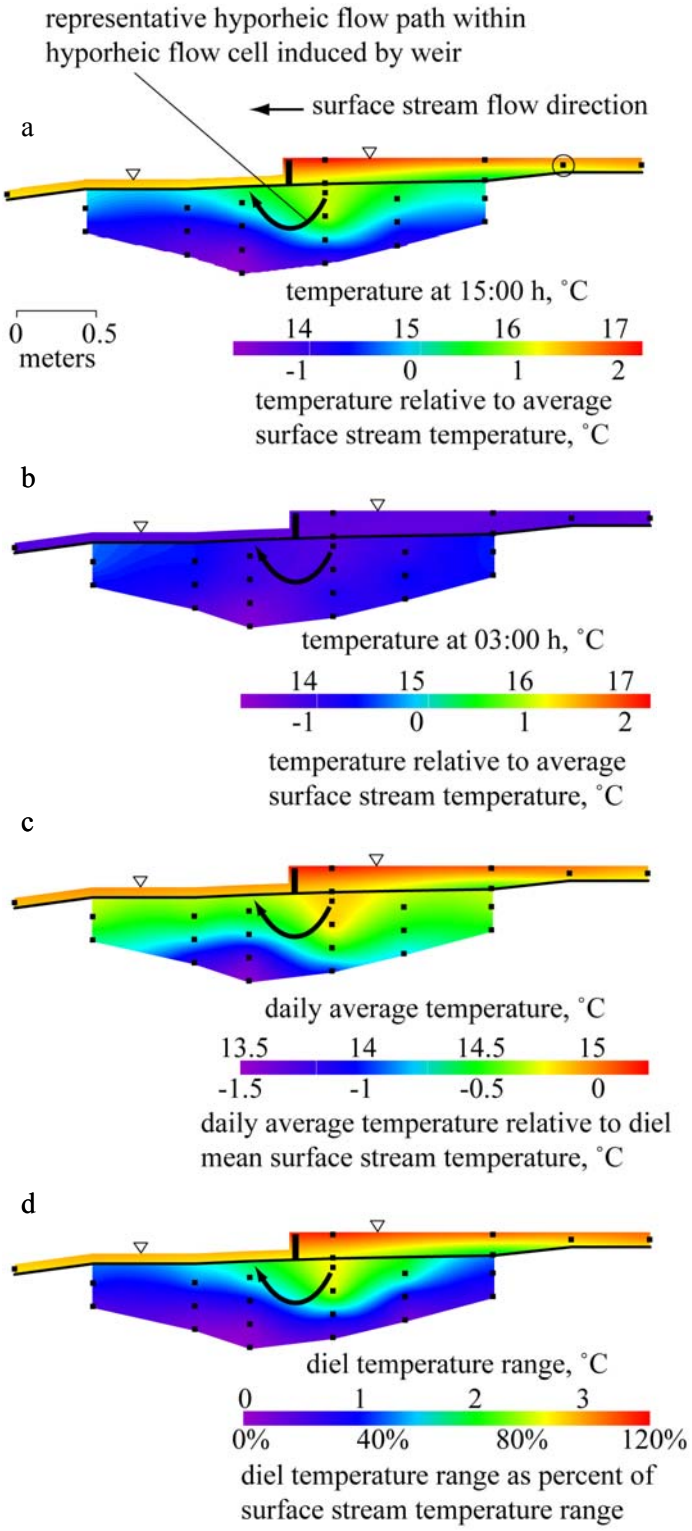

Figure 3.5 Example longitudinal vertical slices through subsurface and surface water temperature data for 15.2 cm weir on representative day (10 June 2007). Shown are temperatures at (a) 15:00 h, (b) 03:00 h the next morning, (c) daily average temperature, and (d) diel temperature range. Relative temperature scales beneath color bars are relative to temperatures (panels a, b), daily average temperatures (panel c), or diel temperature ranges (panel d) for surface stream location marked by open circle in panel a. Filled squares show locations of ibutton sensors; inverted triangles indicate water surface. Subsurface ibuttons were for left column of ibuttons (see Methods, Figure 3.2) due to more complete data set. The surface water ibutton locations downstream and upstream of the hyporheic zone measurements are not shown to scale (horizontal scale is compressed relative to rest of figure). Plots created using Surfer with kriging interpolation using default settings.

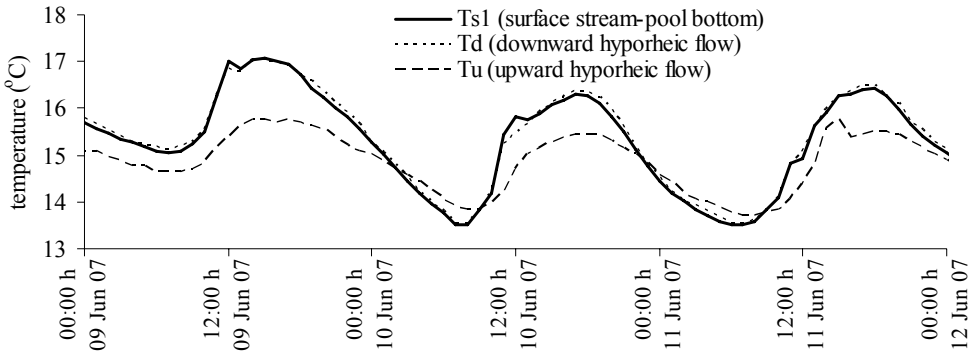

Figure 3.6 Example hourly temperatures at beginning (downward hyporheic flow, T_d) and end (upward hyporheic flow, T_u) of weir-induced hyporheic flow cell, and at bottom of pool behind weir (T_{s1}) for 15.2 cm weir scenario in 2007. Locations are shown in Figure 3.2.

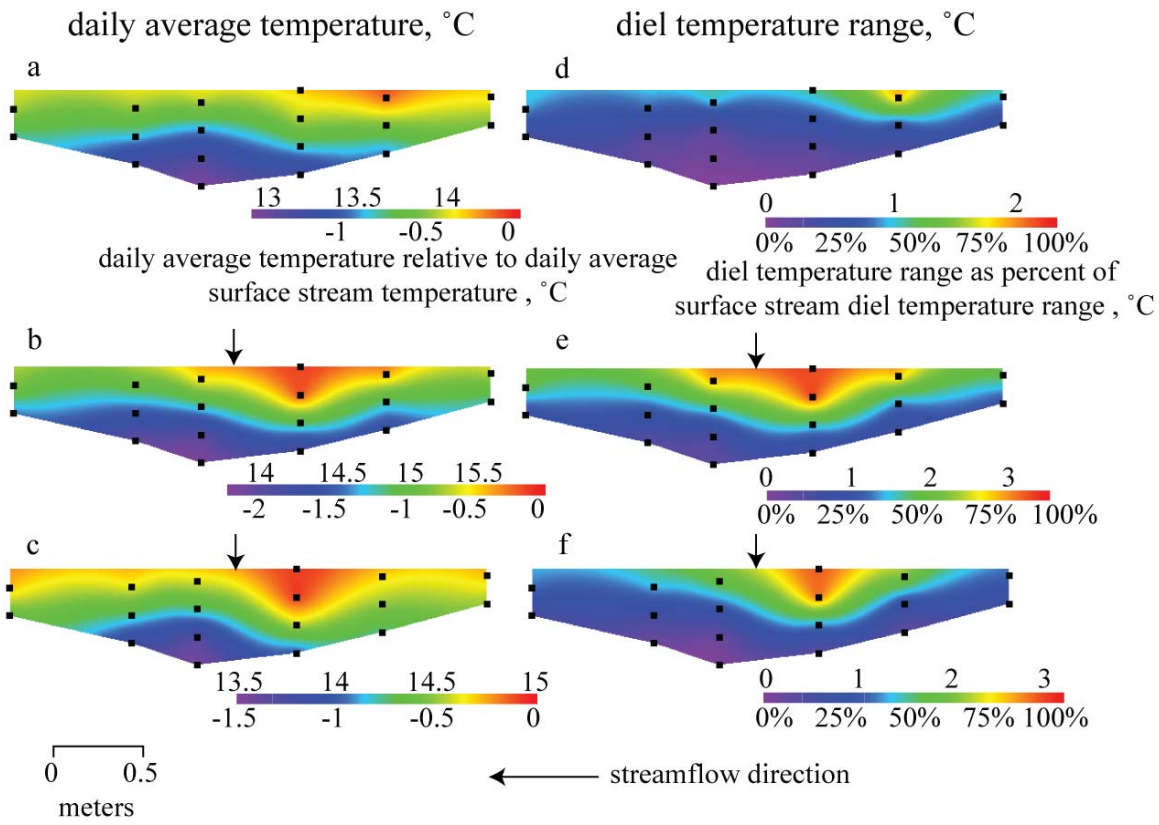

Figure 3.7 Longitudinal vertical slices through subsurface water temperature data showing daily average temperature for (a) no weir, (b) 7.6 cm weir, and (c) 15.2 cm weir and diel temperature range for (d) no weir, (e) 7.6 cm weir, and (f) 15.2 cm weir. Data shown are for representative dates within each weir height experimental period in 2007 (05 Jun 07 for panels a and d, 17 Jun 07 for panels b and e, and 10 Jun 07 for panels c and f). Patterns in 2006 data (not shown) are similar. Arrows show location of weir; filled squares show locations of ibutton sensors. Relative temperature scales beneath color bars are relative to daily average temperatures (panels a, b, c) or diel temperature ranges (panels d, e, f) for surface stream location marked by circle in Figure 3.5a. Data are from left column of ibuttons (see Methods, Figure 3.2) due to more complete data set. Plots created using Surfer with kriging interpolation using default settings.

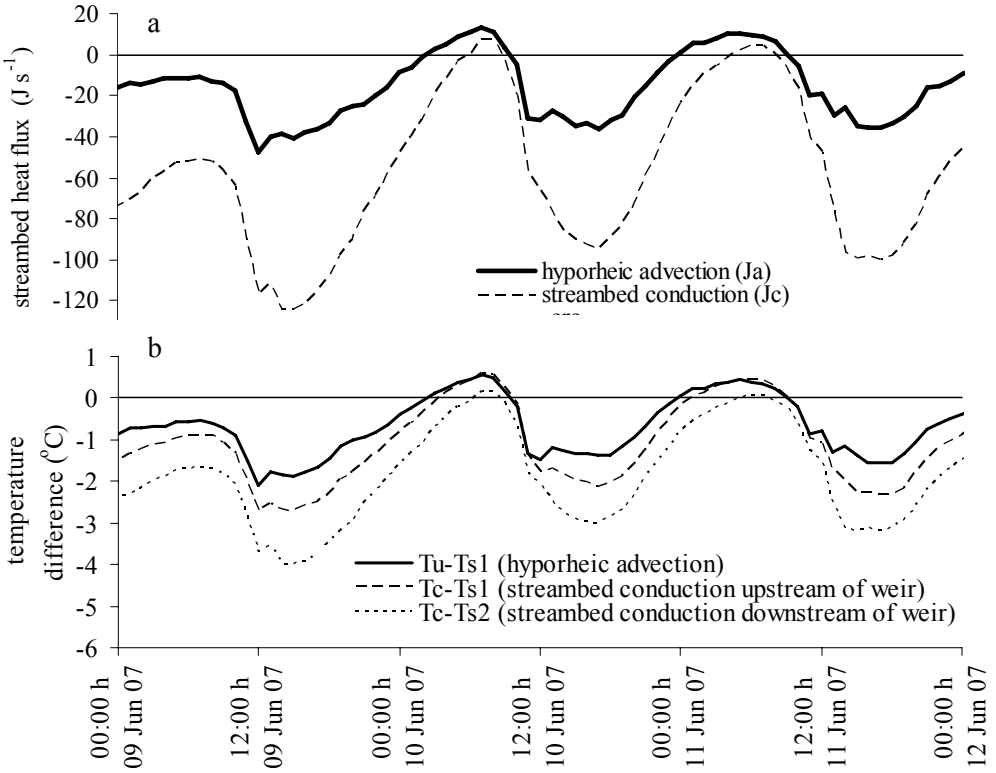

Figure 3.8 (a) Example hourly net streambed heat fluxes (net streambed heat conduction, J_c, and net weir-induced hyporheic heat advection, J_a) for 15.2 cm weir, and (b) example hourly temperature differences used in streambed heat conduction and weir-induced hyporheic heat advection calculations. Net heat fluxes are from perspective of surface stream, so negative values indicate cooling of the surface stream and corresponding warming of the subsurface.

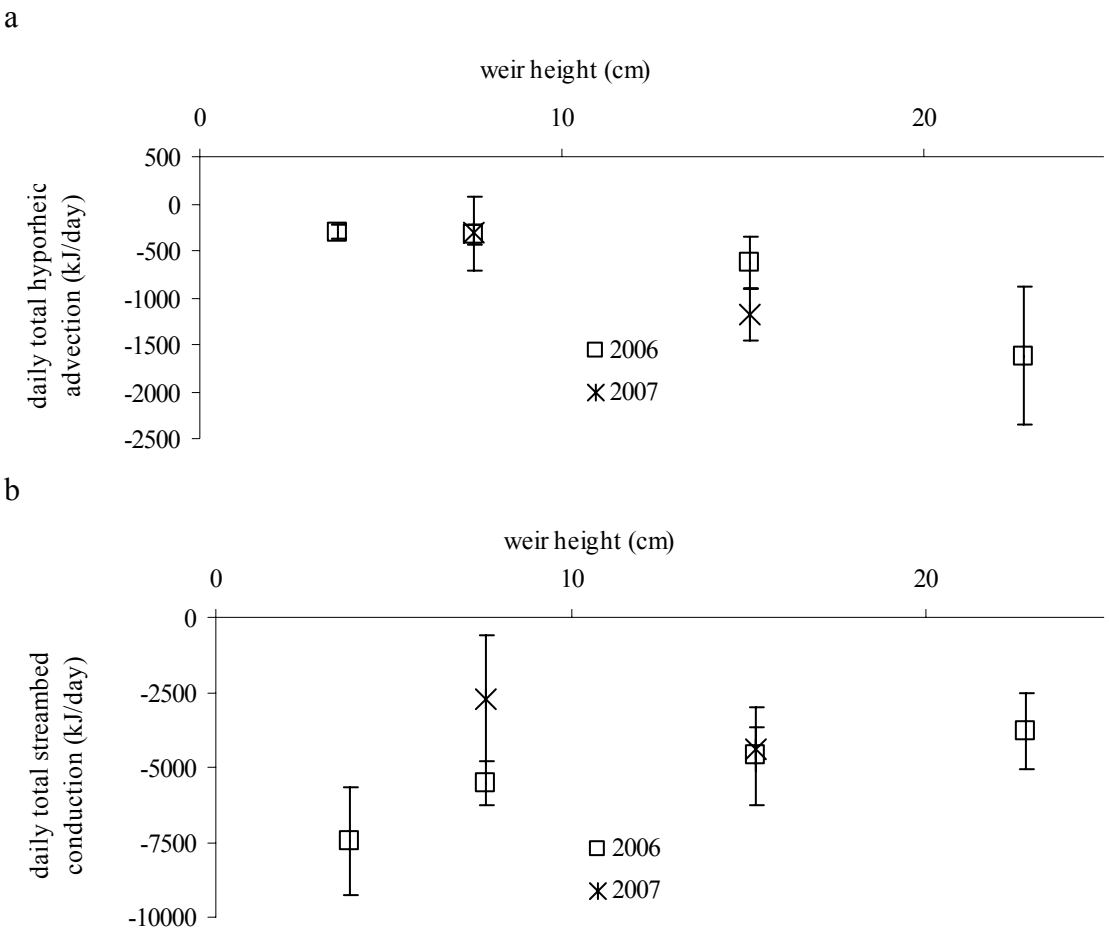

Figure 3.9 Daily total streambed heat flux versus weir height: (a) net weir-induced hyporheic heat advection, J_a, and (b) net streambed heat conduction, J_c. Boxes and whiskers represent averages and standard deviations, respectively, of the daily total fluxes for entire period that weir was at the given height. Net heat fluxes are from perspective of surface stream, so negative values indicate cooling of the surface stream and corresponding warming of the subsurface. Note difference in y-axis scales between panels a and b.

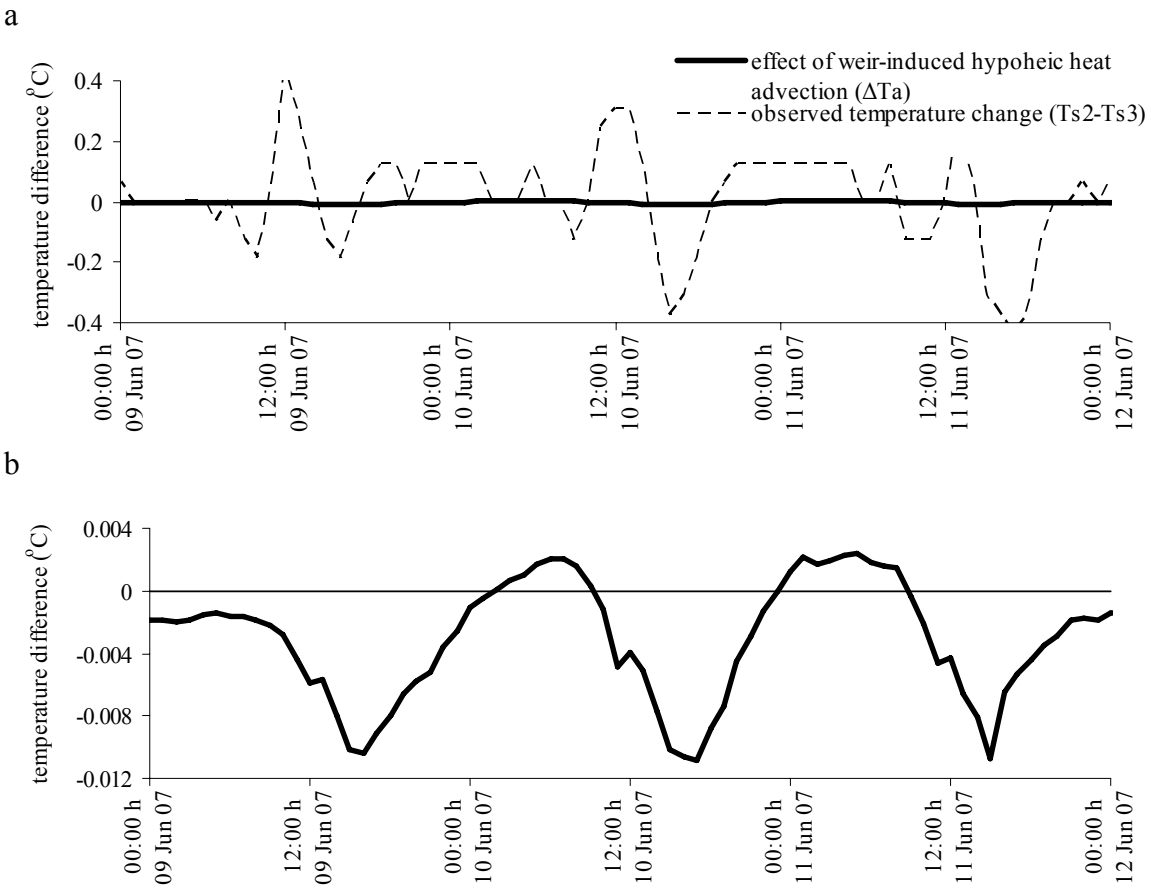

Figure 3.10 Example measured temperature change of surface stream water upstream to downstream across weir (T_{s2}-T_{s3}, Figure 3.5a, panel a), and estimated impact of weir-induced hyporheic heat advection on surface stream temperature (ΔT_a, panels a and b). Discretization of measured temperature change in panel a is due to resolution of the sensors (0.125°C). Note difference in y-axis scales between panel a and panel b.

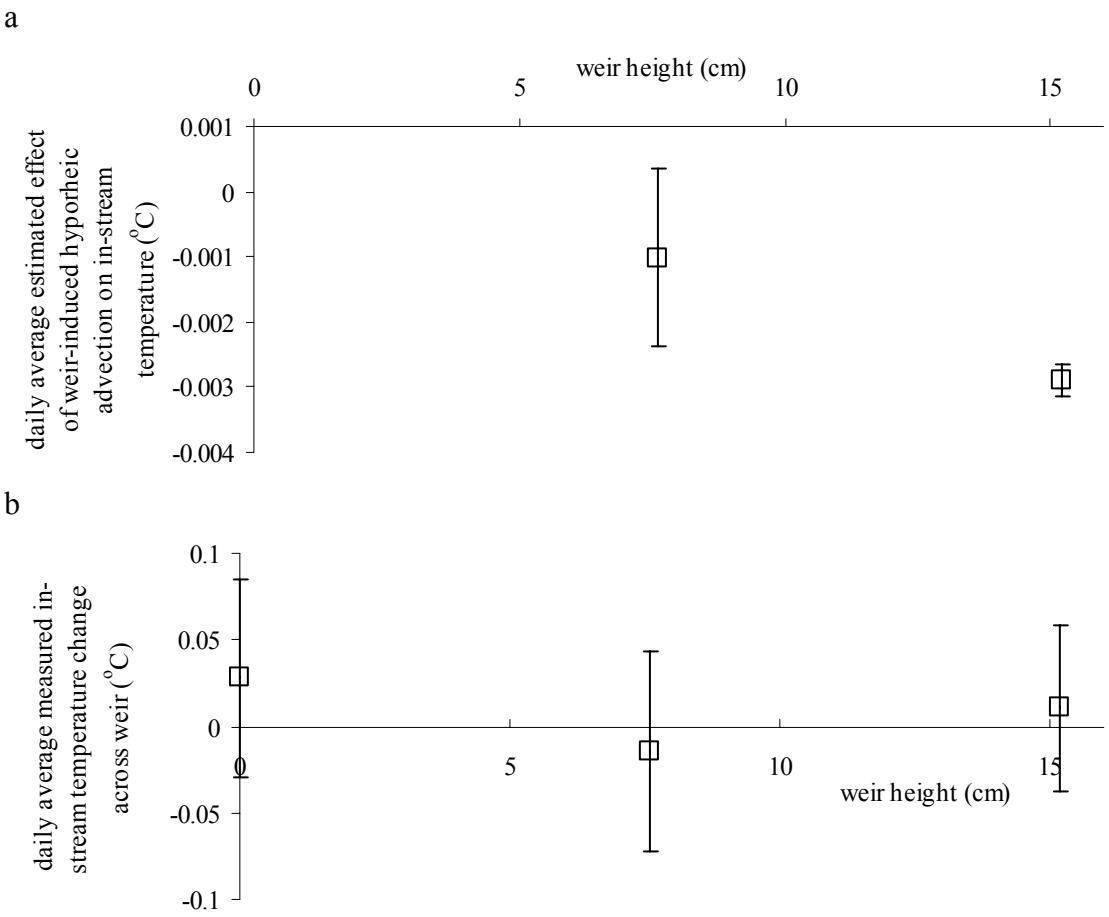

Figure 3.11 (a) Daily average estimated effect of net weir-induced hyporheic heat advection on surface stream temperature (daily average ΔT_a, Eq. 6) versus weir height, and (b) daily average measured temperature change of water upstream to downstream across weir (daily average Ts_2-Ts_3, Fig. 1) versus weir height for 2007 experiment. Boxes and whiskers represent means and standard deviations, respectively, of the daily averages for entire period that weir was at the given height. Note that 1) negative net heat flux cools the surface stream and warms the subsurface water, and 2) while the magnitude of the ordinate values for both y-axes are less than the accuracy and precision of the ibutton sensors, because the values are averages of temperature differences that have at least one significant figure, the rules of significant figures indicate at least one significant figure in the averages.

4 Sensitivity of stream and river organisms to temperature change

4.1 Introduction

Temperature is the single most important condition affecting the lives of organisms (Begon et al. 2006, Brown et al. 2004, Clarke 2006). Aquatic autotrophs and the majority of aquatic heterotrophs are ectotherms, whose temperature fluctuates directly with ambient water temperature (Giller and Malmqvist 1998). Ectotherms are adapted to the spatial and temporal patterns of the thermal regimes typically experienced in their native ranges (Hill et al. 2004, Salisbury and Ross 1985, Lomolino et al. 2006, Begon et al. 2006, Huey and Kingsolver 1989), and are therefore sensitive to thermal shifts (Walther et al. 2002, Sweeney and Vannote 1978). Intact stream and river (lotic) ecosystems are critical for the health of biosphere and humanity alike (Postel and Richter 2003). Humans have profoundly altered stream and river temperatures regimes via dams and diversions, deforestation, urbanization, and channelization, all in addition to projected impacts associated with climate change (Caissie 2006, Webb 1996, LeBlanc et al. 1997). If sufficiently large, such water temperature changes will impact populations and therefore communities of lotic species.

The relationships between temperature and many individual organism level processes that affect population dynamics (thermal performance curves) are similarly shaped across plants, animals, and microbes, both aquatic and terrestrial. All thermal performance curves have a humped shape, with minimum and maximum temperatures outside which the process

ceases, and an optimum temperature associated with maximum rate of functioning (Begon et al. 2006, Huey and Kingsolver 1989). Thermal performance curves are necessary for constructing population and community models to predict ecological response to human thermal impacts (Scheuerell et al. 2006). However, a basic inventory of thermal performance curves is not available for lotic organisms. Furthermore, previous studies have examined the effect of particular temperature shifts on specific lotic species (e.g., climate change impacts on salmon, Battin et al. 2007), but have not provided a quantitative synthesis to evaluate patterns of ecological sensitivity to environmental temperature change across taxonomic groups and organism level processes.

We inventory organism level thermal performance curves from 49 existing papers and population level response to temperature from another 10 papers to synthesize and compare the thermal sensitivity of lotic species across various processes and taxonomic groups. We then compare these thermal sensitivities to typical human impacts on lotic temperatures and discuss implications for human management of aquatic systems. We focus on species (organism and population) sensitivity rather than ecosystem function (e.g., nutrient retention) because ecological conservation policy is typically formulated at the species level (e.g., Endangered Species Act) (Stein et al. 2000).

4.2 Methods

We searched the peer-reviewed scientific literature for thermal performance curves for organism level processes that directly affect lotic population dynamics, including survival (=1-mortality) rate and reproduction (birth) rate (Begon et al. 2006). Because reproduction rate is a function of body size (Beitinger and Fitzpatrick 1979, Sweeney and Vannote 1978),

we also quantified processes that contribute to body size, including growth rate and development rate (Begon et al. 2006). Other processes, like migration, were not included because their importance varies substantially among species and depends heavily on geographic context, which is not considered in this study. Finally, the effect of temperature on disease was considered beyond the scope of our study. Although not strictly performance curves, we also searched the literature for relationships between population level abundance metrics and temperature. We searched Web of Science for citations that contain the keywords temperature or thermal and stream, river, or lotic, and a keyword associated with either one of the processes of interest (growth, development, reproduction, spawn, hatch, egg, birth, death, survival, mortality) or the population level keywords density and abundance. For all searches, wildcard characters and synonyms were included to retrieve citations containing variants of the keywords.

We limited our review to thermal performance curves in graphical form with constant, average, or specified percentile (most commonly maximum) water temperature as the independent variable for lotic species or lotic populations of more cosmopolitan species. Data from both field and laboratory studies were included as they complemented each other well, with field conditions being more realistic, but laboratory data more precisely isolating the effect of temperature. Field data often had considerable scatter, so studies were included if a trend line was drawn by the original authors. Laboratory data often had less scatter than field data, so we drew trend lines connecting laboratory data where three or more temperatures were included on the x-axis. Different findings from the same paper were considered independent results and therefore included separately in our analysis if they were from separate taxa, developmental stages, ages, streams/rivers, resource levels, or seasons.

Different findings from the same paper were not considered independent results if they were from different portions of the same cohort (e.g., different size classes of similar age individuals from a single taxa) undergoing the same experiment, in which case a single median, average, or moderate condition was included as representative in our analysis. Taxonomic resolution varied between papers, and data were included separately in our analysis at as fine a resolution as possible for a given paper, down to the species level. We performed basic calculations to transform literature data into forms used in our study. For example, development duration data were inverted to give development rate (Cossins and Bowler 1987). Mortality rate data were subtracted from 1.0 to give survival rate (Begon et al. 2006). We defined reproduction as the creation of a viable new organism (i.e. an organism is born, hatches, or germinates) rather than intermediate events which may or may not lead to the creation of a new viable organism (e.g., egg production, fertilization) in keeping with our population level focus.

Organisms respond physiologically to temperature change over three timescales of increasing duration: acute response, acclimated response, and evolutionary response (Hill et al. 2004). Here we are concerned with acclimated response where changes in performance due to temperature change account for physiological adaptation that can occur in organisms over days to weeks. Acclimated response is most relevant for evaluating the response to many anthropogenic thermal impacts because such impacts are generally of sufficient duration for organisms to acclimate to the extent possible, and because human mitigation of such thermal impacts, to be most beneficial, should occur before significant evolutionary response has occurred. We therefore limited our review to thermal performance curves based on acclimated organisms. Organisms were considered to be acclimated if data were from

field studies, or in the case of laboratory studies, if the paper stated the organisms were acclimated, if the previous lifestage was also spent at the acclimation temperature, if the majority of the organisms were present at experimental temperatures >3 days for invertebrates and >3 weeks for fish (Hill et al. 2004, Buchanan et al. 1988), or if the experiments were performed on eggs.

For each thermal performance curve from the literature we calculated $\Delta T_{e\text{-}50}$, the temperature change required to reduce the organism level biological process below its maximum value by 50%, and $\Delta T_{e\text{-}10}$, the temperature change required to reduce the function by 10% of its maximum value at the steepest part of the performance curve (Figure 4.1). We chose 50% of the full range to represent overall sensitivity to temperature shifts for comparison among taxa and other groupings (less sensitive to details of data and least arbitrary), and 10% at the steepest portion of curve to allow calculation of nonlinearity (see below). We adopted this approach because were not able to locate precedents in the literature for calculating such ecologically relevant temperature changes, and most performance curves did not have obvious thresholds. Separate values of ΔT_e were calculated for the rising (temperatures below the optimum) and falling (temperatures above the optimum) portions of each curve if data were available (Figure 4.1). Asymmetry of a thermal performance curve about the optimum temperature was evaluated by comparing the magnitude of ΔT_e for the rising portions of curves with that for the falling portions. Nonlinearity of either the rising or falling parts of the curve was calculated as the deviation of the ratio $\Delta T_{e\text{-}50} : \Delta T_{e\text{-}10}$ from 5.0. For performance curves that did not explicitly show a peak temperature, the highest part on the curve that was supported by data was used as the peak. For performance curves exhibiting a sigmoidal or logistic shape, peak was assigned to

point on the curve whose y-value was approximately 95% of the peak, to avoid counting flat portions of the curve in the resulting ΔT_e. We included only thermal performance curves where the y-axis range was large enough to calculate $\Delta T_{e\text{-}50}$ on at least one side of the thermal optimum.

We performed two-sample t-tests to determine if the mean sensitivity (ΔT_e) of various subsets of the data were statistically different. First, we split the entire dataset into rising and falling data, and conducted a t-test to determine if the thermal performance curves were asymmetric overall. All taxa and processes were lumped together for this test to assess the overall asymmetry of the dataset. Second, we split the entire dataset into two taxonomic groups (fish and invertebrates) and conducted a t-test to determine if these groups differed in thermal sensitivity. Data for rising and falling as well as all processes were lumped together for this test to assess the overall difference between fish and invertebrates. Because data were relatively sparse for survival and reproduction (Table 4.1), a similar comparison of thermal sensitivity among processes across the entire dataset was not possible. However, rising curve data were sufficient to allow t-test comparisons of thermal sensitivity between growth and development for both fish and invertebrates (Table 4.1). Further, to determine if differences observed between fish and invertebrates for the entire dataset also held for individual processes, we conducted t-tests between those taxa for growth and development. We also tested whether subsets of the thermal performance curves in the dataset were on average nonlinear. We accomplished this using one-tailed t-tests to determine whether the mean ratio $\Delta T_{e\text{-}50} : \Delta T_{e\text{-}10}$ was significantly different from 5.0. T-tests to determine nonlinearity were performed using natural logarithms of the ratio $\Delta T_{e\text{-}50} : \Delta T_{e\text{-}10}$ because the ratio itself is approximately log-normally distributed. All t-tests performed for this study

were two sample one-tailed t-tests run only when n>9 for both subsets of the data being compared and only when assumptions of normality were met (verified by visual inspection of histograms and skew and kurtosis in the range -2 to +2).

Our quantitative synthesis deviates from a formal meta-analysis (Hunter and Schmidt 1990) because our aim is not to determine whether the effect of temperature is real (there is already consensus in the literature that there is a significant effect (Begon et al. 2006)), nor even primarily to determine the magnitude of the effect, but rather we focus on how this effect varies among subsets of the data. In formal meta-analysis, results from various studies are typically weighted by variance (Hunter and Schmidt 1990), but variance data are too sparse among the studies used in our analysis. Alternatively, results can be weighted by number of data points (n), but there is relatively little precedent for this approach in the literature, and our combination of field and laboratory data means that n varies in significance between different types of studies. For these reasons we concluded that weighting would be as arbitrary as not weighting, and therefore did not weight.

4.3 Ecological sensitivity to temperature

We analyzed 120 organism level thermal performance curves from 49 papers, and 43 additional relationships from 10 population abundance papers. At the organism level, $\Delta T_{e\text{-}50}$ averaged 7.4ºC (n = 145) and $\Delta T_{e\text{-}10}$ averaged 1.0ºC (n = 143) across the entire dataset (all taxa, all processes, including both rising and falling). Corresponding overall averages for population abundance were 4.2ºC (n=48) and 0.5ºC (n=31). Small values of ΔT_e indicate high sensitivity to thermal change, and large values indicate low sensitivity. Thermal performance curves that met our criteria were available for organism level processes for lotic

fish and invertebrates, but not for microbes and macrophytes. All fish organism level thermal performance curves (n=58) were for individual species, and included 21 species from 14 genera and 9 families, including Acipenseridae (n=2), Clupeidae (n=2), Cottidae (n=5), Cyprinidae (7), Esocidae (n=2), Moronidae (n=4), Percichthyidae (n=1), Percidae (n=1), and Salmonidae (n=34). The taxonomic resolution of the invertebrate data (n=62) was typically species or genus, although it was occasionally as coarse as the family level. Most invertebrate organism level thermal performance curves were for insects (n=40), including Diptera (n=19), Ephemeroptera (n=15), Plecoptera (n=3), and Trichoptera (n=3). The remaining invertebrate curves were for crustaceans (n=22), including Amphipoda (10), Cladocera (8), Copepoda (1), and Decapoda (3). The vast majority of the thermal performance curves were from temperate organisms (n=110) with only a few tropical (n=10). Most data were from laboratory experiments, with less than 20% from field studies, although a significant number of semi-controlled field experiments blurred this distinction. A detailed list of results is provided in the Appendix.

Organism level processes for fish were more sensitive to temperature shifts than for invertebrates when compared across all processes, both rising and falling ($p=1.9x10^{-15}$, Figure 4.2). This pattern was also observed for just growth and just development for just the rising portion of the curves ($p=1.5x10^{-4}$ for growth, $p=4.5x10^{-4}$ for development, Figure 4.3). At the population level, fish abundance was somewhat more sensitive to temperature shifts overall (Figure 4.6, $p=0.03$) than invertebrate abundance. This variation with taxonomic group is reasonable, as invertebrates are known to tolerate a wider range of temperatures than fish, due probably to their relative structural and biochemical simplicity (Hardy 1979). Sensitivity appeared to vary among organism level processes (Figure 4.4), but sample size

was generally too small to allow statistical comparison (Table 4.1). Development was slightly more sensitive to temperature than growth among the rising data (Figure 4.3) but this difference was not significant for invertebrates ($p=0.43$) and not very significant for fish ($p=0.083$). Among the comparisons we were able to make, thermal sensitivity therefore appears more sensitive to taxonomic grouping than organism level process.

On the whole, organism level processes were more sensitive on the falling portion of the curve than the rising portion ($p=1.9\text{x}10^{-10}$, Figure 4.5), indicating an asymmetry to many thermal performance curves. This asymmetry appeared to maintain itself across different taxonomic groups and processes (Figure 4.2, Figure 4.4), but sample sizes were sufficient to confirm this only for fish ($p=1.6\text{x}10^{-6}$) and growth ($p=1.8\text{x}10^{-6}$). This asymmetry has been occasionally discussed in general terms (Alexandrov 1977, Huey and Kingsolver 1989), and also specifically for plant growth, where it has been attributed to the balance of gross photosynthesis and respiration costs which vary with increasing temperature, as does the balance of activation energies and enzyme denaturing at the molecular level (Fitter and Hay 2002, Sutcliffe 1977). Such growth asymmetry is evident but not often discussed among the studies summarized in our analysis (Takeshita et al. 2005, Jonsson et al. 2001, Elliott and Hurley 1997, Ojanguren et al. 2001, Brannon et al. 2004). Interestingly, population abundance exhibits the opposite pattern (Figure 4.7), but in that case it was not statistically significant.

The organism level thermal performance curves used in this study were on average nonlinear ($p=5.8\text{x}10^{-15}$ for rising, $p=1.7\text{x}10^{-11}$ for falling, from log transformed values), with falling more nonlinear than rising (back-transformed average $\Delta T_{e\text{-}50} : \Delta T_{e\text{-}10}$ ratios of 9.7 and 6.9, respectively). Nonlinearity maintained itself across individual taxonomic groupings and

processes (back-transformed average rising/falling ratios of 7.0/8.6 for invertebrates, 7.0/10.3 for fish, 7.9/11.0 for growth, 6.1/NA for development, 11.1/9.7 for reproduction, and 8.7/8.8 for survival; NA=not applicable), but sample size was large enough and the log transformed values distributed sufficiently normally to verify this only for growth ($p=1.7x10^{-5}$ for rising, $p=3.0x10^{-4}$ for falling). Because the papers summarized in our study commonly used linear regression to analyze thermal data, our quantification of nonlinearity is likely an underestimate. This degree of both asymmetry and nonlinearity underlines the necessity of knowing existing temperature conditions in order to meaningfully interpret the ecological effects of temperature change.

This study reveals potentially important trends from a broad survey of existing data, but also highlights areas necessary for further research. First, this comparative study of temperature sensitivity is based on arbitrary reductions in process rates. More accurate thermal response curves (i.e. less studies relying on linear regression) might enable such comparisons to be based on thresholds observed within the curves that better reflect underlying biology. Second, most existing data concerning the response of organisms to temperature are anecdotal or entail comparisons among categorical data. The thermal performance curves used in this study are comparatively rare in the literature, particularly for macrophytes, and for certain processes (e.g., the falling part of the curve for development). Such performance curves are necessary as inputs to advanced population viability models currently being developed to predict impacts of human induced stresses like climate change (e.g., Scheuerell et al. 2006). A full suite of such curves for a range of organisms will be necessary to extend such models to the multi-species community models that are necessary to predict human impacts on biodiversity.

4.4 Anthropogenic temperature change

Most human impacts on stream or river temperature affect both the heat budget (heat fluxes with environment) and the heat capacity (discharge rate) of the water (Webb 1996). Overall, human activities tend to increase temperatures more often than decrease, with some notable exceptions (Table 4.2). Each category of impacts exhibits considerable variability in time and space due to corresponding variability in the magnitude of human activity and discharge in stream and river systems. Impacts tend to be greater in low velocity areas within the channel than in overall bulk mainstem flow. Table 4.2 focuses on longer term effects with impacts that last years or decades, and on baseflow (i.e. not storm) conditions, which are present most of the time, and have higher thermal susceptibility due to lower channel discharge.

Loss of riparian shading can be caused by a wide range of human activities, including forestry, urbanization, road cuts, and forest fire (Caissie 2006, Ward 1985, Moore et al. 2005a, Beschta et al. 1987). Loss of riparian shading has an important thermal effect primarily in small waterways where canopy can reach a significant way across the channel (Allan 1995), and is most often reported as a warming effect on peak or average stream temperatures in summer (Table 4.2). The thermal impact of riparian shade loss in winter can be either warming or cooling, and is generally of smaller magnitude than summer effects (not shown in Table 4.2, but see Beschta et al. 1987). In forestry, loss of riparian vegetation can be partial or complete, usually together with loss of upland vegetation. Impacts from loss of vegetation are generally greatest with complete loss of both riparian and upland vegetation and least with loss of only upland vegetation (i.e. vegetative buffers are maintained along

stream margins) (Table 4.2). The effect of stream buffers varies with width of buffer, degree of thinning in buffer, and aspect of stream (Moore et al. 2005a).

Climate change will affect stream and river temperatures in many important ways, including by altering precipitation amounts, precipitation forms, and snow and glacier melt. However, data are available in the literature primarily for the impact of rising air temperatures directly on water temperatures (global warming in Table 4.2). Globally, greater increases in minimum than maximum temperatures are already apparent (Karl et al. 1993, Walther et al. 2002), and greater atmospheric warming is expected in winter than summer (Millenium-Ecosystem-Assessment 2005), but greater stream warming is expected in spring than in summer or winter in the USA (Mohseni et al. 1999). Warming values from the literature reflect this with slightly higher thermal impacts on an annual basis than in summer (Table 4.2), although this difference may not significant. Increasing air temperatures in urban areas due to urban heat islands should also increase temperatures in streams, although there is little data to isolate this effect from other urban impacts (e.g., loss of riparian shading).

The thermal effect of reduction of groundwater input has rarely been directly quantified (but see LeBlanc et al. 1997), but can be estimated by studies that quantify the effect of groundwater on stream heat budgets, which have generally been conducted during summer in non-meltwater dominated conditions (Table 4.2). Humans can also reduce water exchange occurring with groundwater along shorter flowpaths (hyporheic exchange) by channel straightening and simplification (Poole and Berman 2001). This reduction of hyporheic exchange, depending on the length of the flowpaths, can reduce average and/or daily maximum temperatures in summer, with the opposite occurring in winter (Poole and

Berman 2001). The opposite occurs in alpine or arctic systems during periods when glacial- or snow-melt dominates (Brown et al. 2007), or from increases in baseflow. These impacts can be estimated via the small number of studies that quantify the effect of hyporheic exchange on bulk stream temperatures or temperatures in lower velocity areas such as pool bottoms or alcoves (Table 4.2). Changes in channel morphology can impact hyporheic exchange (Chapter 2), but also impact atmospheric heat exchange, for example by increasing channel width-to-depth ratio (Table 1, LeBlanc et al. 1997).

The increased thermal mass of water behind reservoir dams generally damps annual temperature cycles in downstream reaches relative to free flowing conditions (Caissie 2006, Ward 1985, Webb 1996). In addition, thermal stratification and water releases below the thermocline in summer often lead to greater summer cooling than winter warming (Table 4.2). Tributary input has mostly been reported as a cooling influence on bulk stream temperatures or more isolated patches during summer (Webb 1996, Bilby 1984, Nielsen et al. 1994). Consequently, human diversion of tributary input would often have a warming effect (Table 4.2). Nevertheless, some tributaries should have a warming influence on streams, and diversion of these tributaries would have a cooling effect (Danehy et al. 2005). Effluent discharges from municipal sewage treatment plants, power plants, and other industry also typically warm receiving water (Webb 1996)(Table 4.2).

In sum, most human impacts warm streams, particularly in summer (Table 4.2). Some warming impacts, like global warming and input of effluent discharges, have a warming effect in all seasons. Others, like reduction of groundwater input via urbanization or cutting off hyporheic flowpaths have a warming effect in summer, but a cooling effect in winter, increasing the annual water temperature range. Loss of riparian or upland vegetation

has an important thermal effect, inducing considerable warming in summer, with more variable effects in winter. Large bottom-release reservoirs greatly reduce temperatures in summer and increase temperatures in winter, reducing the annual temperature range. The overall magnitude of these anthropogenic effects varies significantly, with reservoir dams having the greatest potential for cooling and loss of riparian and upland vegetation having the greatest potential for warming during summer. These impacts also vary in spatial and temporal scope. Most types of individual human actions (e.g., cutting riparian vegetation) have fairly immediate thermal impacts on temperature that are relatively local in nature. Nevertheless, most types of short-term local impacts are quite common, and can accumulate through time and space to create long term, widespread impacts. On the other hand, global warming impacts take decades to materialize and span the planet, although they too will exhibit geographic variability. Human stream and watershed restoration activities theoretically have the potential to reverse many of these human thermal impacts (e.g., via reforestation or restoration of hyporheic exchange). A major exception is global warming, which may put significant constraints on the degree of restoration to historic conditions that is possible (e.g., Battin et al. 2007).

4.5 Ecological implications of anthropogenic temperature change

Comparing human impacts to ecological sensitivity, the magnitudes of many typical and maximum human-induced temperature changes (Table 4.2) exceed the average $\Delta T_{e\text{-}50}$ for both organism level processes and population abundance (Figure 4.2, Figure 4.3, Figure 4.4, Figure 4.5, Figure 4.6, Figure 4.7). Human impacts therefore clearly have substantial potential for reducing ecological functions in streams. Human thermal impacts are likely to

affect fish more than invertebrates (Figure 4.2, Figure 4.3, Figure 4.6). While this may mean that middle rungs of the food chain might be disturbed less than predatory fish, predatory fish are often more important to human consumption, recreation, and even sense of place (Lackey et al. 2006). Further, higher trophic levels are often especially sensitive to other aspects of human environmental degradation beyond temperature (Hill et al. 1996), compounding their overall risk. Finally, impacts to predatory fish in lotic systems can strongly impact other parts of both aquatic (McIntosh and Townsend 1996) and terrestrial (Willson and Halupka 1995) food webs.

The result of increasing temperature on organism level functions depends on the location of the existing thermal regime relative to the optimum temperature. For organisms that typically operate close to the optimum, the human tendency to warm streams more often than cool them is of particular concern, because growth is more sensitive on the falling than the rising portions of thermal performance curves (Figure 4.4, Figure 4.5). For example, growth and survival in many coldwater and some warmwater fishes are expected to decline as temperatures rise with global warming and other human impacts (Carveth et al. 2007, Bear et al. 2007). On the other hand, for organisms that operate below the optimum, at least at certain times or places, human warming impacts would occur on the rising curve, possibly providing a benefit (Leach and Houde 1999), particularly for introduced species (Whitledge and Rabeni 2002). Warming will also benefit species negatively impacted by coldwater releases from large dams (Todd et al. 2005). In the end, the net impact of temperature shifts on an individual organism is a complex function of different thermal performance curves for multiple processes, each of which can be affected by temperature duration and variability (Cossins and Bowler 1987, Hokanson et al. 1977). Furthermore, the cumulative ecological

impact of temperature shifts depends on thermal performance curves that vary across multiple species and lifestages within communities and play out across a landscape that is thermally heterogeneous in time and space. Predictions of response to temperature shifts therefore must involve careful evaluations on a case by case basis.

Overall then, human impacts on stream and river thermal conditions are large enough relative to organism and population thermal sensitivities that significant ecological responses are expected. Impacts would vary significantly among taxa and geographic setting, but human actions to reduce our "thermal footprint" are clearly necessary to avoid or mitigate significant ecological impacts, particularly those due to warming. Some mitigation would entail local action, such as encouraging riparian re-vegetation and hyporheic restoration. Other actions would require regional coordination, such as scheduling hypolimnetic water releases in larger rivers to coincide with peak summer temperatures. Finally, global impacts like climate change must be addressed on an international basis.

Table 4.1 Distribution of thermal performance curves among taxonomic groups and processes.

	Invertebrates	**Fish**	**Total**
Growth	27 (25R/6F)	34 (25R/26F)	61 (50R/32F)
Development	32 (32R/0F)	10 (10R/0F)	42 (42R/0F)
Reproduction	3 (2R/3F)	4 (2R/4F)	7 (4R/7F)
Survival	0 (0R/0F)	10 (2R/8F)	10 (2R/8F)
Total	62 (59R/9F)	58 (39R/38F)	120 (98R/47F)

Values are number of thermal performance curves in each category. Values in parentheses give split in each category between rising (R) and falling (F).

Table 4.2 Human impacts on lotic temperatures.

		Typical or annual average		Seasonal			
Human impact[1]	**Impact Type**	**Typical ΔT[2]**	**Max ΔT**	**Season**	**Typical ΔT[2]**	**Max ΔT**	**References[3]**
Loss of riparian shading, loss of upland vegetation	Warming			Summer	5.4	13.0	Reviews: (Ward 1985, Moore et al. 2005a, Smith 1972, Beschta et al. 1987); individual study: (Lynch et al. 1984)
Loss of riparian shading[4]	Warming			Summer	3.1	7.6	Reviews: (Allan 1995, Webb 1996, Beschta et al. 1987); individual studies: (Johnson 2004, Dunham et al. 2007, LeBlanc et al. 1997, Ebersole et al. 2003)
Reduction of riparian shading, loss of upland vegetation	Warming			Summer	2.8	6.7	Reviews: (Moore et al. 2005a, Beschta et al. 1987)
Reduction of riparian shading[4]	Warming			Summer	3.7	5.0	Reviews: (Caissie 2006); individual study: (Rutherford et al. 2004)
Loss of upland vegetation (riparian buffer maintained)	Warming			Summer	1.1	2.6	Reviews: (Moore et al. 2005a, Beschta et al. 1987); individual study: (Bourque and Pomeroy 2001)
Global warming (due to air temps changes, not flow alteration)	Warming	3.2	8.4	Summer	2.8	7.0	Review: (Webb 1996); individual studies: (Pedersen and Sand-Jensen 2007, Ferrari et al. 2007, Morrison et al. 2002, Pilgrim et al. 1998, Mohseni et al. 1999)
Reduction of groundwater input	Warming[5]			Summer	1.2	4.0	Individual studies: (Story et al. 2003, Loheide and Gorelick 2006, LeBlanc et al. 1997)
Reduction of groundwater input – effect on lower velocity areas	Warming[5]			Summer	5.6	12.4	Individual studies: (Bilby 1984, Ebersole et al. 2003, Nielsen et al. 1994)

		Typical or annual average			Seasonal		
Human impact[1]	**Impact Type**	**Typical ΔT[2]**	**Max ΔT**	**Season**	**Typical ΔT[2]**	**Max ΔT**	**References[3]**
Reduction of hyporheic exchange	Warming[5]			Summer	1.0 (A) 0.1 (G)	2.0	Individual studies: (Story et al. 2003, Loheide and Gorelick 2006, Burkholder et al. 2008, Chapter 3 of this dissertation)
Reduction of hyporheic exchange – effect on lower velocity areas	Warming[5]			Summer	5.1	7.2	Individual studies: (Bilby 1984, Fernald et al. 2006, Nielsen et al. 1994)
Increased width-to-depth ratio	Warming			Summer		1.7	Individual study: (LeBlanc et al. 1997)
Large bottom-release reservoir dams	Warming			Winter		4.0	Review: (Allan 1995)
Large bottom-release reservoir dams	Cooling			Summer	-8.4	-14.0	Reviews: (Allan 1995, Smith 1972)
Diversion of tributary input	Warming			Summer	0.7	1.1	Review: (Webb 1996); individual study: (Danehy et al. 2005)
Diversion of tributary input – effect on lower velocity areas	Warming			Summer	5.1	5.3	Individual studies: (Bilby 1984, Nielsen et al. 1994)
Diversion of tributary input	Cooling			Summer	-0.8	-1.0	Individual study: (Danehy et al. 2005)
Input of effluent discharges	Warming	3.4	12.0				Reviews: (Webb 1996, Smith 1972); individual study: (Kinouchi et al. 2007)

[1]Temperature changes are for bulk mainstem flow except where noted.

[2] To calculate typical values we took ranges of average, minimum, or maximum temperature changes given in the literature, calculated their midrange values, and took an arithmetic mean of the midranges. The exception was reduction of hyporheic exchange, where impacts ranged over several orders of magnitude, and we present both arithmetic (A) and geometric (G) means.

[3] Table is representative of the literature, but is not an exhaustive compilation. Some data are from direct manipulations (e.g., loss of riparian shading), some are from studies that attribute portions of a stream heat budget to particular processes (e.g., groundwater and hyporheic contributions), and some are from predictive modeling (e.g., global warming). In order to characterize each type of impact separately, only data for single impacts were used in making the table (data from cumulative effects of multiple impacts were excluded).

[4] Some values reported as loss of riparian shade probably also include loss of upland vegetation. We relied on the descriptions provided in the reviews.

[5] Values are for non-meltwater dominated conditions during summer. Reverse is also true, but little data is available.

Note: table may be internally inconsistent in some places due to multiple sources used in the compilation.

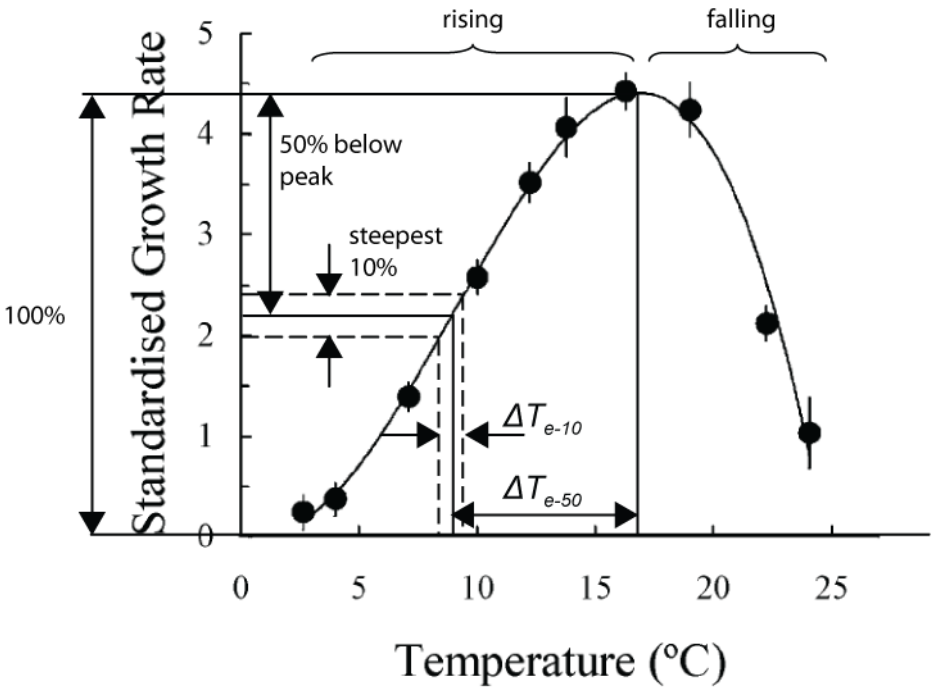

Figure 4.1 Example calculation of ΔT_{e-50} (=8°C) and ΔT_{e-10} (=1.2°C) for rising. Calculation for falling is analogous but not shown. Growth rate plot reprinted from Journal of Thermal Biology, Vol 26, Ojanguren A.F., Reyes-Gavilan F.G. & Brana F., Thermal sensitivity of growth, food intake and activity of juvenile brown trout, 165-170, Copyright 2001, with permission from Elsevier.

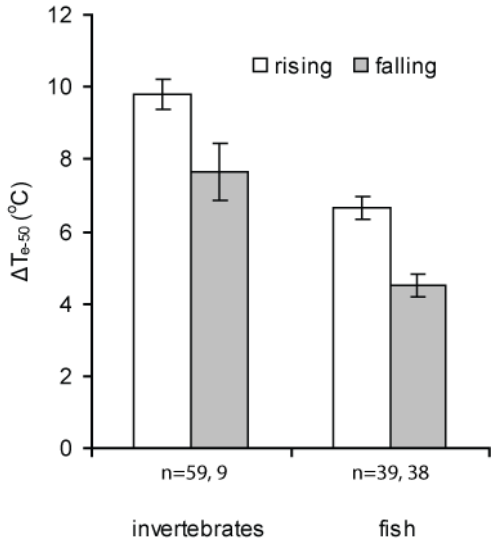

Figure 4.2 Average temperature shift required to reduce organism level process below maximum by 50% (ΔT_{e-50}), segregated by taxonomic group. Includes all organism level processes (growth, development, reproduction, and survival). Bar heights indicate means, error bars represent +/- standard error.

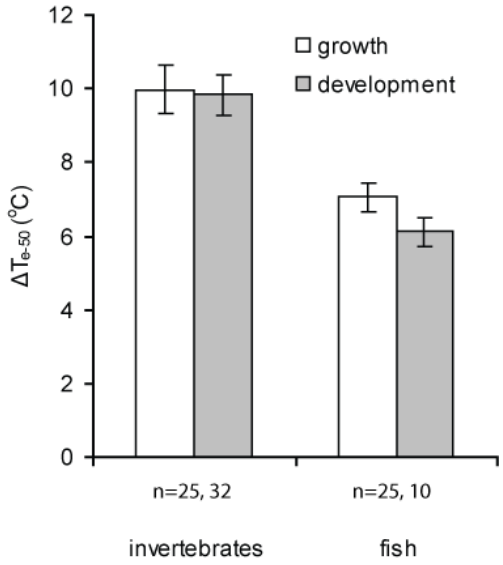

Figure 4.3 Average temperature shifts required to reduce organism level process below maximum by 50% (ΔTe-50), segregated by both taxonomic group and process. Only data for the rising portions of curves where n>9 are included. Bar heights indicate means, error bars represent +/- standard error.

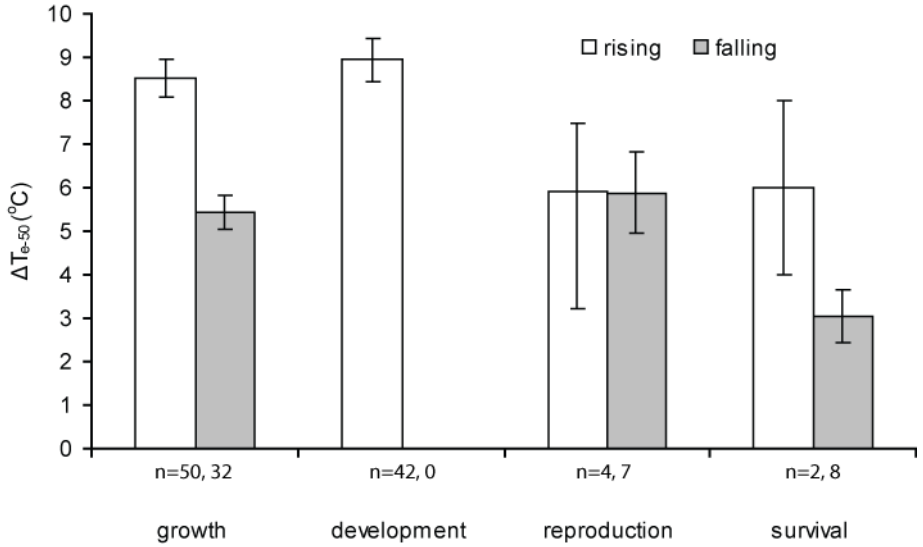

Figure 4.4 Average temperature shifts required to reduce organism level process below maximum by 50% (ΔTe-50), segregated by process. Includes all taxonomic groups (invertebrates and fish). Bar heights indicate means, error bars represent +/- standard error except where n<5 where error bars represent range.

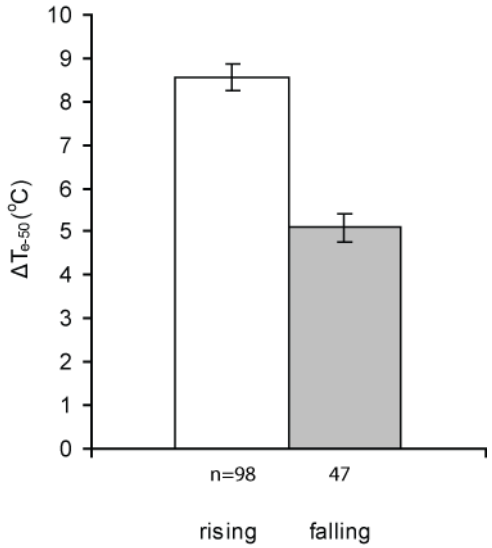

Figure 4.5 Average temperature shifts required to reduce organism level process below maximum by 50% (ΔTe-50). Includes all taxonomic groups and processes. Bar heights indicate means for entire dataset, error bars represent +/- standard error.

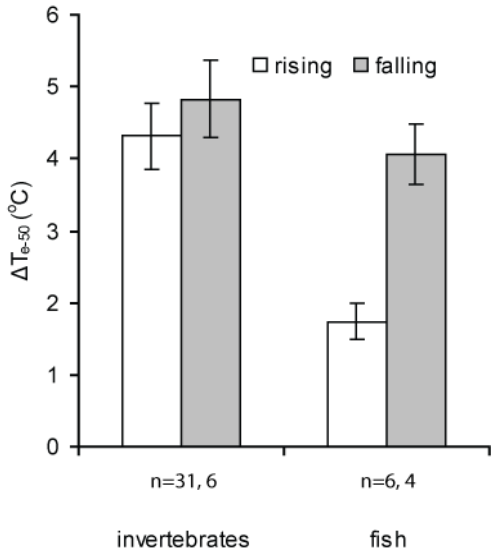

Figure 4.6 Temperature shift required to reduce population abundance below peak value by 50% ($\Delta T_{e\text{-}50}$), segregated by taxonomic group. Bar heights indicate means, error bars represent +/- standard error.

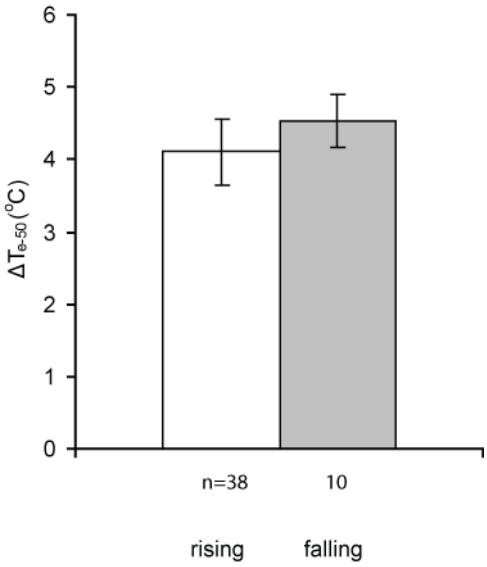

Figure 4.7 Temperature shift required to population abundance below peak value by 50% ($\Delta T_{e\text{-}50}$). Bar heights indicate means, error bars represent +/- standard error.

5 Conclusions

5.1 Answers to Research Questions

Chapters 2-4 of this dissertation each generated new insights concerning how IGSs impact stream hydraulics and temperature, and how those impacts affects stream biota and ecology. These insights address the questions posed in Chapter 1 of this dissertation:

1. How do basic characteristics of in-stream geomorphic structures (IGSs) and their hydrogeologic setting impact hyporheic exchange in streams?
    - IGS types analyzed (weirs, steps, lateral structures) drive significant hyporheic exchange in streams under baseflow conditions mainly by inducing Darcy flux through both local steepening of the streambed and creating backwater behind obstructions.
    - Induced downwelling flux rate and hyporheic zone size generally increase with IGS height, while hyporheic residence time peaks at small or intermediate size.
    - Hydrogeologic setting appears to be important, with reduced background groundwater discharge, increased depth to bedrock, and low to intermediate slopes tending to maximize hyporheic exchange, while the impact of substrate hydraulic conductivity varies depending on the exchange metric of interest.

- Channel spanning structures (weirs, steps) are generally more effective than partially spanning structures (lateral structures), and weirs more effective than steps.
- Overall, IGS size, background groundwater discharge rate, and hydraulic conductivity appear to be the most important factors controlling hyporheic exchange, followed by structure type, depth to bedrock, and channel slope.
- A field experiment determined that our modeling approach anticipates key trends of hyporheic response to driving factors observed in a more heterogeneous field setting.
- Trends observed in both field and model results appear reasonable when interpreted with simple hydraulic theory, indicating that IGSs modulate hyporheic exchange mainly through their effect on head drop in the stream.
- Because it is necessary to understand hyporheic hydraulics to understand hyporheic function, the hydraulic results presented in this chapter provide a foundation for understanding many ecologically important hyporheic functions that may be enhanced by IGSs such nutrient processing, toxics mineralization, and thermal moderation.
- Because IGSs are common in natural streams and frequently installed in stream restoration projects, such hyporheic functions are potentially widespread across the landscape. This study therefore provides a foundation for understanding hyporheic function in natural streams, understanding the hyporheic function of stream restoration projects designed for other purposes, and for designing restoration projects specifically for hyporheic restoration.

2. How does IGS presence and size affect heat exchange across the streambed and temperatures in the hyporheic zone and surface stream?
    - Weir-type IGSs induce a curvilinear hyporheic flow cell.
    - Advection of heat along the induced flow cell during summer created a drop in average temperature in the shallow hyporheic zone upstream to downstream across the weir, inducing a slight advective cooling on the surface stream.
    - Streambed conduction in the vicinity of the structure also induced a net cooling on surface water of similar magnitude to hyporheic advection.
    - Despite the cooling influence of conduction and weir-induced hyporheic advection, obvious cooling of surface stream water as it flowed downstream across the weir site was not observed, indicating the greater importance of other heat flux processes.
    - Atmospheric heat flux process, such as solar radiation, sensible heat transfer, and evaporation/condensation, although not measured at the site, were probably responsible for the observed temperature changes.
    - An increase in weir height led to an increase in daily total weir-induced hyporheic heat advection, and therefore an increase in advective cooling from the perspective of the surface stream. The positive slope of this trend is probably independent of the hydraulic conductivity of the sediments and expected in most hydrologically neutral or gaining streams.

- Sediment hydraulic conductivity, and therefore sediment texture, by controlling the rate of hyporheic water exchange, was critical to determining the importance of hyporheic advection on surface stream temperatures.
- While the importance of weir-induced hyporheic heat advection for surface stream temperatures appears to vary widely with stream context, its importance for subsurface temperatures, including the hyporheic and benthic zones, should be more widespread.
- Because variations in temperature have significant impacts on many ecological and biogeochemical processes in streams, structure-induced hyporheic heat advection has the potential to be ecologically relevant in natural and restored streams, especially in the context of anthropogenic thermal impacts.

3. How does ecological sensitivity to temperature vary by organism level process and taxonomic grouping, and how do those sensitivities compare to human induced temperature impacts in streams?
    - Organism level response to temperature is characterized by thermal performance curves, which exhibit a humped-shape with minimum, optimum, and maximum temperatures.
    - Thermal performance curves have characteristic shapes for processes like metabolism, growth, development, reproduction, and survival that are generally consistent across taxonomic groups.

- Lotic organisms are on average more sensitive to warming than cooling, particularly for growth.
- Fish are on average more sensitive to temperature changes than are invertebrates.
- The falling portion of the thermal response curve (temperature > optimum) is on average more nonlinear than the falling portion (temperature < optimum) for lotic organisms.
- Human impacts to stream and river temperature include global warming, input of effluent discharges, diversion of tributary inputs, cutting of riparian vegetation, reduction of groundwater inputs, reduction of hyporheic exchange, and bottom release from large reservoirs.
- The overall magnitude of these anthropogenic effects varies significantly, with reservoir dams having the greatest potential for cooling and loss of riparian and upland vegetation having the greatest potential for warming.
- Human impacts from reduction of hyporheic exchange have not been explicitly quantified, but effects of hyporheic exchange on stream temperature appear to vary from negligible (Chapter 3) to as much a 7ºC.
- Human effects on temperature are often of similar magnitude to that required to induce a 50% reduction in organism level functioning, indicating that human activities can significantly impair ecological functioning via their "thermal footprint."

- Human activities induce warming more often than cooling, which is particularly troubling as organisms are generally more sensitive to warming than cooling.

5.2 Major Themes and Larger Context

Considered together, the conclusions from the individual chapters presented above provide some intriguing conceptual developments in several important areas of stream and river science and management.

5.2.1 In-stream geomorphic structures and hyporheic exchange

Chapter 2 demonstrated that in-stream geomorphic structures (IGSs) are important drivers of hyporheic exchange in streams, but that importance varies depending on the hyporheic function of interest, and the hydrogeologic setting. For all hyporheic functions, IGSs are most effective in areas of minimal background groundwater discharge, deep bedrock, and intermediate channel slope. For hyporheic functions that correlate with volumetric flux rate of induced hyporheic exchange, IGSs are most effective in areas with high sediment hydraulic conductivity. This explains why the hyporheic impact of the experimental IGS utilized in Chapter 3 on surface stream temperatures was negligible – the hydraulic conductivity was too low in the sandy sediment for the structure to induce sufficient downwelling water flux. Had sediment hydraulic conductivity been higher (gravels or cobbles), the thermal effect on the surface stream would probably have been considerably larger.

For hyporheic functions that correlate with the residence time of the induced hyporheic flow cell, IGSs in areas of lower sediment hydraulic conductivity may be more effective. Functions that might correlate with hyporheic residence time to some extent include anaerobic processes like denitrification, which require complete utilization of oxygen to have already occurred. Denitrification potential may therefore be more significant than temperature modification at the field experimental site used for Chapter 3. Nevertheless, the rates of most hyporheic functions will probably not correlate solely with one hyporheic exchange metric, but rather will be functions of all three metrics: hyporheic flow rate, hyporheic residence time, and hyporheic path length. Understanding how hyporheic functions depend on these three metrics will be important to utilizing the results of Chapter 2 to better understand hyporheic function.

Understanding the total impact of IGSs on streams will require putting their hyporheic functions in context of the many other functions they provide. For instance, IGSs have significant geomorphic functions, including scouring areas downstream and sometimes creating pools upstream. Despite these local scour effects, IGSs can also have an overall stabilizing effect on sediment in a stream reach by trapping sediment behind them. This geomorphic function is probably the most common stated function for installing IGSs in stream restoration projects. IGSs can also have significant ecological effects independent of their hyporheic function. For instance, pools and scour holes generated by IGSs can have significant ecological value, providing habitats that vary in flow velocity, water depth, sediment texture, shade, and cover.

5.2.2 In-stream geomorphic structures, stream temperature, and stream ecology

IGSs appear to influence temperature in lotic systems in three basic ways. First, they induce hyporheic exchange, which can affect surface stream temperatures (cooling in summer, warming in winter). For the experimental IGSs in Chapter 3, this effect on bulk water column temperatures was on the order of 0.01ºC, which is probably not significant for organisms based on the results in Chapter 4. On the other hand, such cooling or warming may be more significant in certain portions of the surface stream, such as boundary layers or pool bottoms, although the experiment described in Chapter 3 did not address this question. The second way that IGSs influence lotic temperatures is by inducing hyporheic exchange which can affect benthic and hyporheic temperatures. This effect was not directly quantified in the experiments in Chapter 3, but was probably nearly 1.0 ºC in some places and times, which should be significant for benthic or hyporheic fauna, based on the results of Chapter 4. Finally, certain types of IGSs (e.g., weirs) can affect surface stream temperatures by creating backwater which can accentuate any differentials in magnitude between stream heat budget components (e.g., streambed vs. atmospheric heat fluxes, see Chapter 3). This also was not directly quantified in the experiments in Chapter 3, but may have been nearly 1.0ºC at certain times of the day, which would be significant for surface stream organisms (e.g., fish) in light of the results of Chapter 4. The relative importance of these three effects depends on many factors including sediment hydraulic conductivity, riparian shading, and structure type.

Within the context of the various human impacts on lotic temperatures laid out in Chapter 4 (Table 4.2), the observed impacts of hyporheic exchange in Chapter 3 are small. Nevertheless the range of hyporheic thermal impacts listed in Table 4.2 are more substantial,

and are of similar magnitude to the ERTCs from Chapter 4 that correspond to 50% reductions in biological processes. This means that restoring hyporheic exchange has the potential to shift temperatures in ways that are beneficial ecologically. This is particularly true in summer, when the tendency of human activities to warm streams more than cool them, and the greater biological sensitivity to warming (see Chapter 4) puts lotic organisms at greater risk. Moderation of stream temperatures or creation of thermal refugia via increased hyporheic exchange can be assisted in the short run by including hyporheic restoration as an integral part of stream restoration. Restoration projects already typically include construction of geomorphic forms that enhance hyporheic exchange (e.g., IGSs, meander bends), but maximizing hyporheic exchange could be more explicitly incorporated into their design. Potential for hyporheic exchange could even be included as a criterion for stream restoration site selection within a watershed.

While active direct intervention in streams may help restore hyporheic function and moderate lotic temperatures in the short term, a long term solution requires a watershed management approach that recreates self-sustaining watershed level processes that create and maintain IGSs and therefore hyporheic function. For example, many IGSs are formed when riparian trees fall into streams and create weir or step type structures. Self sustaining IGS formation in watersheds therefore requires self sustaining riparian forest corridors. Riparian forest restoration also directly moderates stream temperatures by providing shading, particularly in summer. Maintenance of IGSs can also benefit from stewardship of upland areas. For instance, certain forms of forestry and agriculture encourage significant runoff of sediment that can bury or colmate IGSs, or generate unnaturally high flows that can damage or destroy IGSs. Finally, while stream and watershed restoration will facilitate mitigating

human induced thermal shifts in streams and rivers, certain causes of thermal impairment (e.g., global warming) will require international actions.

5.3 Future Research

While this dissertation provides unprecedented understanding of the hydraulic and thermal hyporheic functions of IGSs (Chapters 2 and 3), many interesting questions remain unanswered. For example, the hydraulic analysis presented in Chapter 2 assumes IGSs are static. In reality, these structures are created, evolve in place, and are destroyed. Quantifying the effect of this lifecycle on hydraulic and thermal function would be necessary to fully understand the contribution of these structures to hyporheic function. This would require evaluating the effect of evolving scour patterns and associated turbulent flux in surface sediment, particularly downstream of structure, probably through use of a flume. In addition, beginning to understand how important hyporheic functions like biogeochemical processing and mineralization of toxics correlate with the three metrics of hyporheic exchange (downwelling flux rate, hyporheic residence time, hyporheic pathlength) will be necessary to using the results of Chapter 2 to better understand the impact of IGSs on hyporheic function.

Chapter 3 is one of the first field studies to document heat flux mechanisms in detail within the hyporheic zone and link them to specific temperature changes in bulk stream or river flow. Another is Burkholder et al. (2008), which showed that flow through gravel bars in a large river had temperature impacts on bulk flow on the order of 0.01ºC. These studies contrast with others that have quantified the impact of hyporheic exchange on bulk stream or river temperatures in more indirect ways, and have shown greater temperature effects (Story et al. 2003, Loheide and Gorelick 2006, Moore et al. 2005b). Additional studies like that in

Chapter 3 are warranted to determine if these differences in estimated impact are due to assumptions and methodology, or simply due to natural variability among field sites. In addition, modeling studies would be necessary to determine at what sediment hydraulic conductivity the hyporheic effect of IGSs on surface stream temperatures become significant. The effect of other factors like background groundwater discharge rate, also lend themselves to a modeling sensitivity analysis approach. Finally, field experiments with a weather station would be necessary to quantify the impact of IGSs on atmospheric heat exchange and the effect of shade.

In addition to clarifying many important patterns of ecological sensitivity to a variety of human induced temperature changes in lotic systems, Chapter 4 also highlights key holes in the literature. First, more accurate thermal response curves that are able to resolve thresholds that may be present in biological function are important for anticipating ecological response to temperature change. Second, developing thermal performance curves for organisms at the base of the food chain in lotic systems (e.g., macrophytes like moss, macroalgae) will be necessary to populate models that can predict ecological response to human induced temperature change like that due to global warming. An ecologically consistent way to include other parts of the base of the food chain (e.g., microbes, allochthonous input) into such models will also be necessary.

Appendix

Table A.1 Organism level process data.

[1]organism types: f = fish, i = invertebrate; [2]processes: g = growth, d = development, s = survival; r = reproduction; [3]units: h = hour, d = day, y = year

Taxa	Organism type[1]	Process[2]	$\Delta T_{e\text{-}50,}$ rising	$\Delta T_{e\text{-}50,}$ falling	$\Delta T_{e\text{-}10,}$ rising	$\Delta T_{e\text{-}10,}$ falling	Unit[3]	Source
Acipenser medirostris	f	d	7.2		1.18		1/h	(Van Eenennaam et al. 2005)
Acipenser medirostris	f	r		8		0.6	%	(Van Eenennaam et al. 2005)
Acroperus harpae	i	d	7.7		1.32		1/d	(Bottrell 1975)
Afronurus (Ephemeroptera)	i	g	12		2.4		%/d	(Salas and Dudgeon 2001)
Alona affinis	i	d	9		1.6		1/d	(Bottrell 1975)
Alosa sapidissima	f	s	8		0.7		%	(Leach and Houde 1999)
Alosa sapidissima	f	g	9		1.6		%	(Leach and Houde 1999)
Ameletus (Ephemeroptera)	i	g	11.1		1.42		%/d	(Pritchard and Zloty 1994)
Apatania fimbriata (Trichoptera)	i	d	11.2		1.98		1/d	(Enders and Wagner 1996)
Australopelopia prionoptera - temperate	i	d	12.5		1.52		1/d	(McKie et al. 2004)
Australopelopia prionoptera - temperate	i	d	13.5		2.2		1/d	(McKie et al. 2004)
Australopelopia prionoptera - tropical	i	d	14.5		1.8		1/d	(McKie et al. 2004)
Australopelopia prionoptera - tropical	i	d	12.5		1.46		1/d	(McKie et al. 2004)
Baetidae (Ephemeroptera)	i	g	14		2.8		%/d	(Salas and Dudgeon 2001)
Baetis (Ephemeroptera)	i	g	14		2.8		g/d	(Benke et al. 1992).
Baetis alpinus	i	d	4.2		0.79		1/d	(Knispel et al. 2006)
Cheumatopsyche brevilineata (Trichoptera)	i	g	12		2.4		%	(Mochizuki et al. 2006)
Cheumatopsyche brevilineata (Trichoptera)	i	d	9		1.8		1/dev perio d	(Mochizuki et al. 2006)
Chironomini (Chironomidae)	i	g	12		0.86		%/d	(Hauer and Benke 1991)
Chironomini (subset of Chironominae)	i	g	10.5		0.86		%/d	(Reynolds and Benke 2005)
Chondrostoma nasus	f	g	4		0.8		%/d	(Schiemer et al. 2003)

Taxa	Organ-ism type[1]	Pro-cess[2]	$\Delta T_{e\text{-}50,}$ rising	$\Delta T_{e\text{-}50,}$ falling	$\Delta T_{e\text{-}10,}$ rising	$\Delta T_{e\text{-}10,}$ falling	Unit[3]	Source
Chondrostoma nasus	f	g	7		1.4		%/d	(Schiemer et al. 2003)
Choroterpes (Ephemeroptera)	i	g	5		1		%/d	(Salas and Dudgeon 2001)
Chydorus sphaericus	i	d	8.9		1.56		1/d	(Bottrell 1975)
Cinygmina (Ephemeroptera)	i	g	14		2.8		%/d	(Salas and Dudgeon 2001)
Cottus gobio	f	g		1.5		0.3	1/y	(Abdoli et al. 2007)
Cottus gobio	f	g		1.6		0.32	1/y	(Abdoli et al. 2007)
Cottus gobio	f	g		1.7		0.34	1/y	(Abdoli et al. 2007)
Cottus gobio	f	g		1.8		0.36	1/y	(Abdoli et al. 2007)
Cottus kazika	f	g	10	6.5	1.4	0.5	%	(Takeshita et al. 2005)
Deleatidium (Ephemeroptera, leptohlebiidae) - stony creek	i	g	6		0.56		%/d	(Huryn 1996)
Deleatidium (Ephemeroptera, leptohlebiidae) - sutton stream	i	g	6.6		0.68		%/d	(Huryn 1996)
Dinocras (Plecoptera, Perlidae)	i	r	6	10	0.5	0.5	%	(Zwick 1996)
Dinocras cephalotes (Plecoptera, Perlidae)	i	d	12		2.4		1/d	(Frutiger 1996)
Ecdyonurus picteti	i	d	4		0.8		1/d	(Knispel et al. 2006)
Echinocladius martini	i	d	10.8		1.95		1/d	(McKie and Pearson 2006)
Echinocladius martini - temperate	i	d	13		1.28		1/d	(McKie et al. 2004)
Echinocladius martini - tropical	i	d	14		2.8		1/d	(McKie et al. 2004)
Echinocladius martini - tropical	i	d	12		1.6		1/d	(McKie et al. 2004)
Esox lucius	f	d	6.6		1.08		1/d	(Farrell et al. 2006)
Esox lucius	f	d	4.3		0.74		1/d	(Farrell et al. 2006)
Eucyclops agilis	i	d	8		1.4		1/d	(Bottrell 1975)
Eurycercus lamellatus	i	d	7.5		1.35		1/d	(Bottrell 1975)
Gammarus fossarum	i	d	8.5		1.7		1/d	(Pockl 1992)
Gammarus fossarum	i	g	9.5		1.7		%/d	(Pockl 1992)
Gammarus fossarum	i	g	7		1.5		%/d	(Pockl 1992)
Gammarus fossarum	i	g	12		2.5		%/d	(Pockl 1992)

Taxa	Organ-ism type[1]	Pro-cess[2]	$\Delta T_{e\text{-}50,}$ rising	$\Delta T_{e\text{-}50,}$ falling	$\Delta T_{e\text{-}10,}$ rising	$\Delta T_{e\text{-}10,}$ falling	Unit[3]	Source
Gammarus pulex	i	g	13		1		%/d	(Sutcliffe et al. 1981)
Gammarus pulex	i	g	9	11	0.4		%/d	(Sutcliffe et al. 1981)
Gammarus roeseli	i	d	7.8		1.56		1/d	(Pockl 1992)
Gammarus roeseli	i	g	8.5		1.3		%/d	(Pockl 1992)
Gammarus roeseli	i	g	8		1.2		%/d	(Pockl 1992)
Gammarus roeseli	i	g	11		2.5		%/d	(Pockl 1992)
Graptoleberis testudinaria	i	d	7.3		1.38		1/d	(Bottrell 1975)
Iotichthus phlegethontis	f	g	7		0.56		mg/d	(Billman et al. 2006)
Maccullochella peelii peelii	f	s	4		0.6		%	(Todd et al. 2005)
Meda fulgida	f	s		2.1		0.2	%	(Carveth et al. 2007)
Meda fulgida	f	g		6		1.2	mm/d	(Carveth et al. 2007)
Morone saxatilis	f	g	2.7		0.54		%/d	(Hurst and Conover 1998)
Morone saxatilis	f	g	6.2		1.24		mg/d	(Secor and Houde 1995)
Morone saxatilis	f	s		5		0.36	%/d	(Secor and Houde 1995)
Morone saxatilis	f	s		4.2		0.38	%/d	(Secor and Houde 1995)
Nanocladius	i	d	13		2.04		1/d	(McKie et al. 2004)
Notropis topeka - with tapeworms	f	g	5.1	4	0.7	0.18	%/d	(Koehle and Adelman 2007)
Notropis topeka - without tapeworms	f	g	6.9	5.4	0.92	0.34	%/d	(Koehle and Adelman 2007)
Oncorhynchus clarki utah	f	s		1.2		0.2	%	(Johnstone and Rahel 2003)
Oncorhynchus clarkii lewisi	f	s		3		0.35	%	(Bear et al. 2007)
Oncorhynchus clarkii lewisi	f	g	5.9	5.8	0.4	0.4	%	(Bear et al. 2007)
Oncorhynchus mykiss	f	s		2.3		0.28	%	(Bear et al. 2007)
Oncorhynchus mykiss	f	g		8		1	%	(Bear et al. 2007)
Oncorhynchus mykiss	f	d	6.8		1.18		1/d	(Brannon et al. 2004)
Oncorhynchus mykiss	f	g		3.7		0.74	%	(Magoulick and Wilzbach 1998)
Oncorhynchus nerka	f	r		2.65		0.53	%	(Hendry et al. 1998)
Oncorhynchus tshawytscha	f	s		5.5		0.54	%	(Baker et al. 1995)
Oncorhynchus tshawytscha	f	d	7.7		1.34		1/d	(Crisp 1981)

Taxa	Organ-ism type[1]	Pro-cess[2]	$\Delta T_{e\text{-}50,}$ rising	$\Delta T_{e\text{-}50,}$ falling	$\Delta T_{e\text{-}10,}$ rising	$\Delta T_{e\text{-}10,}$ falling	Unit[3]	Source
Oncorhynchus tshawytscha	f	s		0.92		0.184	%	(Crozier and Zabel 2006)
Oncorhynchus tshawytscha 3.0% ration	f	g	7	5	1.14	0.54	%/d	(Brannon et al. 2004)
Oncorhynchus tshawytscha 5.0% ration	f	g	8.7	4.4	1.24	0.32	%/d	(Brannon et al. 2004)
Oncorhynchus tshawytscha 7.5% ration	f	g	10.2	5	1.58	0.34	%/d	(Brannon et al. 2004)
Oncorhynchus tshawytscha max ration	f	g	11.3	5.3	1.66	0.14	%/d	(Brannon et al. 2004)
Oncorhynchus tshawytscha min ration	f	g	5	5	0.84	0.6	%/d	(Brannon et al. 2004)
Orconectes eupunctus	i	g		8		1.6	%/d	(Whitledge and Rabeni 2002)
Orconectes punctimanus	i	g	4		0.8		%/d	(Whitledge and Rabeni 2002)
Orconectes virilis	i	g		4		0.8	%/d	(Whitledge and Rabeni 2002)
Orthocladiinae (subset of Chironomidae)	i	g	8	9	0.5	1	%/d	(Reynolds and Benke 2005)
Parameletus chelifer	i	g	16.86		1.1025		mm/d	(Soderstrom 1988)
Paramerina	i	d	6.9		1.38		1/d	(McKie et al. 2004)
Paramerina	i	d	18		1.36		1/d	(McKie et al. 2004)
Perla grandis + Perlis marginata (Plecopetera, Perlidae)	i	d	9		1.8		1/d	(Frutiger 1996)
Pleuroxus uncinatus	i	d	7.5		1.4		1/d	(Bottrell 1975)
Polypedilum australotropicus	i	d	10		2.2		1/d	(McKie and Pearson 2006)
Polypedilum australotropicus	i	d	10		1.46		1/d	(McKie et al. 2004)
Polypedilum australotropicus	i	d	12.6		1.78		1/d	(McKie et al. 2004)
Rhithrogena loyolaea (Ephemeroptera)	i	r		4.8		0.9	%	(Humpesch and Elliott 1980)
Rhithrogena semicolorata (Ephemeroptera)	i	r	7.5	5.5	0.5		%	(Humpesch and Elliott 1980)
Rhithrogena semicolorata (Ephemeroptera)	i	d	6		0.98		1/d	(Humpesch and Elliott 1980)
Salmo gairdneri	f	d	5.8		0.94		1/d	(Crisp 1981)
Salmo gairdneri	f	g	8.7		1.66		%/d	(Hokanson et al. 1977)

Taxa	Organ-ism type[1]	Pro-cess[2]	$\Delta T_{e-50,}$ rising	$\Delta T_{e-50,}$ falling	$\Delta T_{e-10,}$ rising	$\Delta T_{e-10,}$ falling	Unit[3]	Source
Salmo salar	f	g	5.7		0.5		%	(Bacon et al. 2005)
Salmo salar	f	d	5.3		0.86		1/d	(Crisp 1981)
Salmo salar	f	g	5.5	3.5	1.1	0.7	%	(Elliott and Hurley 1997)
Salmo salar - river alta	f	g	8	4	1.2	0.2	%	(Jonsson et al. 2001)
Salmo salar - river imsa	f	g	8	5	1	0.3	%	(Jonsson et al. 2001)
Salmo salar - river lone	f	g	7	5	0.8	0.3	%	(Jonsson et al. 2001)
Salmo salar - river stryn	f	g	7	5	1	0.3	%	(Jonsson et al. 2001)
Salmo salar - river suidai	f	g	7	6	1	0.5	%	(Jonsson et al. 2001)
Salmo trutta	f	d	4.2		0.62		1/d	(Crisp 1981)
Salmo trutta	f	g	8	6.5	1.2	0.4	%	(Ojanguren et al. 2001)
Salmo trutta	f	r	3.2	6	0.3	0.44	%	(Vernier 1969)
Salmo trutta	f	r	7	4.2	0.9	0.5	%	(Vernier 1969)
Salvelinus confluentus	f	g	5.7	5.7	0.6	0.6	g/d	(Selong et al. 2001)
Salvelinus confluentus - with Salvelinus fontinalis	f	g		6.8		0.56	g/d	(McMahon et al. 2007)
Salvelinus confluentus - without Salvelinus fontinalis	f	g		7.2		0.76	g/d	(McMahon et al. 2007)
Salvelinus fontinalis	f	d	5.6		0.94		1/d	(Crisp 1981)
Sander lucioperca	f	d	7.6		1.26		1/h	(Lappalainen et al. 2003)
Sida crystallina	i	d	6.5		1.14		1/d	(Bottrell 1975)
Simocephalus vetulus	i	d	7.3		1.3		1/d	(Bottrell 1975)
Stenonema (Ephemeroptera)	i	g	7		1		g/d	(Benke et al. 1992)
Tanytarsini (Chironomidae)	i	g	10	9	0.8	1	%/d	(Hauer and Benke 1991)
Tanytarsini (subset of Chironominae)	i	g	8.4	7.6	0.68	0.8	%/d	(Reynolds and Benke 2005)

Table A.2 Population level abundance data

[1]organism types: f = fish, i = invertebrate

Taxa	Organ-ism type[1]	$\Delta T_{e\text{-}50,}$ rising	$\Delta T_{e\text{-}50,}$ falling	$\Delta T_{e\text{-}10,}$ rising	$\Delta T_{e\text{-}10,}$ falling	Unit	Source
Baetidae	i	2.5		0.4		#/m^2	(Castella et al. 2001)
Baetidae	i	1.3				#/m^2	(Milner et al. 2001)
Chironominae	i	4.5	4	0.5	0.5	#/m^2	(Castella et al. 2001)
Chironominae	i	1.3				#/m^2	(Milner et al. 2001)
Cottus cognatus	f		5		1	#/100m^2	(Edwards and Cunjak 2007)
Diamesinae	i	4	4	0.4	0.4	#/m^2	(Castella et al. 2001)
Diamesinae	i	4.8	4			#/m^2	(Milner et al. 2001)
Empididae	i	7.5	7	0.7	0.7	#/m^2	(Castella et al. 2001)
Empididae	i	4.8				#/m^2	(Milner et al. 2001)
Gastropoda and others	i	2.2		0.44		#/m^2	(Zivic et al. 2006)
Heptageniidae	i	1.5		0.3		#/m^2	(Castella et al. 2001)
Heptageniidae	i	1.1				#/m^2	(Milner et al. 2001)
Leuctridae	i	3		0.5		#/m^2	(Castella et al. 2001)
Leuctridae	i	3				#/m^2	(Milner et al. 2001)
Limnephilidae	i	4.5	6	0.5	0.6	#/m^2	(Castella et al. 2001)
Limnephilidae	i	4.5				#/m^2	(Milner et al. 2001)
Limoniidae	i	9.5		0.7		#/m^2	(Castella et al. 2001)
Limoniidae	i	8.2				#/m^2	(Milner et al. 2001)
Nemouridae	i	9		0.4		#/m^2	(Castella et al. 2001)
Nemouridae	i	1.5				#/m^2	(Milner et al. 2001)
Oligochaeta	i	5				#/m^2	(Milner et al. 2001).
Oncorhynchus mykiss 2004	f	1.7		0.34		#	(Sutton et al. 2007)
Oncorhynchus mykiss 2006	f	2.4		0.48		#	(Sutton et al. 2007)
Oncorhynchus nerka	f	1.4	3.5	0.1	0.2	%	(Lorenz and Eiler 1989)
Oncorhynchus tshawytscha 2004	f	1.5		0.3		#	(Sutton et al. 2007)
Oncorhynchus tshawytscha 2006	f	2.5		0.5		#	(Sutton et al. 2007)
Orthocladiinae	i	4		0.4		#/m^2	(Castella et al. 2001)
Orthocladiinae	i	4				#/m^2	(Milner et al. 2001)
Perlodidae	i	3.5		0.5		#/m^2	(Castella et al. 2001)
Perlodidae	i	3				#/m^2	(Milner et al. 2001)
Rhyacophilidae	i	3.5		0.5		#/m^2	(Castella et al. 2001)
Rhyacophilidae	i	2.3				#/m^2	(Milner et al. 2001)
Salmo trutta	f	0.9		0.18		#/m^2	(Lobon-Cervia and Mortensen 2005)
Salvelinus confluentus	f		4.5		0.8	%	(Dunham et al. 2003)
Salvelinus confluentus	f		3.25		0.39	%	(Rieman et al. 2006)
Simuliidae	i	4.5	4	0.4	0.4	#/m^2	(Castella et al. 2001)

Taxa	Organ-ism type[1]	$\Delta T_{e\text{-}50,}$ rising	$\Delta T_{e\text{-}50,}$ falling	$\Delta T_{e\text{-}10,}$ rising	$\Delta T_{e\text{-}10,}$ falling	Unit	Source
Simuliidae	i	6.5				#/m^2	(Milner et al. 2001)
Taeniopterygidae	i	3		0.5		#/m^2	(Castella et al. 2001)
Taeniopterygidae	i	4.3				#/m^2	(Milner et al. 2001)
Tipulidae	i	11.5				#/m^2	(Milner et al. 2001)

References

Abbe, T., G. Pess, D. R. Montgomery, and K. L. Fetherston. 2003. Integrating Engineering Log Jam Technology into River Rehabilitation. Pages 443-482 *in* D. R. Montgomery, S. Bolton, D. Booth, and L. Wall, editors. Restoration of Puget Sound Rivers University of Washington Press, Seattle, WA.

Abdoli, A., D. Pont, and P. Sagnes. 2007. Intrabasin variations in age and growth of bullhead: the effects of temperature. Journal of Fish Biology **70**:1224-1238.

Alexandrov, Y. Y. 1977. Cells, Molecules and Temperature: Conformational Flexibility of Macromolecules and Ecological Adaptation. Spring-Verlag, Berlin.

Allan, J. D. 1995. Stream Ecology: Structure and function of running waters. Kluwer Academic Publishers, Dordrecht, The Netherlands.

Anderson, M. P. 2005. Heat as a ground water tracer. Ground Water **43**:951-968.

Arrigoni, A. S., G. C. Poole, L. A. K. Mertes, S. J. O'Daniel, W. W. Woessner, and S. A. Thomas. In Press. Buffered, lagged, or cooled? Disentangling hyporheic influences on temperature cycles in stream channels. Water Resources Research.

Bacon, P. J., W. S. C. Gurney, W. Jones, I. S. McLaren, and A. F. Youngson. 2005. Seasonal growth patterns of wild juvenile fish: partitioning variation among explanatory variables, based on individual growth trajectories of Atlantic salmon (Salmo salar) parr. Journal of Animal Ecology **74**:1-11.

Baker, P. F., T. P. Speed, and F. K. Ligon. 1995. Estimating the Influence of Temperature on the Survival of Chinook Salmon Smolts (Oncorhynchus-Tshawytscha) Migrating through the Sacramento-San-Joaquin River Delta of California. Canadian Journal of Fisheries and Aquatic Sciences **52**:855-863.

Battin, J., M. W. Wiley, M. H. Ruckelshaus, R. N. Palmer, E. Korb, K. K. Bartz, and H. Imaki. 2007. Projected impacts of climate change on salmon habitat restoration. Proceedings of the National Academy of Sciences of the United States of America **104**:6720-6725.

Bear, E. A., T. E. McMahon, and A. V. Zale. 2007. Comparative thermal requirements of westslope cutthroat trout and rainbow 11-out: Implications for species interactions and development of thermal protection standards. Transactions of the American Fisheries Society **136**:1113-1121.

Begon, M., C. R. Townsend, and J. L. Harper. 2006. Ecology, Fourth edition. Blackwell Publishing, Malden, MA.

Beitinger, T. L., and L. C. Fitzpatrick. 1979. Physiological and ecological correlates of preferred temperature in fish. American Zoologist **19**:319-329.

Bencala, K. E., and R. A. Walters. 1983. Simulation of Solute Transport in a Mountain Pool-and-Riffle Stream - a Transient Storage Model. Water Resources Research **19**:718-724.

Benke, A. C., F. R. Hauer, D. L. Stites, J. L. Meyer, and R. T. Edwards. 1992. Growth of Snag-Dwelling Mayflies in a Blackwater River - the Influence of Temperature and Food. Archiv Fur Hydrobiologie **125**:63-81.

Berg, D. R., A. McKee, and M. J. Maki. 2003. Restoring Floodplain Forests. Pages 248-291 *in* D. R. Montgomery, S. Bolton, D. Booth, and L. Wall, editors. Restoration of Puget Sound Rivers University of Washington Press, Seattle, WA.

Beschta, R. L., R. E. Bilby, G. W. Brown, L. B. Holtby, and T. D. Hofstra. 1987. Stream Temperature and Aquatic Habitat: Fisheries and Forestry Interactions. *in* E. O. Salo and T. W. Cundy, editors. Streamside Management: Forestry and Fishery Interactions. University of Washington, Seattle, WA.

Bethel, J., and K. Neal. 2003. Stream Enhancement Projects: A King County Perspective. *in* D. R. Montgomery, S. Bolton, D. Booth, and L. Wall, editors. Restoration of Puget Sound Rivers University of Washington Press, Seattle, WA.

Bilby, R. E. 1984. Characteristics and Frequency of Cool-Water Areas in a Western Washington Stream. Journal of Freshwater Ecology **2**:593-602.

Billman, E. J., E. J. Wagner, and R. E. Arndt. 2006. Effects of temperature on the survival and growth of age-0 least chub (Iotichthys phlegethontis). Western North American Naturalist **66**:434-440.

Boano, F., C. Camporeale, R. Revelli, and L. Ridolfi. 2006. Sinuosity-driven hyporheic exchange in meandering rivers. Geophysical Research Letters **33**.

Bottrell, H. H. 1975. Relationship between Temperature and Duration of Egg Development in Some Epiphytic Cladocera and Copepoda from River Thames, Reading, with a Discussion of Temperature Functions. Oecologia **18**:63-84.

Boulton, A. J. 2007. Hyporheic rehabilitation in rivers: restoring vertical connectivity. Freshwater Biology **52**:632-650.

Boulton, A. J., S. Findlay, P. Marmonier, E. H. Stanley, and H. M. Valett. 1998. The functional significance of the hyporheic zone in streams and rivers. Annual Review of Ecology and Systematics **29**:59-81.

Bourque, C. P. A., and J. H. Pomeroy. 2001. Effects of forest harvesting on summer stream temperatures in New Brunswick, Canada: an inter-catchment, multiple-year comparison. Hydrology and Earth System Sciences **5**:599-613.

Brannon, E. L., M. S. Powell, T. P. Quinn, and A. Talbot. 2004. Population structure of Columbia River Basin chinook salmon and steelhead trout. Reviews in Fisheries Science **12**:99-232.

Brown, G. W. 1969. Predicting Temperatures of Small Streams. Water Resources Research **5**:68-75.

Brown, J. H., J. F. Gillooly, A. P. Allen, V. M. Savage, and G. B. West. 2004. Toward a metabolic theory of ecology. Ecology **85**:1771-1789.

Brown, L. E., A. M. Milner, and D. M. Hannah. 2007. Groundwater influence on alpine stream ecosystems. Freshwater Biology **52**:878-890.

Brunke, M., and T. Gonser. 1997. The ecological significance of exchange processes between rivers and groundwater. Freshwater Biology **37**:1-33.

Buchanan, J. A., B. A. Stewart, and B. R. Davies. 1988. Thermal-Acclimation and Tolerance to Lethal High-Temperature in the Mountain Stream Amphipod Paramelita-Nigroculus (Barnard). Comparative Biochemistry and Physiology a-Physiology **89**:425-431.

Burkholder, B. K., G. E. Grant, R. Haggerty, T. Khangaonkar, and P. J. Wampler. 2008. Influence of hyporheic flow and geomorphology on temperature of a large, gravel-bed river, Clackamas River, USA. Hydrological Processes **2**:941-953.

Caissie, D. 2006. The thermal regime of rivers: a review. Freshwater Biology **51**:1389-1406.

Calver, A. 2001. Riverbed permeabilities: Information from pooled data. Ground Water **39**:546-553.

Cardenas, M. B., and J. L. Wilson. 2006. The influence of ambient groundwater discharge on exchange zones induced by current-bedform interactions. Journal of Hydrology **331**:103-109.

Cardenas, M. B., and J. L. Wilson. 2007. Effects of current-bed form induced fluid flow on the thermal regime of sediments. Water Resources Research **43**:W08431.

Cardenas, M. B., J. L. Wilson, and V. A. Zlotnik. 2004. Impact of heterogeneity, bed forms, and stream curvature on subchannel hyporheic exchange. Water Resources Research **40**.

Cardenas, M. B., and V. A. Zlotnik. 2003. Three-dimensional model of modern channel bend deposits. Water Resources Research **39**:1141.

Carveth, C. J., A. M. Widmer, S. A. Bonar, and J. R. Simms. 2007. An examination of the effects of chronic static and fluctuating temperature on the growth and survival of spikedace, Meda fulgida, with implications for management. Journal of Thermal Biology **32**:102-108.

Castella, E., H. Adalsteinsson, J. E. Brittain, G. M. Gislason, A. Lehmann, V. Lencioni, B. Lods-Crozet, B. Maiolini, A. M. Milner, J. S. Olafsson, S. J. Saltveit, and D. L. Snook. 2001. Macrobenthic invertebrate richness and composition along a latitudinal gradient of European glacier-fed streams. Freshwater Biology **46**:1811-1831.

Clarke, A. 2006. Temperature and the metabolic theory of ecology. Functional Ecology **20**:405-412.

Cossins, A. R., and K. Bowler. 1987. Temperature Biology of Animals. Chapman and Hall, London, UK.

Crisp, D. T. 1981. A Desk Study of the Relationship between Temperature and Hatching Time for the Eggs of 5 Species of Salmonid Fishes. Freshwater Biology **11**:361-368.

Crisp, D. T. 1990. Water Temperature in a Stream Gravel Bed and Implications for Salmonid Incubation. Freshwater Biology **23**:601-612.

Crozier, L., and R. W. Zabel. 2006. Climate impacts at multiple scales: evidence for differential population responses in juvenile Chinook salmon. Journal of Animal Ecology **75**:1100-1109.

Danehy, R. J., C. G. Colson, K. B. Parrett, and S. D. Duke. 2005. Patterns and sources of thermal heterogeneity in small mountain streams within a forested setting. Forest Ecology and Management **208**:287-302.

Doll, B. A., G. L. Grabow, K. R. Hall, J. Halley, W. A. Harman, G. D. Jennings, and D. E. Wise. 2003. Stream Restoration: A Natural Channel Design Handbook. NC Stream Restoration Institute, NC State University, Raleigh, NC.

Doyle, M. W., E. H. Stanley, D. L. Strayer, R. B. Jacobson, and J. C. Schmidt. 2005. Effective discharge analysis of ecological processes in streams. Water Resources Research **41**.

Dunham, J., B. Rieman, and G. Chandler. 2003. Influences of temperature and environmental variables on the distribution of bull trout within streams at the southern margin of its range. North American Journal of Fisheries Management **23**:894-904.

Dunham, J. B., A. E. Rosenberger, C. H. Luce, and B. E. Rieman. 2007. Influences of wildfire and channel reorganization on spatial and temporal variation in stream temperature and the distribution of fish and amphibians. Ecosystems **10**:335-346.

Ebersole, J. L., W. J. Liss, and C. A. Frissell. 2003. Cold water patches in warm streams: Physicochemical characteristics and the influence of shading. Journal of the American Water Resources Association **39**:355-368.

Edwards, P. A., and R. A. Cunjak. 2007. Influence of water temperature and streambed stability on the abundance and distribution of slimy sculpin (Cottus cognatus). Environmental Biology of Fishes **80**:9-22.

Elliott, A. H., and N. H. Brooks. 1997. Transfer of nonsorbing solutes to a streambed with bed forms: Theory. Water Resources Research **33**:123-136.

Elliott, J. M., and M. A. Hurley. 1997. A functional model for maximum growth of Atlantic Salmon parr, Salmo salar, from two populations in northwest England. Functional Ecology **11**:592-603.

Enders, G., and R. Wagner. 1996. Mortality of Apatania fimbriata (Insecta: Trichoptera) during embryonic, larval and adult life stages. Freshwater Biology **36**:93-104.

Ensign, S. H., and M. W. Doyle. 2005. In-channel transient storage and associated nutrient retention: Evidence from experimental manipulations. Limnology and Oceanography **50**:1740-1751.

Evans, E. C., G. R. McGregor, and G. E. Petts. 1998. River energy budgets with special reference to river bed processes. Hydrological Processes **12**:575-595.

Evans, E. C., and G. E. Petts. 1997. Hyporheic temperature patterns within riffles. Hydrological Sciences Journal-Journal Des Sciences Hydrologiques **42**:199-213.

Farrell, J. M., J. V. Mead, and B. A. Murry. 2006. Protracted spawning of St Lawrence River northern pike (Esox lucius): simulated effects on survival, growth, and production. Ecology of Freshwater Fish **15**:169-179.

Federal Interagency Stream Restoration Working Group. 1998. Stream corridor restoration: principles, processes, and practices, Washington, DC.

Fernald, A. G., D. H. Landers, and P. J. Wigington. 2006. Water quality changes in hyporheic flow paths between a large gravel bed river and off-channel alcoves in Oregon, USA. River Research and Applications **22**:1111-1124.

Ferrari, M. R., J. R. Miller, and G. L. Russell. 2007. Modeling changes in summer temperature of the Fraser River during the next century. Journal of Hydrology **342**:336-346.

Fitter, A., and R. Hay. 2002. Environmental Physiology of Plants, Third edition. Academic Press, London, UK.

Freeze, R. A., and J. A. Cherry. 1979. Groundwater. Prentice-Hall, Inc, Englewood Cliffs, NJ.

Frutiger, A. 1996. Embryogenesis of Dinocras cephalotes, Perla grandis and P-marginata (Plecoptera: Perlidae) in different temperature regimes. Freshwater Biology **36**:497-508.

Giller, P. S., and B. Malmqvist. 1998. The biology of streams and rivers. Oxford University Press, Oxford, UK.

Gooseff, M. N., J. K. Anderson, S. Wondzell, J. LaNier, and R. Haggerty. 2006. A modeling study of hyporheic exchange pattern and the sequence, size, and spacing of stream bedforms in mountain stream networks, Oregon, USA (Retraction of vol 19, pg 2915, 2005). Hydrological Processes **20**:2441-+.

Gooseff, M. N., J. LaNier, R. Haggerty, and K. Kokkeler. 2005. Determining in-channel (dead zone) transient storage by comparing solute transport in a bedrock channel-alluvial channel sequence, Oregon. Water Resources Research **41**.

Gooseff, M. N., D. M. McKnight, R. L. Runkel, and J. H. Duff. 2004. Denitrification and hydrologic transient storage in a glacial meltwater stream, McMurdo Dry Valleys, Antarctica. Limnology and Oceanography **49**:1884-1895.

Groffman, P. M., A. M. Dorsey, and P. M. Mayer. 2005. N processing within geomorphic structures in urban streams. Journal of the North American Benthological Society **24**:613-625.

Hansen, E. A. 1975. Some Effects of Groundwater on Brown Trout Redds. Transactions of the American Fisheries Society **104**:100-110.

Harbaugh, A. W. 1990. A Computer Program for Calculating Subregional Water Budgets Using Results from the U.S. Geological Survey Modular Three-dimensional Finite-difference Ground-water Flow Model. Open-File Report 90-392. . United States Geological Survey Reston, VA.

Harbaugh, A. W., and M. G. McDonald. 1996. User's Documentation for MODFLOW-96, an update to the U.S. Geological Survey Modular Finite-Difference Ground-Water Flow Model. Open-File Report 96-485. United States Geological Survey Reston, VA.

Hardy, R. N. 1979. Temperature and Animal Life, Second edition. The Camelot Press, Ltd., Southampton, UK.

Harvey, J. W., and B. J. Wagner. 2000. Quantifying hydrologic interactions betweens streams and their subsurface hyporheic zones. *in* J. B. Jones and P. J. Mulholland, editors. Streams and ground waters. Academic Press, San Diego, CA.

Hauer, F. R., and A. C. Benke. 1991. Rapid Growth of Snag-Dwelling Chironomids in a Blackwater River - the Influence of Temperature and Discharge. Journal of the North American Benthological Society **10**:154-164.

Hendricks, S. P., and D. S. White. 1991. Physicochemical Patterns within a Hyporheic Zone of a Northern Michigan River, with Comments on Surface-Water Patterns. Canadian Journal of Fisheries and Aquatic Sciences **48**:1645-1654.

Hendry, A. P., J. E. Hensleigh, and R. R. Reisenbichler. 1998. Incubation temperature, developmental biology, and the divergence of sockeye salmon (Oncorhynchus nerka) within Lake Washington. Canadian Journal of Fisheries and Aquatic Sciences **55**:1387-1394.

Hill, R. W., G. A. Wyse, and M. Anderson. 2004. Animal Physiology. Sinauer Associates, Inc., Sunderland, MA.

Hill, W. R., A. J. Stewart, and G. E. Napolitano. 1996. Mercury speciation and bioaccumulation in lotic primary producers and primary consumers. Canadian Journal of Fisheries and Aquatic Sciences **53**:812-819.

Hokanson, K. E. F., C. F. Kleiner, and T. W. Thorslund. 1977. Effects of Constant Temperatures and Diel Temperature-Fluctuations on Specific Growth and Mortality-Rates and Yield of Juvenile Rainbow-Trout, Salmo-Gairdneri. Journal of the Fisheries Research Board of Canada **34**:639-648.

Hondzo, M., and H. G. Stefan. 1994. Riverbed Heat-Conduction Prediction. Water Resources Research **30**:1503-1513.

Huey, R. B., and J. G. Kingsolver. 1989. Evolution of Thermal Sensitivity of Ectotherm Performance. Trends in Ecology & Evolution **4**:131-135.

Humpesch, U. H., and J. M. Elliott. 1980. Effect of Temperature on the Hatching Time of Eggs of 3 Rhithrogena Spp (Ephemeroptera) from Austrian Streams and an English Stream and River. Journal of Animal Ecology **49**:643-661.

Hunter, J. E., and F. L. Schmidt. 1990. Methods of Meta-Analysis: Correcting Error and Bias in Research Findings. Sage Publications, Newbury Park, CA.

Hurst, T. P., and D. O. Conover. 1998. Winter mortality of young-of-the-year Hudson River striped bass (Morone saxatilis): size-dependent patterns and effects on recruitment (vol 55, pg 1122, 1998). Canadian Journal of Fisheries and Aquatic Sciences **55**:2709-2709.

Huryn, A. D. 1996. Temperature-dependent growth and life cycle of Deleatidium (Ephemeroptera: Leptophlebiidae) in two high-country streams in New Zealand. Freshwater Biology **36**:351-361.

Hutchinson, P. A., and I. T. Webster. 1998. Solute uptake in aquatic sediments due to current-obstacle interactions. Journal of Environmental Engineering-Asce **124**:419-426.

Hynes, H. B. N. 1970. The Ecology of Running Waters. University of Toronto Press, Suffolk, UK.

Jobson, H. E. 1977. Bed conduction computation for thermal models. Journal of the Hydraulics Division, Proceedings of the American Society of Civil Engineers **103**:1213-1217.

Johnson, A. N., B. R. Boer, W. W. Woessner, J. A. Stanford, G. C. Poole, S. A. Thomas, and S. J. O'Daniel. 2005. Evaluation of an inexpensive small-diameter temperature logger for documenting ground water-river interactions. Ground Water Monitoring and Remediation **25**:68-74.

Johnson, S. L. 2004. Factors influencing stream temperatures in small streams: substrate effects and a shading experiment. Canadian Journal of Fisheries and Aquatic Sciences **61**:913-923.

Johnstone, H. C., and F. J. Rahel. 2003. Assessing temperature tolerance of Bonneville cutthroat trout based on constant and cycling thermal regimes. Transactions of the American Fisheries Society **132**:92-99.

Jones, J. B., and P. J. Mulholland. 2000. Streams and ground waters. Academic Press, San Diego, CA.

Jonsson, B., T. Forseth, A. J. Jensen, and T. F. Naesje. 2001. Thermal performance of juvenile Atlantic Salmon, Salmo salar L. Functional Ecology **15**:701-711.

Karl, T. R., P. D. Jones, R. W. Knight, G. Kukla, N. Plummer, V. Razuvayev, K. P. Gallo, J. Lindseay, R. J. Charlson, and T. C. Peterson. 1993. A New Perspective on Recent Global Warming - Asymmetric Trends of Daily Maximum and Minimum Temperature. Bulletin of the American Meteorological Society **74**:1007-1023.

Kasahara, T., and S. M. Wondzell. 2003. Geomorphic controls on hyporheic exchange flow in mountain streams. Water Resources Research **39**.

Kinouchi, T., H. Yagi, and M. Miyamoto. 2007. Increase in stream temperature related to anthropogenic heat input from urban wastewater. Journal of Hydrology **335**:78-88.

Knispel, S., M. Sartori, and J. E. Brittain. 2006. Egg development in the mayflies of a Swiss glacial floodplain. Journal of the North American Benthological Society **25**:430-443.

Koehle, J. J., and I. R. Adelman. 2007. The effects of temperature, dissolved oxygen, and Asian tapeworm infection on growth and survival of the Topeka shiner. Transactions of the American Fisheries Society **136**:1607-1613.

Lackey, R. T., D. H. Lach, and S. L. Duncan. 2006. Salmon 2100: The future of wild pacific salmon. American Fisheries Society, Bethesda, MD.

Lapham, W. W. 1989. Use of temperature profiles beneath streams to determine rates of vertical ground-water flow and vertical hydraulic conductivity. U.S. Geological Survey

Lappalainen, J., H. Dorner, and K. Wysujack. 2003. Reproduction biology of pikeperch (Sander lucioperca (L.)) - a review. Ecology of Freshwater Fish **12**:95-106.

Lautz, L. K., and D. I. Siegel. 2006. Modeling surface and ground water mixing in the hyporheic zone using MODFLOW and MT3D. Advances in Water Resources **29**:1618-1633.

Leach, S. D., and E. D. Houde. 1999. Effects of environmental factors on survival, growth, and production of American shad larvae. Journal of Fish Biology **54**:767-786.

LeBlanc, R. T., R. D. Brown, and J. E. FitzGibbon. 1997. Modeling the effects of land use change on the water temperature in unregulated urban streams. Journal of Environmental Management **49**:445-469.

Leopold, L. B., and T. Maddock. 1953. The Hydraulic Geomometry of Stream Channels and Some Physiographic Implications. Geological Survey Professional Paper 252. United States Geological Survey, United States Government Printing Office, Washington, DC.

Lindeburg, M. R. 2001. Civil Engineering Reference Manual, 8th edition. Professional Publications, Inc., Belmont, CA.

Lobon-Cervia, J., and E. Mortensen. 2005. Population size in stream-living juveniles of lake-migratory brown trout Salmo trutta L.: the importance of stream discharge and temperature. Ecology of Freshwater Fish **14**:394-401.

Loheide, S. P., and S. M. Gorelick. 2006. Quantifying stream-aquifer interactions through the analysis of remotely sensed thermographic profiles and in situ temperature histories. Environmental Science & Technology **40**:3336-3341.

Lomolino, M. V., B. R. Riddle, and J. H. Brown. 2006. Biogeography, Third edition. Sinauer Associates, Inc., Sunderland, MA.

Lorenz, J. M., and J. H. Eiler. 1989. Spawning Habitat and Redd Characteristics of Sockeye-Salmon in the Glacial Taku River, British-Columbia and Alaska. Transactions of the American Fisheries Society **118**:495-502.

Lynch, J. A., G. B. Rishel, and E. S. Corbett. 1984. Thermal Alteration of Streams Draining Clear-Cut Watersheds - Quantification and Biological Implications. Hydrobiologia **111**:161-169.

Magoulick, D. D., and M. A. Wilzbach. 1998. Effect of temperature and macrohabitat on interspecific aggression, foraging success, and growth of brook trout and rainbow trout pairs in laboratory streams. Transactions of the American Fisheries Society **127**:708-717.

Manners, R., and M. W. Doyle. 2008. A mechanistic model of woody debris jam evolution and its application to wood-based restoration and management. River Research and Applications **in press**.

Manners, R. B., M. W. Doyle, and M. J. Small. 2007. Structure and hydraulics of natural woody debris jams. Water Resources Research **43**.

McIntosh, A. R., and C. R. Townsend. 1996. Interactions between fish, grazing invertebrates and algae in a New Zealand stream: A trophic cascade mediated by fish induced changes to grazer behaviour? Oecologia **108**:174-181.

McKie, B. G., P. S. Cranston, and R. G. Pearson. 2004. Gondwanan mesotherms and cosmopolitan eurytherms: effects of temperature on the development and survival of Australian Chironomidae (Diptera) from tropical and temperate populations. Marine and Freshwater Research **55**:759-768.

McKie, B. G., and R. G. Pearson. 2006. Environmental variation and the predator-specific responses of tropical stream insects: effects of temperature and predation on survival and development of Australian Chironomidae (Diptera). Oecologia **149**:328-339.

McMahon, T. E., A. V. Zale, F. T. Barrows, J. H. Selong, and R. J. Danehy. 2007. Temperature and competition between bull trout and brook trout: A test of the elevation refuge hypothesis. Transactions of the American Fisheries Society **136**:1313-1326.

Mertes, L. A. K. 1997. Documentation and significance of the perirheic zone on inundated floodplains. Water Resources Research **33**:1749-1762.

Millenium-Ecosystem-Assessment. 2005. Ecosystems and human well-being. Island Press.

Milner, A. M., J. E. Brittain, E. Castella, and G. E. Petts. 2001. Trends of macroinvertebrate community structure in glacier-fed rivers in relation to environmental conditions: a synthesis. Freshwater Biology **46**:1833-1847.

Mochizuki, S., Y. Kayaba, and K. Tanida. 2006. Larval growth and development in the caddisfly Cheumatopsyche brevilineata under natural thermal regimes. Entomological Science **9**:129-136.

Mohseni, O., T. R. Erickson, and H. G. Stefan. 1999. Sensitivity of stream temperatures in the United States to air temperatures projected under a global warming scenario. Water Resources Research **35**:3723-3733.

Montgomery, D. R., J. M. Buffington, R. D. Smith, K. M. Schmidt, and G. Pess. 1995. Pool Spacing in Forest Channels. Water Resources Research **31**:1097-1105.

Moore, R. D. 2005. Slug Injection Using Salt Solution. Streamline Watershed Management Bulletin **8**:1-6.

Moore, R. D., D. L. Spittlehouse, and A. Story. 2005a. Riparian microclimate and stream temperature response to forest harvesting: A review. Journal of the American Water Resources Association **41**:813-834.

Moore, R. D., P. Sutherland, T. Gomi, and A. Dhakal. 2005b. Thermal regime of a headwater stream within a clear-cut, coastal British Columbia, Canada. Hydrological Processes **19**:2591-2608.

Morrison, J., M. C. Quick, and M. G. G. Foreman. 2002. Climate change in the Fraser River watershed: flow and temperature projections. Journal of Hydrology **263**:230-244.

Munson, B. R., D. F. Young, and T. H. Okiishi. 1994. Fundamentals of Fluid Mechanics. John Wiley and Sons, Inc, New York, NY.

Nielsen, J. L., T. E. Lisle, and V. Ozaki. 1994. Thermally Stratified Pools and Their Use by Steelhead in Northern California Streams. Transactions of the American Fisheries Society **123**:613-626.

Nimick, D. A., C. H. Gammons, T. E. Cleasby, J. P. Madison, D. Skaar, and C. M. Brick. 2003. Diel cycles in dissolved metal concentrations in streams: Occurrence and possible causes. Water Resources Research **39**.

Ojanguren, A. F., F. G. Reyes-Gavilan, and F. Brana. 2001. Thermal sensitivity of growth, food intake and activity of juvenile brown trout. Journal of Thermal Biology **26**:165-170.

Packman, A., M. Salehin, and M. Zaramella. 2004. Hyporheic exchange with gravel beds: Basic hydrodynamic interactions and bedform-induced advective flows. Journal of Hydraulic Engineering-Asce **130**:647-656.

Packman, A. I., and K. E. Bencala. 2000. Modeling surface-subsurface hydrologic interactions. *in* J. B. Jones and P. J. Mulholland, editors. Streams and Ground Waters Academic Press, San Diego, CA.

Packman, A. I., and M. Salehin. 2003. Relative roles of stream flow and sedimentary conditions in controlling hyporheic exchange. Hydrobiologia **494**:291-297.

Pedersen, N. L., and K. Sand-Jensen. 2007. Temperature in lowland Danish streams: contemporary patterns, empirical models and future scenarios. Hydrological Processes **21**:348-358.

Pilgrim, J. M., X. Fang, and H. G. Stefan. 1998. Stream temperature correlations with air temperatures in Minnesota: Implications for climate warming. Journal of the American Water Resources Association **34**:1109-1121.

Pockl, M. 1992. Effects of Temperature, Age and Body Size on Molting and Growth in the Fresh-Water Amphipods Gammarus-Fossarum and Gammarus-Roeseli. Freshwater Biology **27**:211-225.

Pollock, D. W. 1994. User's Guide for MODPATH/MODPATH-PLOT, Version 3. Open File Report 94-464. United States Geological Survey

Poole, G. C., and C. H. Berman. 2001. An ecological perspective on in-stream temperature: Natural heat dynamics and mechanisms of human-caused thermal degradation. Environmental Management **27**:787-802.

Poole, G. C., S. J. O'Daniel, K. L. Jones, W. W. Woessner, E. S. Bernhardt, A. M. Helton, J. A. Stanford, B. R. Boer, and T. J. Beechie. In Press. Hydrologic spiraling: the role of multiple interactive flow paths in stream ecosystems. River Research and Applications.

Poole, G. C., J. A. Stanford, S. W. Running, and C. A. Frissell. 2006. Multiscale geomorphic drivers of groundwater flow paths: subsurface hydrologic dynamics and hyporheic habitat diversity. Journal of the North American Benthological Society **25**:288-303.

Poole, G. C., J. A. Stanford, S. W. Running, C. A. Frissell, W. W. Woessner, and B. K. Ellis. 2004. A patch hierarchy approach to modeling surface and subsurface hydrology in complex flood-plain environments. Earth Surface Processes and Landforms **29**:1259-1274.

Postel, S., and B. Richter. 2003. Rivers for life: managing water for people and nature. Island Press, Washington, DC.

Pritchard, G., and J. Zloty. 1994. Life-Histories of 2 Ameletus Mayflies (Ephemeroptera) in 2 Mountain Streams - the Influence of Temperature, Body-Size, and Parasitism. Journal of the North American Benthological Society **13**:557-568.

Reynolds, S. K., and A. C. Benke. 2005. Temperature-dependent growth rates of larval midges (Diptera : Chironomidae) from a southeastern US stream. Hydrobiologia **544**:69-75.

Rieman, B. E., J. T. Peterson, and D. L. Myers. 2006. Have brook trout (Salvelinus fontinalis) displaced bull trout (Salvelinus confluentus) along longitudinal gradients

in central Idaho streams? Canadian Journal of Fisheries and Aquatic Sciences **63**:63-78.

Ringler, N. H., and J. D. Hall. 1975. Effects of Logging on Water Temperature and Dissolved-Oxygen in Spawning Beds. Transactions of the American Fisheries Society **104**:111-121.

Runkel, R. L. 1998. One dimensional transport with inflow and storage (OTIS): a solute transport model for streams and rivers. US Geological Survey Water-Resources Investigation Report 98-4018. United States Geological Survey, Denver, CO.

Runkel, R. L. 2002. A new metric for determining the importance of transient storage. Journal of the North American Benthological Society **21**:529-543.

Rutherford, J. C., N. A. Marsh, P. M. Davies, and S. E. Bunn. 2004. Effects of patchy shade on stream water temperature: how quickly do small streams heat and cool? Marine and Freshwater Research **55**:737-748.

Saenger, N., P. K. Kitanidis, and R. L. Street. 2005. A numerical study of surface-subsurface exchange processes at a riffle-pool pair in the Lahn River, Germany. Water Resources Research **41**.

Salas, M., and D. Dudgeon. 2001. Laboratory and field studies of mayfly growth in tropical Asia. Archiv Fur Hydrobiologie **153**:75-90.

Salehin, M., A. I. Packman, and M. Paradis. 2004. Hyporheic exchange with heterogeneous streambeds: Laboratory experiments and modeling. Water Resources Research **40**.

Salisbury, F. B., and C. W. Ross. 1985. Plant Physiology, Third edition. Wadsworth Publishing Company, Belmont, CA.

Scheuerell, M. D., R. Hilborn, M. H. Ruckelshaus, K. K. Bartz, K. M. Lagueux, A. D. Haas, and K. Rawson. 2006. The Shiraz model: a tool for incorporating anthropogenic effects and fish-habitat relationships in conservation planning. Canadian Journal of Fisheries and Aquatic Sciences **63**:1596-1607.

Schiemer, F., H. Keckeis, and E. Kamler. 2003. The early life history stages of riverine fish: ecophysiological and environmental bottlenecks. Comparative Biochemistry and Physiology a-Molecular and Integrative Physiology **133**:439-449.

Secor, D. H., and E. D. Houde. 1995. Temperature Effects on the Timing of Striped Bass Egg-Production, Larval Viability, and Recruitment Potential in the Patuxent River (Chesapeake Bay). Estuaries **18**:527-544.

Selong, J. H., T. E. McMahon, A. V. Zale, and F. T. Barrows. 2001. Effect of temperature on growth and survival of bull trout, with application of an improved method for determining thermal tolerance in fishes. Transactions of the American Fisheries Society **130**:1026-1037.

Shimizu, Y., T. Tsujimoto, and H. Nakagawa. 1990. Experiment and macroscopic modeling of flow in highly permeable porous medium under free-surface flow. J. Hydrosc. Hydrol. Eng. **8**:69-78.

Silliman, S. E., and D. F. Booth. 1993. Analysis of Time-Series Measurements of Sediment Temperature for Identification of Gaining Vs Losing Portions of Juday-Creek, Indiana. Journal of Hydrology **146**:131-148.

Sinokrot, B. A., and H. G. Stefan. 1993. Stream Temperature Dynamics - Measurements and Modeling. Water Resources Research **29**:2299-2312.

Smith, K. 1972. River water temperatures - an environmental review. Scottish Geographical Magazine **88**:211-220.

Soderstrom, O. 1988. Effects of Temperature and Food Quality on Life-History Parameters in Parameletus-Chelifer and P-Minor (Ephemeroptera) - a Laboratory Study. Freshwater Biology **20**:295-303.

Stanford, J. A., and A. R. Gaufin. 1974. Hyporheic communities of two Montana rivers. Science **185**:700-702.

Stein, B. A., L. S. Kutner, and J. S. Adams. 2000. Precious Heritage: The Status of Biodiversity in the United States. Oxford University Press, Oxford, UK.

Stonestrom, D. A., and J. Constantz. 2003. Heat as a tool for studying the movement of ground water near streams. U.S. Geological Survey Reston, VA.

Storey, R. G., K. W. F. Howard, and D. D. Williams. 2003. Factors controlling riffle-scale hyporheic exchange flows and their seasonal changes in a gaining stream: A three-dimensional groundwater flow model. Water Resources Research **39**.

Story, A., R. D. Moore, and J. S. Macdonald. 2003. Stream temperatures in two shaded reaches below cutblocks and logging roads: downstream cooling linked to subsurface hydrology. Canadian Journal of Forest Research-Revue Canadienne De Recherche Forestiere **33**:1383-1396.

Sutcliffe, D. W., T. R. Carrick, and L. G. Willoughby. 1981. Effects of diet, body size, age and temperature on growth rates in the amphipod Gammarux pulex. Freshwater Biology **11**:183-214.

Sutcliffe, J. 1977. Plants and Temperature. The Camelot Press, Ltd., Southampton, UK.

Sutton, R. J., M. L. Deas, S. K. Tanaka, T. Soto, and R. A. Corum. 2007. Salmonid observations at a Klamath River thermal refuge under various hydrological and metereological conditions. River Research and Applications **23**:775-785.

Sweeney, B. W., and R. L. Vannote. 1978. Size Variation and Distribution of Hemimetabolous Aquatic Insects - 2 Thermal-Equilibrium Hypotheses. Science **200**:444-446.

Takeshita, N., I. Ikeda, N. Onikura, M. Nishikawa, S. Nagata, S. Matsui, and S. Kimura. 2005. Growth of the fourspine sculpin Cottus kazika in the Gonokawa River, Japan, and effects of water temperature on growth. Fisheries Science **71**:784-790.

Thibodeaux, L. J., and J. D. Boyle. 1987. Bedform-Generated Convective-Transport in Bottom Sediment. Nature **325**:341-343.

Todd, C. R., T. Ryan, S. J. Nicol, and A. R. Bearlin. 2005. The impact of cold water releases on the critical period of post-spawning survival and its implications for Murray cod (Maccullochella peelii peelii): A case study of the Mitta Mitta River, southeastern Australia. River Research and Applications **21**:1035-1052.

Triska, F. J., V. C. Kennedy, R. J. Avanzino, G. W. Zellweger, and K. E. Bencala. 1989. Retention and Transport of Nutrients in a 3rd-Order Stream in Northwestern California - Hyporheic Processes. Ecology **70**:1893-1905.

United State Army Corps of Engineers. 2002a. HEC-RAS River Analysis System Hydraulic Reference Manual Version 3.1. U.S. Army Corps of Engineers, Institute for Water Resources, Hydrologic Engineering Center, Davis, CA.

United State Army Corps of Engineers. 2002b. HEC-RAS River Analysis System User's Manual Version 3.1. U.S. Army Corps of Engineers, Institute for Water Resources, Hydrologic Engineering Center, Davis, CA.

Van Eenennaam, J. P., J. Linares-Casenave, X. Deng, and S. I. Doroshov. 2005. Effect of incubation temperature on green sturgeon embryos, Acipenser medirostris. Environmental Biology of Fishes **72**:145-154.

Vaux, W. G. 1962. Interchange of stream and intragravel water in a salmon spawning riffle. United State Fish and Wildlife Service, Washington, DC.

Vaux, W. G. 1968. Intragravel flow and interchange of water in a streambed. United States Fish and Wildlife Service Fishery Bulletin **66**:479-489.

Vernier, J. M. 1969. Table chronologique du development embryonaire de la truite arc-en-ciel, Salmo gairdneri. Annales d'Embryologie et de Morphogenese **2**:495-520.

Walther, G. R., E. Post, P. Convey, A. Menzel, C. Parmesan, T. J. C. Beebee, J. M. Fromentin, O. Hoegh-Guldberg, and F. Bairlein. 2002. Ecological responses to recent climate change. Nature **416**:389-395.

Ward, J. V. 1985. Thermal-Characteristics of Running Waters. Hydrobiologia **125**:31-46.

Webb, B. W. 1996. Trends in stream and river temperature. Hydrological Processes **10**:205-226.

Webb, B. W., and Y. Zhang. 2004. Intra-annual variability in the non-advective heat energy budget of Devon streams and rivers. Hydrological Processes **18**:2117-2146.

Westrich, J. T., and R. A. Berner. 1988. The Effect of Temperature on Rates of Sulfate Reduction in Marine-Sediments. Geomicrobiology Journal **6**:99-117.

White, D. S., C. H. Elzinga, and S. P. Hendricks. 1987. Temperature patterns within the hyporheic zone of a northern Michigan river. Journal of the North American Benthological Society **6**:85-91.

Whitledge, G. W., and C. F. Rabeni. 2002. Maximum daily consumption and respiration rates at four temperatures for five species of crayfish from Missouri, USA (Decapoda, Orconectes spp.). Crustaceana **75**:1119-1132.

Willson, M. F., and K. C. Halupka. 1995. Anadromous Fish as Keystone Species in Vertebrate Communities. Conservation Biology **9**:489-497.

Woessner, W. W. 2000. Stream and fluvial plain ground water interactions: Rescaling hydrogeologic thought. Ground Water **38**:423-429.

Wondzell, S. M., and F. J. Swanson. 1996. Seasonal and storm dynamics of the hyporheic zone of a 4th-order mountain stream .1. Hydrologic processes. Journal of the North American Benthological Society **15**:3-19.

Wroblicky, G. J., M. E. Campana, H. M. Valett, and C. N. Dahm. 1998. Seasonal variation in surface-subsurface water exchange and lateral hyporheic area of two stream-aquifer systems. Water Resources Research **34**:317-328.

Zivic, I., Z. Markovic, and M. Brajkovic. 2006. Influence of the temperature regime on the composition of the macrozoobenthos community in a thermal brook in Serbia. Biologia **61**:179-191.

Zwick, P. 1996. Variable egg development of Dinocras spp (Plecoptera, Perlidae) and the stonefly seed bank theory. Freshwater Biology **35**:81-99.